Venously printed

Multi-material 3D printed responsive fluidic interfaces with programmable dynamic appearance triggered by mechanical deformation.

Abstract

Venously printed contributes to the field of HCI and digital manufacturing by exploring the scope and possibilities for programmable and responsive fluidic interfaces, using multi-material 3D printing as a manufacturing technique. Novel meta-materials and computational composites have proven to open up new design paradigms and continue to expand the design space for HCI and material design with unprecedented I/O configurations and material experiences. By encoding the computational logic of dynamic and responsive behaviour into the material's structure and properties, these materials allow shifting away from typical 2D (digital) interfaces towards embedded responsive 3D objects and materials without the need for external logical operators or controllers.

A novel concept within this field is fluidic interfaces, which utilise liquid flow as a medium to drive dynamic appearance triggered by mechanical deformation input such as pressure, twisting or bending. Within this research, multi-material 3D printing is explored as a manufacturing tool for such fluidic interfaces to allow for more complex 3D geometries, dynamic visual output and encoded computational logic. A set of demonstrators are developed with programmable dynamic appearance, showcasing the capabilities of this manufacturing workflow and the possibility of being tuned for specific material experiences or temporal form in interaction design.

To allow for the fabrication of these interfaces Venously printed presents a fabrication pipeline, including a computational design and simulation tool for designers to validate the responsive behaviour and iterate on their design before going into manufacturing. Additionally, a voxel-based support structure for 3D printing complex internal cavities is developed to provide better printing quality as opposed to available workflows whilst still being able to be removed from complex internal structures. Finally, a first step for the characterisation of the experiential qualities of fluidic interfaces has been performed via a set of interviews. This led to promising future applications and material experiences which can be explored in future work.

Master Thesis
MSc. Integrated Product Design
Faculty of Industrial Design Engineering
Delft University of Technology

08-12-2022
David van Rijn
ID 4457951

Chair
Dr. ir. Doubrovski, E.L. (Zjenja)
Faculty of Industrial Design Engineering

Mentor
Dr. ir. Elkhuizen, W.S. (Willemijn)
Faculty of Industrial Design Engineering

Special thanks to
MSc. Dam, J.J.F van (Joris)
Prof. dr. Pont, S.C. (Sylvia)
Participating interviewees

TU Delft

Preface

This project will be the completion of my master's at the faculty of Design Engineering at the Delft, University of Technology. Seven years ago I came to this institution as a young dreamer, not knowing about the rich experiences and life lessons waiting in front of me. Seven years ago, I wouldn't have believed that I will do a research project, without a client involved, as a final thesis for my master's. However, as so often in life, it turned out to be going in other directions. This project gave me the final opportunity to dive deep, deep into the future of material and computational design. I would like to thank my supervisors Willemijn en Zjenja for giving me the opportunity to work on such an inspiring project, together with your guidance and inspiration allong the way. This project heavenly inspired me as a designer, and shifted my thoughts from component-based design, towards a more embedded holistic view on materiality and its inherent capabilities and behaviour for interaction design With this project I hope to inspire fellow designers to start thinking differently, asking themselves the question:

What if materials could think, feel or behave, not only as an AI, but like human beings?

Walking around at this faculty for seven years has not only shaped me as a designer, but even more, towards the person, I am today. Over the years I've met wonderful people and had a lot of fun. I would like to give a big shoutout to everyone out there feeling addressed! Thanks for the great times, thanks for all the fun, thanks for the sad times and thanks for helping me out on this final journey towards my graduation! Next to all these fellow student friends, I thought this was a good moment to say a few nice words to some very special people in my life. Hi sister, mom and dad. You were there with me from the beginning (yes, I am the youngest), and you've always given me the room and opportunities to do the things I like, whenever and wherever I wanted them to do. I came to realise that this is not for everyone, and therefore I would like to thank you. Besides I would like to compliment my patents on your ability to make me and my sister always feel comfortable, whatever or whenever, by just being yourself. You are the souls that make my house, my home, and I would love to visit that as long as I can. .

There is one person for which written words could not make up for the feelings that I want to express. Romée, You were there for me <3. Undergoing this project was one of the bigger challenges in my life, but doing it with you on my side made it more fun, easy and with more self-confidence than I could ever imagine. Giving me a helping hand or challenging me when needed, you just seem to know what I need before I do, I love you.

With that being said it is time to read my thesis, enjoy!

Table of contents

01

Introduction

1 Introduction

Traditional 2D user interfaces (UI's) are familiar systems for human-computer interaction (HCI). Typically they consist of multiple components, which each have a single functionality, such as input sensing (keyboard and mouse), computation (computer) and output display or actuation (LCD display). However, researchers have explored the possibility to shift away from such 2D displays (painted bits) and into 3D objects and materials (tangible bits). [36], [35].

Additionally, novel meta-material structures have been researched to be used in HCI by encoding the responsive and dynamic behaviour into the material's structure and properties itself as computational logic [83], [63]. The unique properties and ability of such novel meta-material structures to react in preprogrammed ways to external stimuli have opened up a wide variety of possibilities for dynamic human-material interactions such as dynamic shape, texture, appearance or sound [63], [32], [34], [33], [92], [16].

A recent example showcasing such responsive behaviour is a novel meta-material concept and approach for designing dynamic tangible interfaces using fluidic mechanisms presented by the Tangible Media group at MIT [54]. Within these interfaces, fluids simultaneously function as a sensor, driver and display of tangible information, acting as an analogue dynamic interface. The concept of these interfaces is yet explored as a set of 2D venous structures that respond to the mechanical inputs of the user, which dynamically displays fluid flow and colour change.

Based on the principle of these venous structures, a novel evolution in PolyJet 3D-printing presented by Maccurdy [48], [76] is introduced as a manufacturing technique for fluidic mechanisms [74]. This workflow allows for simultaneously depositing photopolymers and a non-curing liquid to create complex pre-filled fluidic geometries. 3D printing fluidic systems using this manfucturing workflow is explored by Speijer within a graduation project at the faculty of IDE at the Delft University of Technology. The final result of this research is an externally actuated 3D-printed fluidic structure in which the fluid acts as a medium to trigger dynamic material surface texture for corresponding mechanical inputs. Whilst various digital fabrication techniques are explored for manufacturing such computational material composites, the encoded responsive behaviour of these materials and interfaces can lead to unprecedented possibilities for material experiences and HCI. To design for such (novel) meaning material experiences, Karana et al. have presented a Material Driven Design method (MDD) [42] in which (novel) materials are characterised for their experiential qualities on four experiential levels [27]. Another approach to interaction design for material experiences is to use the power of temporal form, which describes the computational structure that enables the temporal expression of responsive computational materials or interfaces [82]. However, both the characterisation of fluidic interfaces for their experiential qualities or temporal form remains completely unexplored in current literature.

This research aims to contribute to the field of HCI and digital manufacturing by expanding the scope and possibilities for programmable responsive materials with a focus on fluidic interfaces. Specifically, the goal is to open up new design paradigms by making use of a multi-material 3D printing workflow, to explore novel embedded, responsive fluidic interface configurations. Ultimately, this exploration has led to the following results:

- Extended design space and basic architecture of the configurations and possibilities of 3D printed fluidic interfaces.
- A design and fabrication pipeline for 3D-printed fluidic interfaces, including a computational design and simulation tool and evaluation of the simulation model
- A novel 3D printing workflow using a voxel-based support material.
- First characterisation of experiential qualities and temporal form of responsive fluidic interfaces.
- Overview of various promising applications for 3D printed fluidic interfaces, driven by their experiential qualities.
- A demonstration concept which showcases the concept of 3D-printed fluidic interfaces by three different 3D-printed fluidic interfaces which are programmed for specific material experiences.

Project scope

This research contributes to the field of HCI and digital manufacturing by exploring the scope and possibilities for programmable responsive material using multi-material 3D printing as a manufacturing technique. Its main focus is 3D-printed fluidic interfaces, which overlaps with multiple research fields such as: meta- and smart-materials, 4D-printing, microfluidics, human visual perception and material experiences.

Within the scope of this project, a demonstration concept of a fluidic interface is developed to showcase the capabilities of multi-material 3D-printing of fluidic interfaces. The demonstration concept is tuned for specific material experiences by adjusting a set of design parameters for programmable dynamic responsive behaviour embedded into the material itself.

Project structure

This project is a research graduation project at the faculty of Industrial Design at the Delft, University of Technology. The main focus of this project is to gather new insights for:

The optimization of the 3D-printing workflow for 3D-printed fluidic interfaces.
Exploration of new human-material interactions using responive fluidic interface.

Both of these directions were explored simultaneously within an interactive process driven by rapid prototyping. The structure of this project can be described using the Double Diamond Design model as shown in Figure 1.

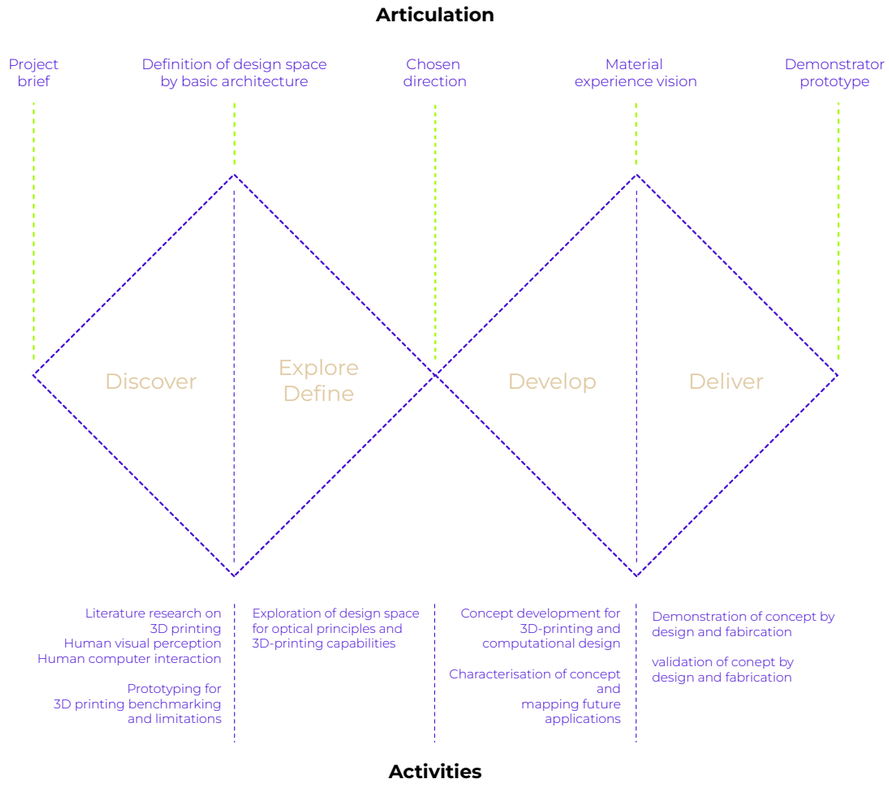

Figure 1: Project structure following a double diamond approach

02

Related work

2 Related work

Traditional 2D user interfaces (UIs) are familiar systems for HCI. Typically they consist of an input device (e.g. a keyboard and mouse), a machine state for computational logic (the computer) and an output device (e.g. an LCD or LED screen). Bachmann et al. visualised a simple version of this HCI loop as shown in Figure 2 [4]. The human layer interacts with the computational layer via the human actuators and sensory system. The human actuators provide input for the sensors of the UI, whilst the human sensory system perceives the output of the UI.

Within this basic HCI loop, each of the components of the computational layer has a single functionality. However, in nowadays common UIs such as touchscreens, the in- and output take place at the same location, integrating the computational sensor and actuator into a single component.

Responsive materials and interfaces

Besides integrating such functionalities into a single location or component, HCI researchers started to investigate how to shift UIs away from 2D screens and into 3D objects and materials [36], [35]. Deformable and foldable screens have been developed as material for visual output [45], and similar touch-sensitive interfaces showcase the integration of in- and output in such a single material. [66], [49].

Other working principles, such as pneumatics, have been widely explored for shape-shifting interfaces [57], [58], [91]. Pneumatics even have been used to design integrated responsive shape- and colour-changing interfaces (output) triggered by touch at the same location (input) [24]. Besides pneumatics, fluidic systems are explored for shape-changing and dynamic visual interfaces as well [64], [46], [81], [72].

However, these digital, pneumatic and liquid interfaces generally still include rigid and bulky electrical components such as batteries, controllers and pumps or actuators. Therefore, researchers have investigated how to embed the computational layer of the HCI loop in the material itself by encoding the responsive behaviour into the material structure and properties [83]. Based upon other examples of categorising integrated functionalities for responsive interfaces and materials [65], [59], this evolution in interactive material design is shown as three levels of integration of the HCI loop for responsive interfaces in Figure 3.

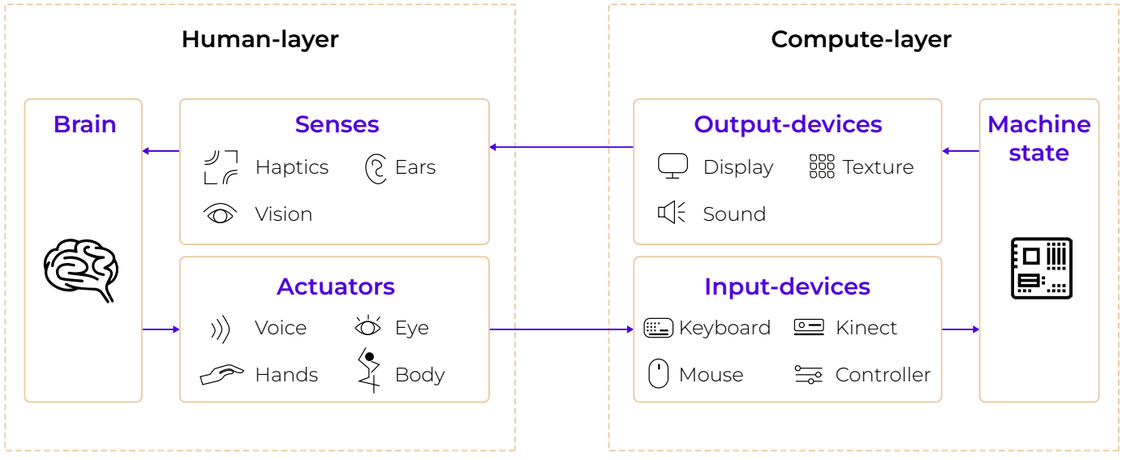

Figure 2: Simple version of the HCI loop by bachmann et al. [3]

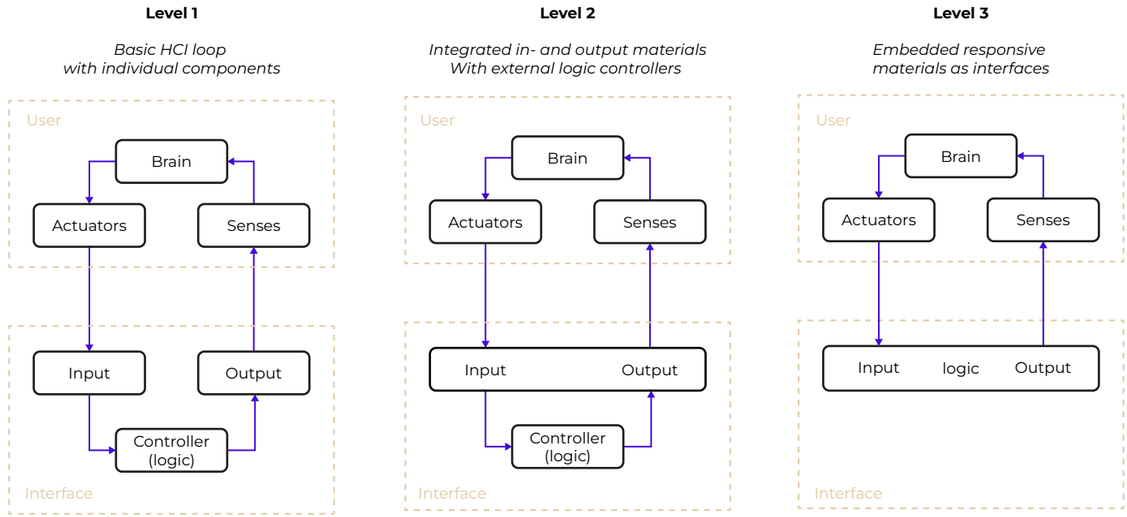

Figure 3: Three levels of integration of the HCI loop for responsive interfaces and materials [64], [58].

The concept of embedded responsive material interfaces (level three), is defined along multiple research concepts and paradigms, including Smart Materials [70], [84], [86] Meta-Materials [60], [32], [17] and 4D Printing [38], [80]. For example, a method to design meta-material structures which output specific mechanical actuation and deformation for input force is presented [32]. This work was later extended with the ability to embed mechanical computation [34] and dynamic textures [33]. A wide variety of such shape-changing structures which are responsive to inputs such as actuation force, deformation and temperature are reviewed for designing dynamic interfaces [63].

Besides embedded mechanical deformation, other types of responsive behaviour are encoded into meta-materials, such as programmable buoyancy [87], centre of mass [3] and light and sound wave manipulation [15], [21], [16].

Materials with dynamic visual appearance

The goal of this research is to explore 3D-printed embedded responsive materials with dynamic visual output. Within this domain, materials with dynamic colour output have been explored as both 3D-printed and non-3D-printed objects triggered by different stimuli, including temperature [6], [41], [67], [85] UV-light [68], [39], [30] deformation [52], and viewing angle [92], [28]. Additionally, materials with dynamic transparency which can be tuned and controlled by mechanical actuation are developed [47], [50]. Next to dynamic colour and transparency as visual output, light-emitting responsive interfaces have been explored with bioluminescence algae which respond to kinetic stimuli [8], and 3D printed embedded optical elements, which act as an interactive display [89].

Fluidic interfaces

The approach of using fluid flow as a driver for dynamic visual appearance has been explored within multiple responsive interfaces. As described, non-embedded (level two, Figure 3) fluidic interfaces have been used for dynamic visual display [64], [46], [81], [72]. Embedded fluidic interfaces (level three, figure 3) have been created which output dynamic colour, haptic texture and biomimetic actuation, triggered by electromagnetic fields [25]. These interfaces make use of embedded layer pumps manufactured with laser and plotting cutting techniques.

Used as a starting point for this research, Mor et al. have presented a novel concept and approach for interactive fluidic mechanisms called Venous Materials [54]. They present a design method for fluidic interfaces with dynamic appearance, that respond to deformation by mechanical input of a user. The concept is presented as a 2D embedded and responsive interface, which is fabricated using PDMS moulding and laser engraving. Venous structures (cavities) within the substrate material are filled with coloured liquid material, displaying fluid flow and colour change in multiple flow patterns. Various configurations and designs of Venous Materials are shown if Figure 4. Figure 5 shows the design space and basic architecture of this material.

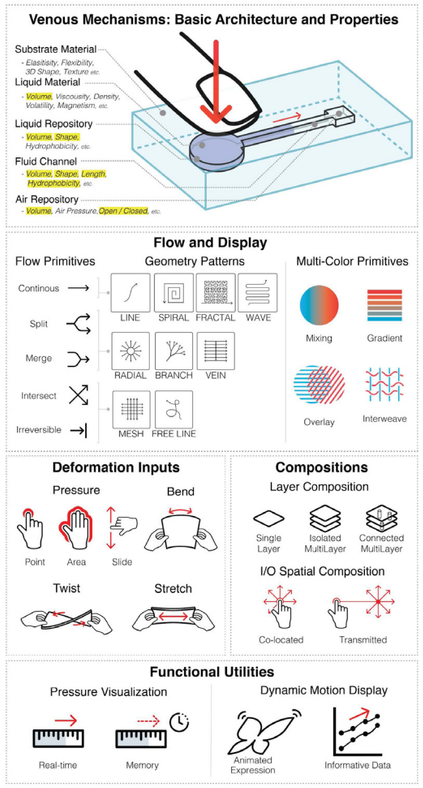

Figure 5: The design space and basic architecture of Venous Materials [53]..

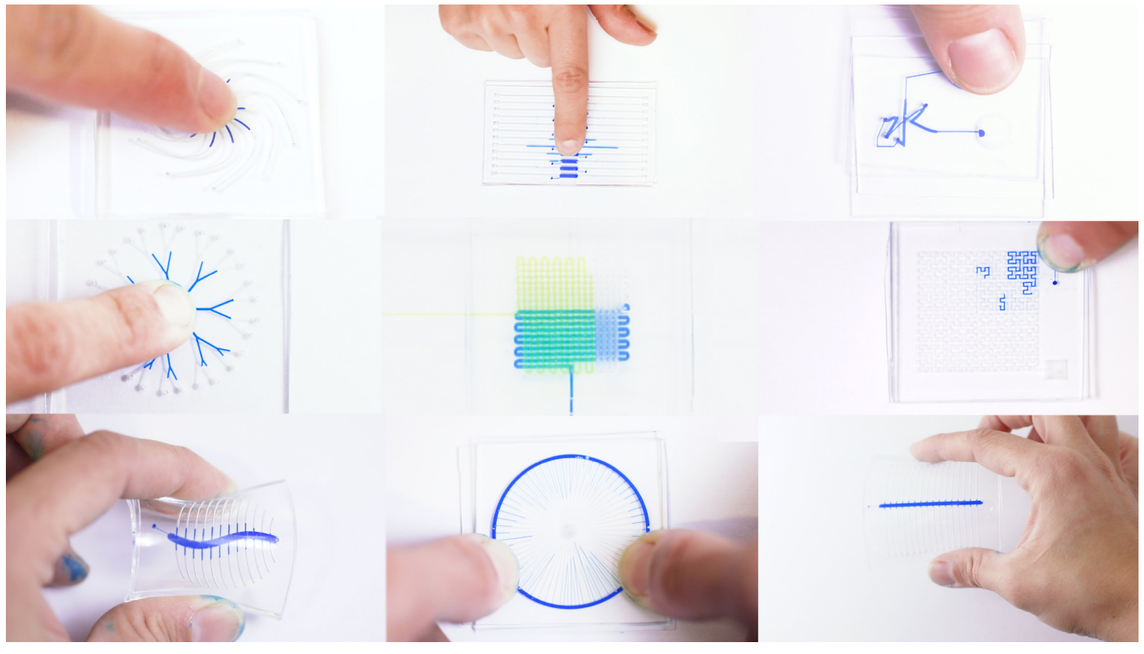

Figure 4: Various configurations and designs of Venous Materials, a 2D embedded and responsive fluidic interface [53]..

(micro)Fluidic 3D printing

The concept of Venous materials has been the starting point for this research. However, Venous Materials are still roughly 2D material geometries, with limited complexity in the third dimension as it is composed as a (manually) layered structure. This research aims to extend the concept of fluidic interfaces by using Multimaterial 3D printing as a means of fabrication.

Multi-material 3D printed fluidic systems have been used as a haptic interface with dynamic texture triggered by mechanical actuation [69]. Other examples showcase the possibility to simultaneously 3D print liquid and substrate materials to fabricate pre-filled liquid channels and geometries, which allow for complex fluidic systems without assembly required after printing. [48], [74]. However, the suggested workflows in those papers still result in poor structural and optical properties and limitations for printing dimensions.

Another research domain which is widely explored in material science, mechanical engineering, microbiology and computational fluidic systems is microfluidics [88]. In soft robotics, microfluidics have been explored by creating soft robots with dynamic colour [53], [64]. As opposed to more typical fabrication methods for microfluidic devices such as laser engraving, PDMS moulding and lithography, (multi-material) 3D-printing has been introduced as a fabrication method. Bader et al. have presented a multi-material 3D printed microfluidic fluidic wearable designed to culture microbial communities [5]. Other examples have shown the possibility to use multi-material 3D printing to encode computational logic into a meta-material structure itself. Operators like mechanical valves , pressure valves, one-way valves and fluidic capacitors have been embedded into 3D printed microfluidic devices [2], [71], [43]. However, the workflows suggested in these papers result in internal cavities which remain very difficult to be cleared from 3D-printed support material. This makes it impossible to manufacture complex internal fluidic structures. To overcome this limitation, researchers have 3D printed enclosed fluidic geometries by pausing the print and injecting non-photocurable viscous liquids or polycarbonate membranes [13]. Although this workflow shows promising structural and optical properties for 3D-printed (micro)fluidic structures, it is limited for the complexity of internal geometries in the third dimension.

Characterisation of responsive interfaces

Karana et al. have developed a material-driven design method (MDD) to design for specific material experiences [42]. The key aspect of this method is to characterise (new) materials not only for their technical properties but also for their experiential qualities in order to design meaningful material interactions and applications. A framework and approach for this experiential characterisation for HCI is presented by Giaccardi & Karana [27]. This method has been applied to characterise experiential qualities of dynamic material interfaces, such as LTM smart-materials [7], and living light material interfaces using (fluidic) bioluminescence algae [8]. Besides, relationships between temporal form and such experiential qualities have been investigated within interaction design and HCI [82].

Although responsive fluidic interfaces have been thoroughly characterised for their technical properties, as presented in Figure 5 [54]. The concept of fluidic interfaces has not been explored for the possibilities of different encoded behaviour in relation towards their expressions and resulting material experience. The experiential qualities and temporal form for fluidic interfaces and materials with such temporal qualities remain still unknown.

Overall insights

The concept of Venous Materials [54] and the workflow for liquid printing using a Stratays PolyJet 3D printer [48], [74] were both used as a starting point for this research to develop a 3D printed responsive fluidic interface with dynamic visual appearance. The most important and inspiring related work for this research is shown in Figure 6.

Materials with dynamic appearance

Fluidic interfaces

(micro)fluidic 3D printing

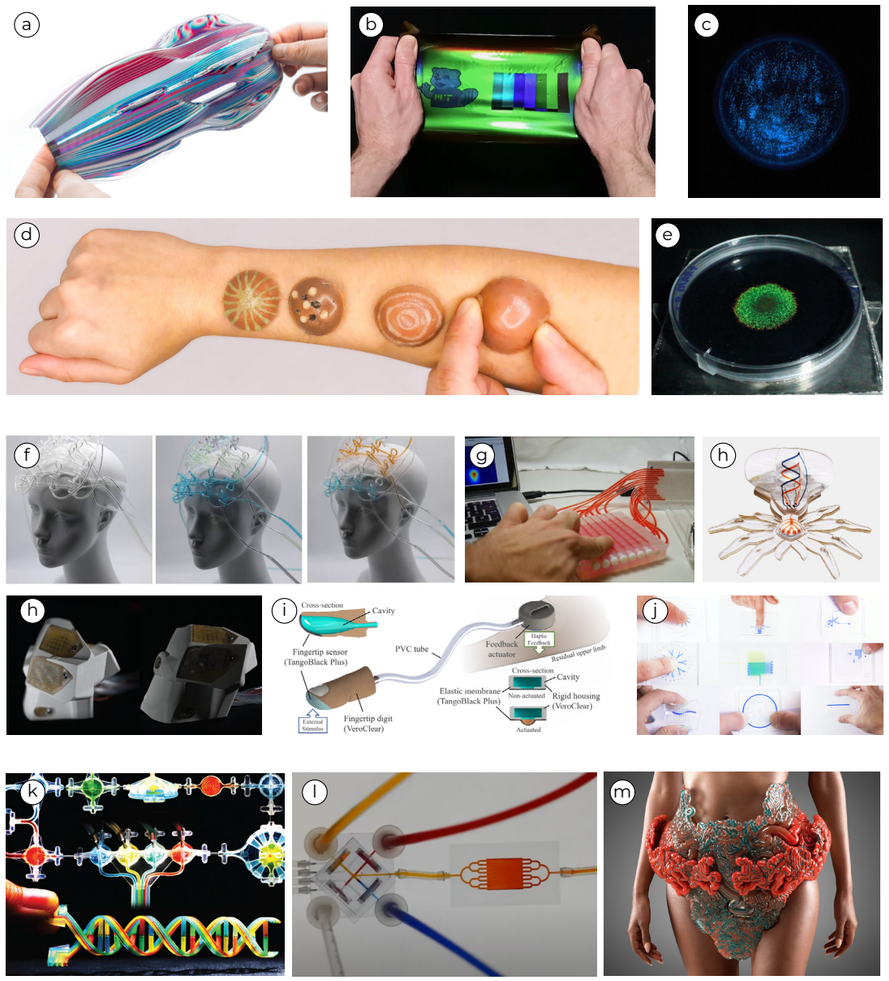

Figure 6: Various configurations and designs of Venous Materials, a 2D embedded and responsive fluidic interface [53].

Knowledge gaps and limitations

Reviewing the related work, several knowledge gaps and limitations can be identified:

Knowledge gaps

- Dynamic visual output, other than colour change by fluidic flow, has not been explored for fluidic interfaces.
- Experiential qualities and temporal form of fluidic interfaces and their effect on different interactive experiences have not been characterised.

Limitations and oppurtunities

- Embedded responsive fluidic interfaces are explored as 2D venous materials [53], but are still limited in complexity in the thrid dimension.
- Additionally, these 2D fluidic interfaces remain very limited in possibilities to encode programable logic within the material structure itself. Due to its fabrication method (laser engraving), they only allow for logic encoded within the 2D flow pattern, such as irreversible flow, as showcased by Mor et al [54].
- Multimaterial 3D printing has been explored as a manufacturing technique for creating (micro)fluidic devices with encoded logic. However, this workflow is limited for complex geometries and printing dimensions as it remains difficult to remove support material from tiny cavities.

03

Design space

3 Design space

To scope the design space for 3D printed fluidic interfaces, a set of requirements is defined to distinguish 3D printed fluidic interfaces from other responsive material interfaces. When developing new fluidic interface configurations, these requirements must be met to classify as a 3D printed fluidic interface.

3D printed fluidic interface requirements

3D printed

A 3D printed fluidic interface must be manufactured with a multi-material 3D printing technique categorised as "Material Jetting" following the ASTM terminology [37].

Fluidic driver

Within a 3D printed fluidic interface a liquid material is used as a medium to drive its responsive behaviour.

Responsive

A 3D printed fluidic interface has a responsive dynamic output. The dynamic output must be controllable, meaning there is a logical relation between in- and output. The dynamic output is typically reversible but can be non-reversible for specific use cases.

Embedded

A 3D printed fluidic interface acts simultaneously as a data sensor, data driver and data actuator with inherent feedback. The computational logic of the interface is programmed into the material itself, and defined by the specific properties of the meta-material structure. Therefore a 3D printed fluidic interface is a completely embedded responsive interface.

Analogue

A 3D printed fluidic interface acts as an analogue, embedded system, which is driven by liquid material. It operates without the need for any external or internal electronics.

Dynamic visual appearance

In order to design for dynamic visual appearance, it is key to have a basic understanding on how humans visually perceive objects and materials within the world surrounding them. Human visual perception is a difficult process to understand, full of ambiguities [56], [10]. In this section, a basic explanation of human visual perception is provided, after which a framework for object appearance properties is drawn from literature. This framework describes a set of visual parameters which can be manipulated in time within the design space to create different dynamic material appearances.

Human visual perception

Following the basic understanding of human visual perception, it is known that a 2D image of the world is projected on the back of our eyes. This is done as light is focused on the cones and rods in the retina. This sensory visual data is transmitted as electrical impulses towards the brain via the optic nerve [1] In fact, our visual image is a mental representation of the 3D world surrounding us based on this 2D projection (Figure 7). It is the brain that enables us to have a clear impression of the 3D world, by reconstructing the 'missing' information in these 2D projections [22], [56]. A constant 'play' takes place between what's 'real' in the 3D world and what is represented in our minds.

The mind can cover up for the 'missing' parts of information in the 2D-image to quite extend as humans do perceive depth. It is even reported humans are able to interpret mechanical properties of materials like stiffness or hardness quite adequately by only looking at it [23] [22]. Our brain gives meaning and interpretation to our visual senses, by categorisation amongst

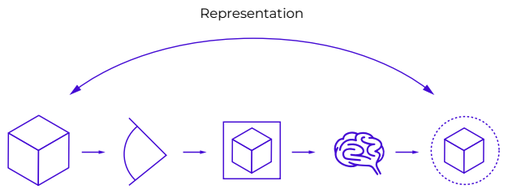

Figure 7: Basic process of human visual perception.

our sensory and semantic memories within the brain [55]. It is this mechanism which helps us act and define our actions in daily life. For example, we know when a banana is rotten by looking at its visual cues, or we avoid stepping on surfaces which appear to be slippery.

However, the main problem in understanding this process is that an infinite number of possible objects or scenes in the 'real' 3D world can arise from the same projected 2D image in our brain. This ambiguity can be experienced as visual illusions [10], [12]. In order to design for dynamic appearances, one must therefore understand which of the visual properties of objects are 'preserved' in the projection of a 3D object towards a 2D-image in our brain.

It must be understood that humans are only able to perceive the visible part of the electromagnetic spectrum as light, as shown in Figure 8. When looking at an object, we perceive the light which is reflected from the object. This is called the luminance (Figure 9).

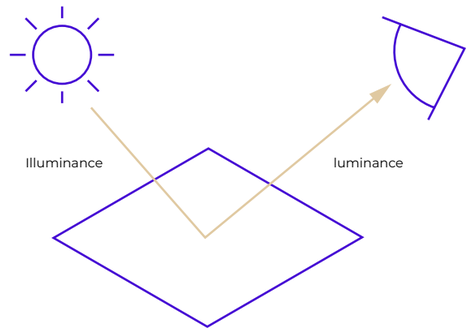

Figure 9: We perceive luminance of an object which is the reflected light of a surface.

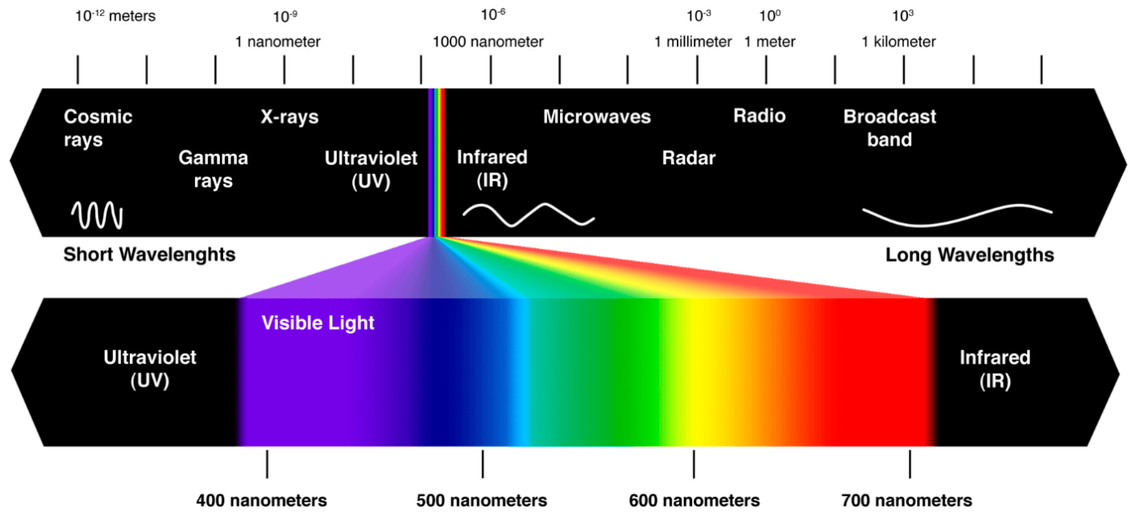

Figure 8: The visible part of the electromagnetic spectrum that humans are able to perceive as light.

Object visual appearance

But what characteristics make objects look the way they do? What parameters define the (dynamic) appearance of a 3D printed fluidic interface?

As described, the visual sensory information, or visual appearance, we perceive of an object are characterised by its luminance. However, the overall appearance of an object is subject to three main variables as described in [61] [22]:

- The object's shape
- The object's Illuminance
- The object's material

The object's shape includes visual information on the form of an object, such as that a football is a sphere. Secondly, the object illuminance is the projected light on an object. Illuminance has a wide variety of properties, including lighting directions, spectral properties and intensity. The light directions can be described as a set of layers as acknowledged by lighting architect Richard Kelly: ambient luminescence, focal glow and play of brilliants [26]. Different variations of these three layers result in other object appearances. For example, shiny objects illuminated by ambient light appear to be matt [61]. Additionally, illuminance spectral properties can also vary in their frequencies; when frequencies are not present in the illuminance, they can't be reflected by the object and won't be present in the luminance as well. This is the reason a blue object appears black when illuminated by red light. The third determining variable is the object's material, which includes the information of colour, reflectance, transparency and texture.

The goal of this research is to design interfaces with dynamic visual output which perform in multiple contexts (lighting conditions) and for different 3D-printed geometries, shapes and forms. Therefore, the object's shape and illumination are left out of scope. The dynamic visual appearance is a result of varying the material optical properties only.

Visual properties framework

Combining multiple explanations, theories and models for visual perception, a simple visual property framework is presented in Figure 10 grounded in literature [56], [61], [22], [93], [23], [12], [20], [62]. It includes a set of optical properties that describe a materials visual appearance.

Colour

- **Selective wavelength reflection**
  Colour by adsorption and reflection of specific frequencies.
- **Structural colour**
  Nanostructures interfering at light frequencies creating specific colour reflections.
- Fluoressence
  Specific materials which can absorb UV-light and emit visible light.

Reflectance

- **BRDF modes**
  The BRDF describes the scattering behaviour of light on a surface:
  - Forward scattering (glossy appearance) [62], [61]
  - Diffuse scattering (matte appearance) [62], [61]
  - Asperity scattering (velvety appearance)[62], [61]
  - Backward scattering (retro-reflective appearance) [9]

Light transmission

- **Transparency**
  The amount of light that can pass through a material without scattering
- **Translucency**
  he amount of scattering that takes place within the material.

Texture

- **Surface colour texture**
  Full-colour variations and patterns at the material surface.
- **Surface texture**
  Topographical variations at the material surface influencing light scattering and shadowing.
- **Volumetric texture**
  Subsurface scattering in transparent and/ or translucent layers and voxels within the material.

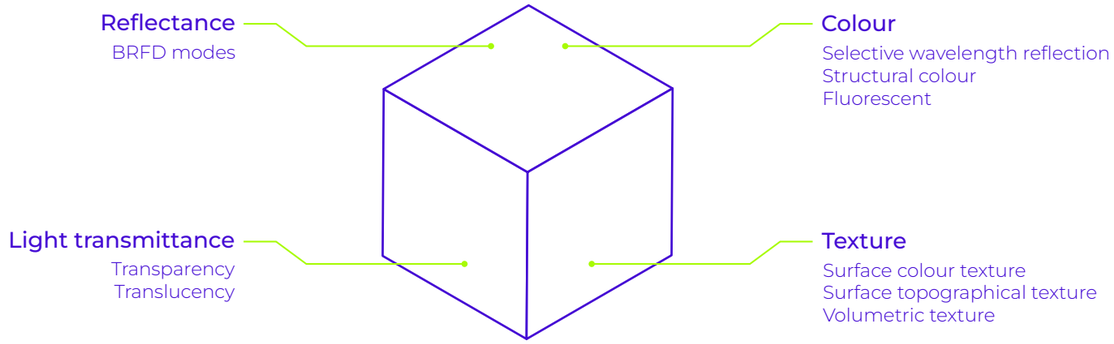

Figure 10: Visual properties framework.

Dynamic appearance

The optical properties from the framework has been validated for the possibility to be used as a parameter for dynamic appearance of 3D printed fluidic interfaces. The optical parameters which have been obtained from the framework are listed below:

- Dynamic Colour via selective wavelength reflection (one- or multidimensional)
- Dynamic fluorescent colour by making use of fluorescent liquids (one-dimensional)
- Dynamic transparency (one dimensional; transparent vs opaque)
- Dynamic translucency (one dimensional; clear vs cloudy)
- Dynamic colour texture at the surface (one or multi-dimensional)
- Dynamic volumetric texture (one or multi-dimensional)

The following optical parameters are excluded as they are subject to distinct tiny features which are not achievable within the printer's resolution (1200DPI). .

- Dynamic BRDF modes, for example, glossiness (one dimensional; matt vs glossy).
  Not achievable with 3D printing resolution.
- Topographical surface texture.
  Not achievable with 3D printing resolution

To design for dynamic visual output of responsive 3D printed fluidic interfaces, these optical parameters must be manipulated by an input trigger in a controllable and reversible manner.

Basic architecture for 3D printed fluidic interfaces

The basic architecture of Venous Material as shown in Figure 5, 5 [54], describes the design space of 2D fluidic interfaces which are triggered by mechanical deformation. Introducing multi-material 3D printing as a manufacturing tool has the ability to expand the design space of fluidic interfaces with new opportunities for 3D geometry and shape, encoded computational logic and in-output configurations. To define this extended design space, an expanded basic architecture for responsive 3D printed fluidic interfaces is presented in Figure 11.

Besides the additional possibilities of 3D printing, other liquid materials and output configurations have been explored in literature. Although these configurations are not further explored within this research, they are shown in Figure xx, to complete the total design space for fluidic interface.

The architecture is both an explanatory tool, and a configuration tool for developing new 3D printed fluidic interface concepts. Due to the novelty of this research domain, the architecture is presented as a living document, grounded by examples found in literature. It is intended that this architecture can be adjusted and/ or expanded on new findings during future research.

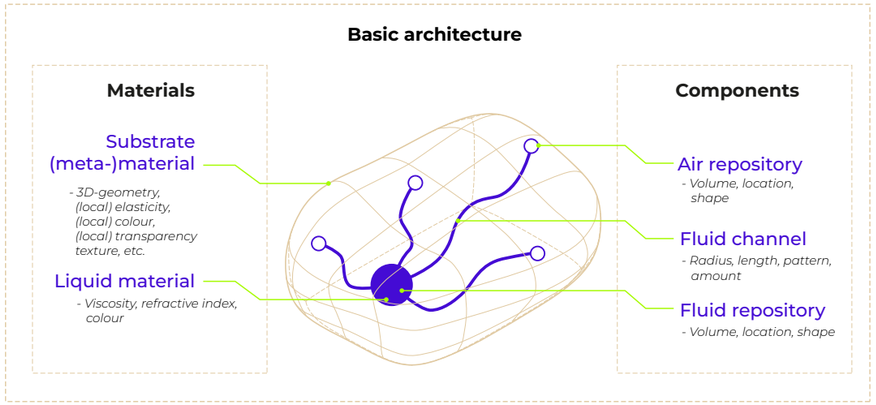

Figure 11: 3D printed fluid interface basic design architecture.

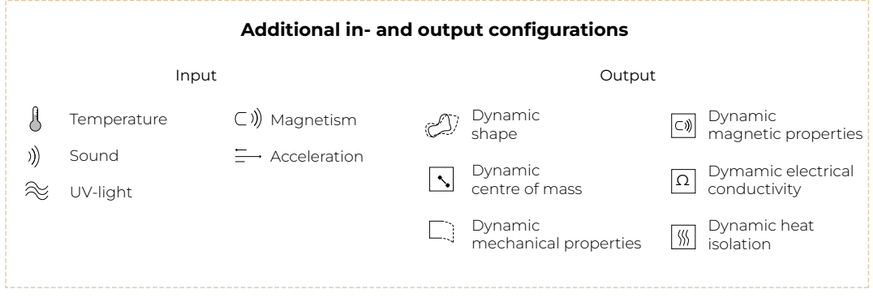

Figure 12: 3D printed fluid interface basic design architecture.

Materials and components

A 3D printing fluidic interface is composed of two main materials. The Substrate (meta) material and the Liquid material. The Substrate Material is a heterogeneous material, also known as a meta-material composed of various (3D-printed) mono-material structures. Cavities in this Substrate material form the three Circuity components; Air repositories, Fluid channels and Fluid Repositories. Together these components define the internal fluidic structure. The Liquid material flows through this structure acting as a sensor, driver and actuator of the responsive behaviour.

The responsive behaviour of the interfaces is encoded within the geometry of the internal fluidic structure and properties of the Substrate (meta)material. For example, various dimensions of Air repositories and Fluid channels can result in different sensitivity and temporality, and coloured or transparant voxels can interact with displaced liquid to create visual output variations.

The substrate (meta-)material

As described, a multi-material 3D printed (meta)material, with cavities.

Liquid material

The liquid material flows through the Fluid repositories and Fluid channels. It can be used in multiple manners to sense, drive and actuates the responsive behaviour of 3D-printed fluidic interfaces:

- Acting as a sensor and display by displacement (e.g. coloured fluid displacement, as presented in [54])
- Acting as a sensor and display without displacement (e.g. thermo- or photochromic dyes changing colour).
- Acting as a (non-coloured) hydraulic network to trigger (coloured) mechanical structures (e.g. displacing or manipulating rigid parts within a flexible substrate material, as presented in [74]).

Logic operators

Logic operators can manipulate and structure the liquid flow inside 3D-printed fluidic interfaces adding towards the possibilities for encoded computational logic. Although within this research the application of logic operators is not further explored multiple examples can be found in literature:

- Mechanical valves (externally operated) [43]
- Pressure valves (operated by pressure) [71]
- One-way valves (allow flow in 1 way) [71]
- Fluidic capacitors (store kinetic flow) [71]

Flow primitives

The basic flow primitives which can be used in different patterns. By combing these patterns in specific geometries, effects such as colour overlay, mixing and interweaving channels can be created.

Substrate (meta-)material structures

PolyJet 3D printing allows for complex geometries and variations in local mechanical and optical properties on a voxel level [18], [29] .This allows for two types of meta-material structures which can be used in 3D-printed fluidic interfaces. Mechanical structures are printed using variations in local elasticity. Optical structures are printed as full-colour or transparent voxels. When designed in specific configurations they can create dynamic visual output or computation logic when interacting with Liquid material.

In- and output

This research focuses on 3D-printed fluidic interfaces with dynamic visual output triggered by actuation pressure. However, other types of I/O configurations found in literature are shown in Figure 12. The dynamic visual output variations in the basic architecture are obtained from the visual property framework presented in figure 10. They are listed as:

- Dynamic Colour by selective wavelength reflection (one- or multidimensional)
- Dynamic transparency (one dimensional; transparent vs opaque)
- Dynamic translucency (one dimensional; clear vs cloudy)
- Dynamic colour texture at the surface (one or multi-dimensional)
- Dynamic volumetric texture (one or multi-dimensional)

Temporal parameters

The temporal form of 3D-printed fluidic interfaces can be tuned for sensitivity and response time by varying the dimensions of the Air repositories and the radius of the liquid channels combined with the viscosity of the Liquid material. Within Section 6 the specific underlying relationships and parameters are presented for tuning 3D-printed fluidic interfaces.

04

Exploration of design space

4 Exploration of design space

The design space for 3D printed fluidic interfaces presented in the previous section is explored by multiple cycles of iterative and rapid prototyping within multiple directions. Various optical principles have been explored to create dynamic visual output. The process of rapid and iterative prototyping simultaneously gained insights into both the optical performance and optimisation of the 3D printing workflow for fluidic interfaces. After validation, one of the directions is chosen for further development within this research.

Protoyping directions

Refractive liquid

The prototype shown in Figure 13 explores dynamic colour, transparency and/ or translucency as visual output. The prototype is primarily used to explore visual output, as it does not act as an embedded interface and is in need for an external operator (syringe). The output is caused by the difference in refractive index for different materials; 3D printed Vero, injected Cleanser and air. Using a liquid printing workflow (described in section 7), a cavity is printed between a coloured (Magenta) and Clear layer 3D printed substrate material. Although not explored within this research, Polyjet printing allows for multicolour textures as a background layer within this interface configuration. After printing, the cavity is cleared from the liquid support material.

The dynamic output is actuated by injecting a non-coloured transparent liquid (Cleanser) through one of the inlets with a syringe. The Cleanser material has a refraction index close to the Vero materials (Clear and Magenta). When the Liquid material is injected, total internal refraction is approached between the material layers. This means no scattering of the incoming light is present at the different material surface interfaces within the interface. This causes the magenta-coloured layer to appear at the top surface of the part as dynamic colour. Subsequently, it increases transparency and degreases the translucency of the part. This effect can be reversed by removing the Cleanser material with negative pressure created by the syringe, replacing it with air which is sucked in via a secondary inlet.

At this point scattering of the incoming light does appear between the material surface interfaces of air and the printed layers due to the larger difference in refractive index.

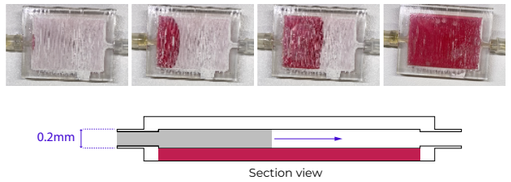

Figure 13: Refractive liquid prototype making use of the difference in refractive index for air and Cleanser material.

Touch- sensitive refractive liquid

The same principle of Total Internal Reflection is used in the prototype shown in Figure 14 However, for this prototype, a flexible layer of Agilus is printed on top of a fully encapsulated (and simultaneously printed) layer of Cleanser material. After printing, a small volume of air is injected into the liquid cavity using a syringe with a thin needle. The puncture hole is sealed with a droplet of CA-glue. The optical principle driving the visual output of this prototype is identical to the previous prototype. However, the encapsulated 'air bubble' can be displaced by applying mechanical pressure on the flexible Agilus material. Therefore this prototype acts as an embedded responsive fluidic interface, triggered by touch input.

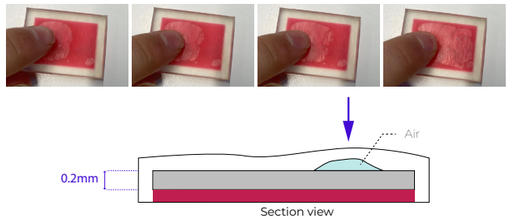

Figure 14: Touch-sensitive embedded refractive liquid prototype making use of the difference in refractive index for air and Cleanser material.

Gravitational liquid

Using Air printing (Appendix B as a workflow for manufacturing, a series of liquid channels are printed on a white background layer in which dyed water is injected (50% volume of the channel). The channels are then sealed on both sides by a thin sheet of Polystyrol with CA-glue. The result is an embedded responsive interface in which a coloured fluid is displaced in lineair motion, triggered by the orientation and movement of the part as shown in Figure 15. A surprising side effect of this prototype is that the fluid appears to be displacing with 'anti gravity' movement as explained in Figure 15.

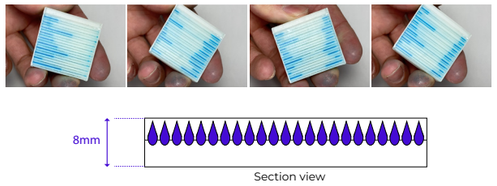

Figure 15: gravitational embedded responsive interface with dynamic colour by displacement of coloured liquid, triggered by orientation and movement of the part.

Fluidic lenticular lenses

Zeng et al. have presented a workflow for 3D-printing objects with lenticular lens surfaces creating viewpoint-dependent dynamic visual appearance [92]. Based on this design, a similar interface is explored using Clear liquid cleanser material to create dynamic cylindrical lenticular lens arrays shown in Figure 16. Injection or removal of the cleanser material within semi-circle-shaped cavities printed in clear Vero material can activate or de-activate the cylindrical lenticular lenses. The semi-circle cavities are printed using liquid printing as a manufacturing workflow.

Based on the principle of lenticular printing [40], colour textures in the substrate material underneath the lens array can be displayed dynamically, dependent on the viewpoint. However, the ability to activate and de-activating the lens arrays via liquid flow creates an additional input source which allows different textures to be displayed for the same viewpoint. Within the prototype, these background colour textures are printed on a piece of paper and placed underneath the lens. It is assumed multi-colour Polyjet 3D printing can integrate these backgrounds into a single 3D-printed part.

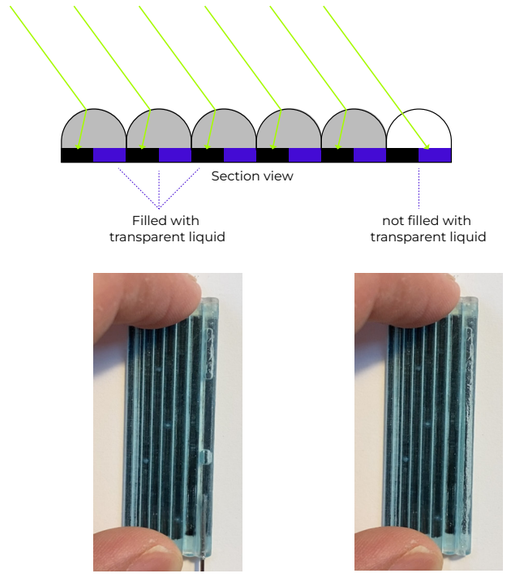

Figure 16: Fluidic lenticular lensen which can be activated and de-activated by liquid flow.

Coloured liquid displacement

Figure 17 shows a set of spherical prototypes which explore embedded responsive fluidic interfaces with dynamic colour, triggered by mechanical deformation. Based on the concept of Venous materials [54], the dynamic visual output is driven by displacing coloured liquid in an encapsulated fluidic structure. The displacement of the fluid is a result of increased pressure in the system by mechanical deformation (Figure 18). The cavities which form the fluidic structure are printed using a liquid printing workflow and are modelled using Rhinoceres and Grasshopper. The printed liquid support was sucked out of the cavities with a syringe, using a needle, after which coloured liquid is injected into the centre liquid repository.

The prototypes explore various fluidic structures which differentiate in the number of channels, channel radii and with and without integrated Air repositories. It was found that channels were very difficult or impossible to clear from printed liquid support via a single inlet at the centre. Additionally, it was found that for samples without Air repositories it was very hard to displace the liquid material. Besides, all of the prototypes were subject to printing imperfections such as delamination, poor surface quality and sinking of the substrate material as described in section 7. However, various prototypes showcase the intended behaviour for numerous channels within the fluidic structure, showcasing its potential.

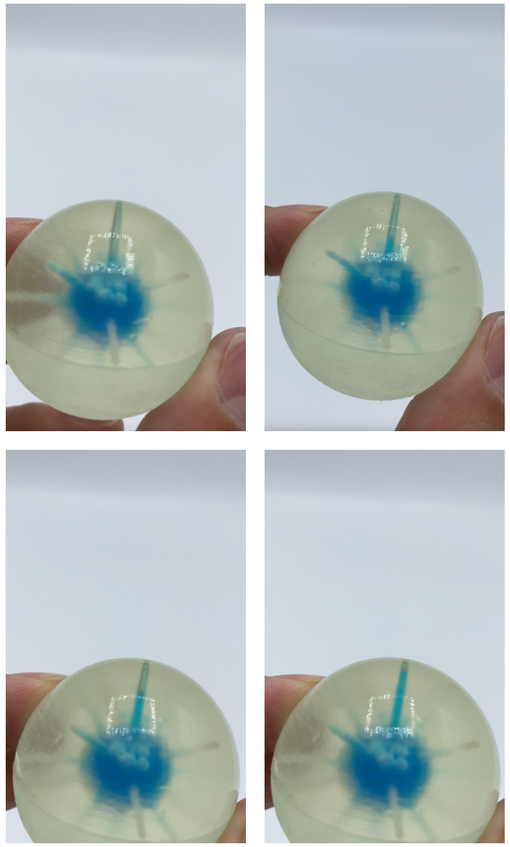

Figure 18: Displacement of liquid in a sample when squeezing.

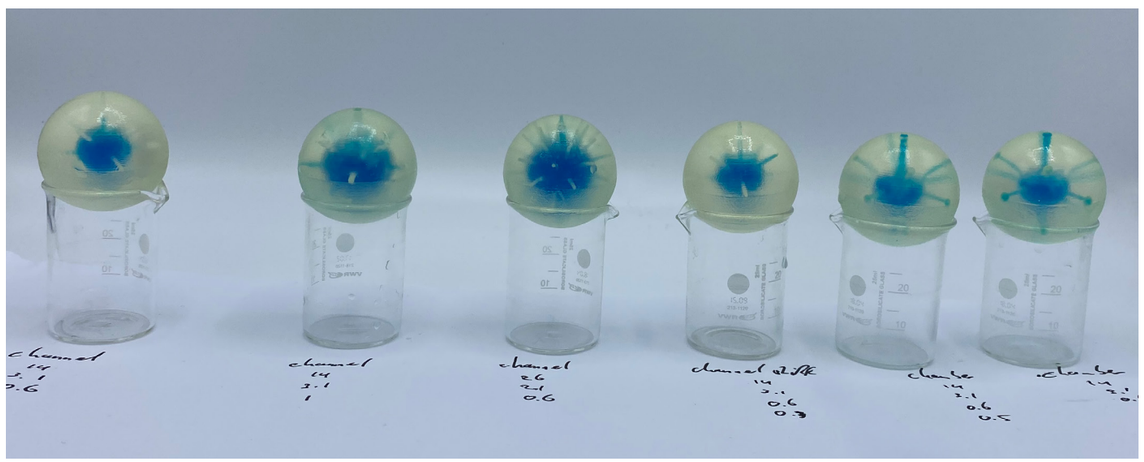

Figure 17: Samples for coloured liquid displacement.

Validation of directions

After multiple iterative prototyping cycles the resulting samples have been validated for their ability to provide the most valuable scientific knowledge within the scope of this research after which, one of the directions is chosen for further development.

Each of the directions showcases promising possibilities for 3D-printed fluidic interfaces. The use of differences between refractive index and fluidic lenticular lenses provides novel, unexplored concepts for responsive fluidic interfaces. However, apart from the touch sensitive-sample shown in Figure 14, these samples do not meet the requirements presented in section 3, as they are underdeveloped as a completely embedded responsive interface. These prototypes act as a level two integrated in-output interface as shown in Figure 3, section 2 which are in need of external fluid flow controllers (syringe). Besides, the concepts of refractive liquids and fluidic lenticular lenses are both reported to be heavily subject to material surface interface quality as presented in section 7. At this point in the research this was still a major limitation for 3D printing fluidic interfaces. .

The concept of displacing coloured liquid by mechanical deformation as shown in Figure 18 showed to be less subject to material surface interface quality. The dynamic visual output was more noticeable even with poor surface qualities. More importantly, it can be concluded that all of the explored directions make use of displacement of the liquid material in order to drive the responsive behaviour, and this principle is the main driver for the latter concept.

Overall, it was experienced that iterations for the printing workflow with the goal to achieve better printing properties are a very time-consuming process. To achieve quantifiable results, multiple steps of parametric testing must be performed (see Appendix B for examples).

Reflecting on these insights and the given time frame of this research, the logical next step for 3D-printed liquid interfaces was to develop further into the direction of coloured liquid displacement. Firstly it allowed to elaborate on previous research [54], and was less subject to printing quality, which makes it more viable to achieve sufficient results within the given time frame. Secondly, and more importantly, exploring the embedding and encoding of programmable liquid displacement in various patterns and fluidic structures could provide valuable knowledge for all of the prototyping directions. Ultimately, this could provide a workflow for manufacturing embedded responsive 3D fluidic interfaces which can be used to further explore the other direction as embedded interfaces in future research.

Further exploration of displacing coloured liquid

The concept of displacement of coloured liquids within 3D printed fluidic interfaces to create dynamic visual output was further explored via multiple 3D printed samples including:

- A set of domes exploring various flow patterns for different visual output and experiences. .
- A set of linear embedded responsive fluidic interfaces.

Domes

The main goal of these samples is to explore various types of patterns and geometries for the internal fluidic structures to design for different visual outputs and experiences. Previous samples as shown in section xx were heavily subject to printing imperfections and difficult to be cleared from internal liquid support. Since these samples focus on the validation of visual output, it is chosen to separate the in- and output functionality into different components connected via inlets in the 3D printed part as shown in Figure 18.

The patterns include a spiral surface pattern shown in Figure 18 which is intented to showcase a simple and predictable flow of liquid, a surface differential grow pattern which is intended to showcase a more organic flow of liquid with a higher surface (colour) density and a volumetric differential growth pattern which is intended to showcase a more unpredictable and organic flow of liquid with higher volumetric (colour)density. The spiral pattern was printed in various channel radii as shown in Figure 18.

The explored patterns were modelled using the Grasshopper environment within Rhinoceres, for both of the differential grow patterns the plugin Kangaroo has been used. At this point in the research, the samples were printed using the voxel-based support material as presented in Section 7. Furthermore, the fabrication process of these samples also provides insights which led to the fabrication pipeline and limitations as presented in Section 5.

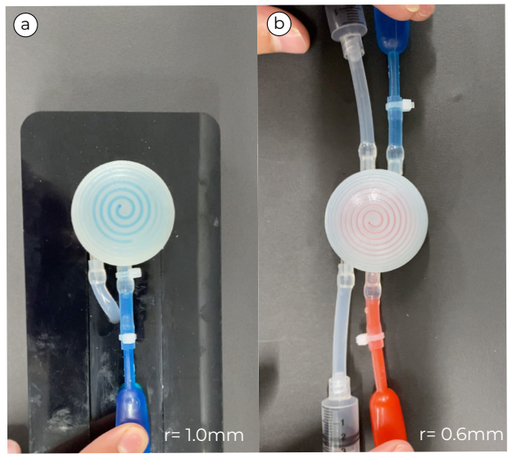

Figure 18: Spiral pattern for various radius.

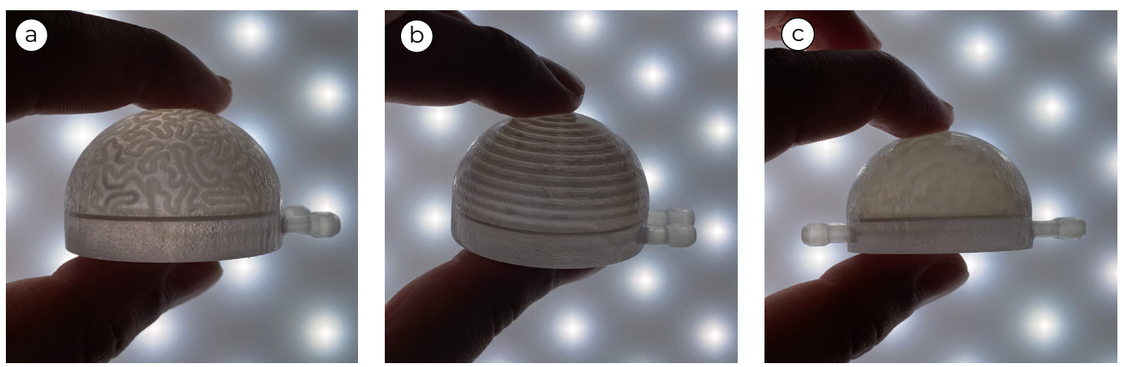

Figure 19: Various flow patterns, before coloured liquid injection (a) surface differential growth pattenr, (b) spiral pattern, (c) volumetric differential growth pattern..

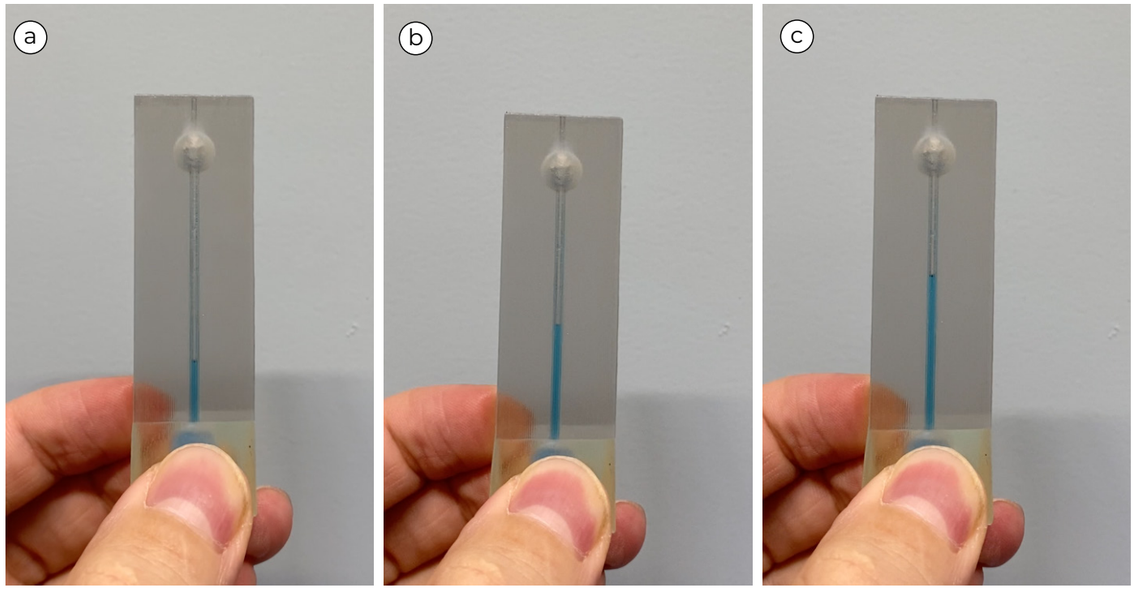

Figure 20: Fluid discplament within multi-material embedded interfaces, for gradually applying pressure. (a) low pressure, (b) medium pressure, (c) high pressure. .

Important insights

These samples were used as a demonstrator for interviewing multiple experts on the experiential qualities of 3D printed fluidic interfaces. An overview of the main insights of these interviews are presented in section 9.

It was found various channel diameters resulted in different response times for the interfaces affecting the temporal form and overall experience.

Linear embedded interfaces

To explore the possibilities to embed en encode the computational logic into single 3D-printed fluidic interfaces with substrate meta-material, a set of linear fluidic interfaces have been printed with filling holes for post-processing as described in section 8.

Important insights

It was found that to clear internal fluidic structures completely from voxel-based support material, the fluidic structure needs a minimum of two filling holes. This allows the internal structure to be flushed after voxel support material has been sucked out with a vacuum as described in section 8. The sample with only one filing was not able to be cleared from internal voxel-based support material.

05

Design and fabrication pipeline

5 Design and fabircation pipeline

The design and fabrication pipeline is divided into three phases: Design and simulation, Fabrication, and Post-processing. It starts with the design and simulation of the fluidic structure, followed by a fabrication process based on Polyjet 3D printing. Finally, parts are cleaned and Liquid material is injected inside the geometry. An overview of this process is shown in Figure 21.

Design and simulation

The design space for 3D printed fluidic interfaces is very broad allowing a variety of flow primitives. However, a few basic design rules must be taken into account:

- Minimum separation of liquid material along X/Y-axis = 0.4mm [48].
- Minimum separation of liquid material along Z-axis = 0.2mm [48].
- The fluidic structure can't intersect with itself.
- For dimensioning tiny features or channels (<0.5mm) the printer resolution and layer height should be taken into account.

A specialised simulation tool is developed in Rhinoceros and Grasshopper in which 3D fluid interfaces can be imported or designed. It can simulate the flow response and fluid distribution for dynamic pressure force input via Arduino, and is subjective to different adjustable parameters. The simulation tool allows for visualisation and validation of the sensitivity and visual output of a fluidic interface, before going into manufacturing. The implementation and grounding of the tool are presented in section 6.

Fabrication

Voxel slicing

A voxel-based workflow is used for 3D-printed fluidic interfaces as described by Dourovski et al. [18] which allows for specific printing capabilities which will be explained section 7.

3D printing

3D fluidic interfaces are printed using the Liquid Printing mode and voxel print utility available in the Research Package of Stratasys [76]. For printing internal cavities, a voxel-based support material composed of 55% support to 45% cleanser is used as a support structure
.

Post-processing

After the part is printed, External support material (SUP706) should be removed with a waterjet. The internal fluidic structures are drained and rinsed with a vacuum pump and water injection, removing the voxel-based support material. Subsequently, the liquid material of choice is injected into the fluid repository after which the part is sealed with clear (flexible) UV-glue.

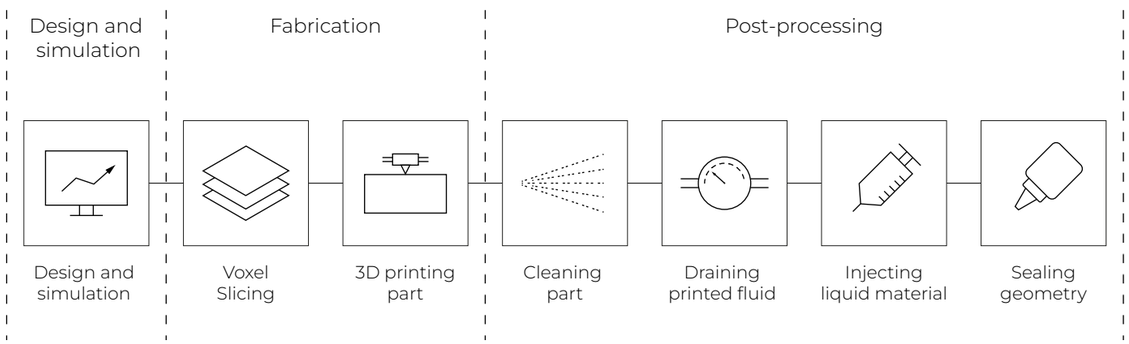

Figure 21: Design and fabrication pipeline for 3D printed fluidic interfaces.

06

Design and simulation

6 Design and simulation

A design and simulation tool is developed in Rhinoceros and the Grasshopper environment to visualise and experience the behaviour of 3D fluidic interfaces. It simulates fluid displacement in relation to the actuation force. Via a set of adjustable design parameters, the user is able to change the interface geometry and sensitivity, allowing designers to iterate on their designs even before manufacturing.

To grasp the real-life experience of dynamic interaction with a fluidic interface, users can interact with the simulation by means of a pressure sensor (input) connected via Arduino, and see real-time fluid flow (output). A screenshot of the simulation in action is shown in Figure 22. The complete simulation tool is available in Appendix D.

User workflow for design and simulation tool

Plan and design

Users can design a fluidic interface within both Rhinoceros and the Grasshopper environment by constructing two elements; the outer shape and a set of channel curves.

Outer shape

A Brep or Mesh body is used to describe the outer shape of the fluidic interface which is printed using the substrate material.

Channel curves

Within this body, multiple curves can be modelled to describe the channel geometry of the fluidic interface.

After the Outer shape and Channel curves are assigned within Grasshopper, it parametrically generates the fluidic geometry, including the Liquid repositories, Liquid channels, and Air repositories based on a set of adjustable parameters.

Adjust parameters

Next, a set of parameters can be adjusted to alter the fluidic geometry by means of a slider. Channel radius r: to set the channel thickness and sensitivity value R: to control the fluidic interface sensitivity. Besides, the normal distance of the actuation force h can be adjusted by changing the geometry of the channel curves.

Apply pressing force

To visualise the fluid flow of the fluidic interface, a pressing force must be initiated. The user can either choose to use a slider for input force, which displays static fluid flow, or use a pressure sensor connected via Arduino to display real-time visual feedback.

Simulate and display

To simulate, the user must enter the render preview mode within the Rhinoceros viewport. Altering the settings and environment of the viewport can result in a more realistic render. During the simulation, and whilst interacting with the fluidic interface, it is still possible to adjust the parameters of the model. Users can see real-time updates of twwwclear heir alterations and make iterations of their design.

Simulation workflow

Mor et al. [54] have presented a design and simulation tool for tangible 2D fluidic interfaces. Since both 2D and 3D fluidic interfaces are based on the principle of fluidic movement caused by deformation of a flexible substrate material, the workflow and fundamental physics for the 2D tool have been used as a starting point for the development of a new 3D simulation model.

In addition to the functionalities as presented in [54], the newly developed simulation tool also allows for real-time tangible interaction via pressure sensors. In order to create a smooth and real-life user interaction, the run-time of the simulation had to be minimised. Therefore the iteration algorithm as used in [54] is substituted for a direct numerical method, using an equilibrium equation to calculate the fluid flow. The complete simulation workflow is shown in Figure 23.

a

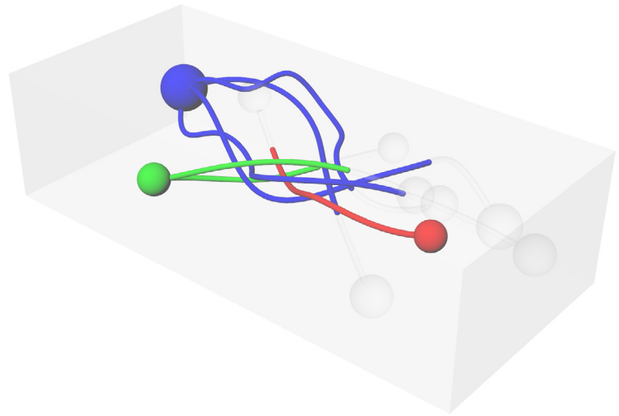

b

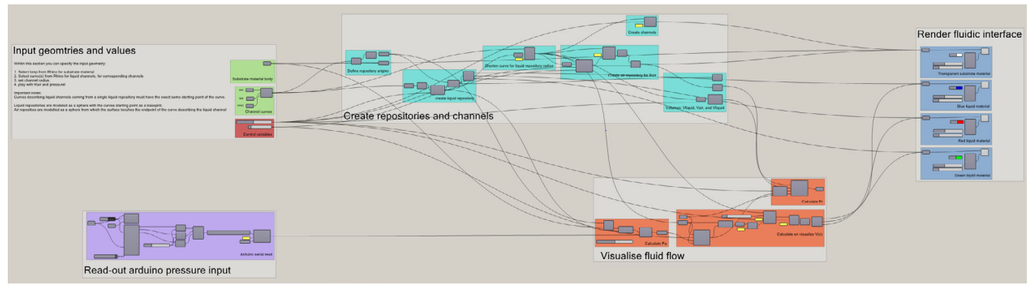

Figure 22: Screenshot of the simulation tool in action. Displaying fluid flow in 3 colours, situated in 3 liquid repositories.

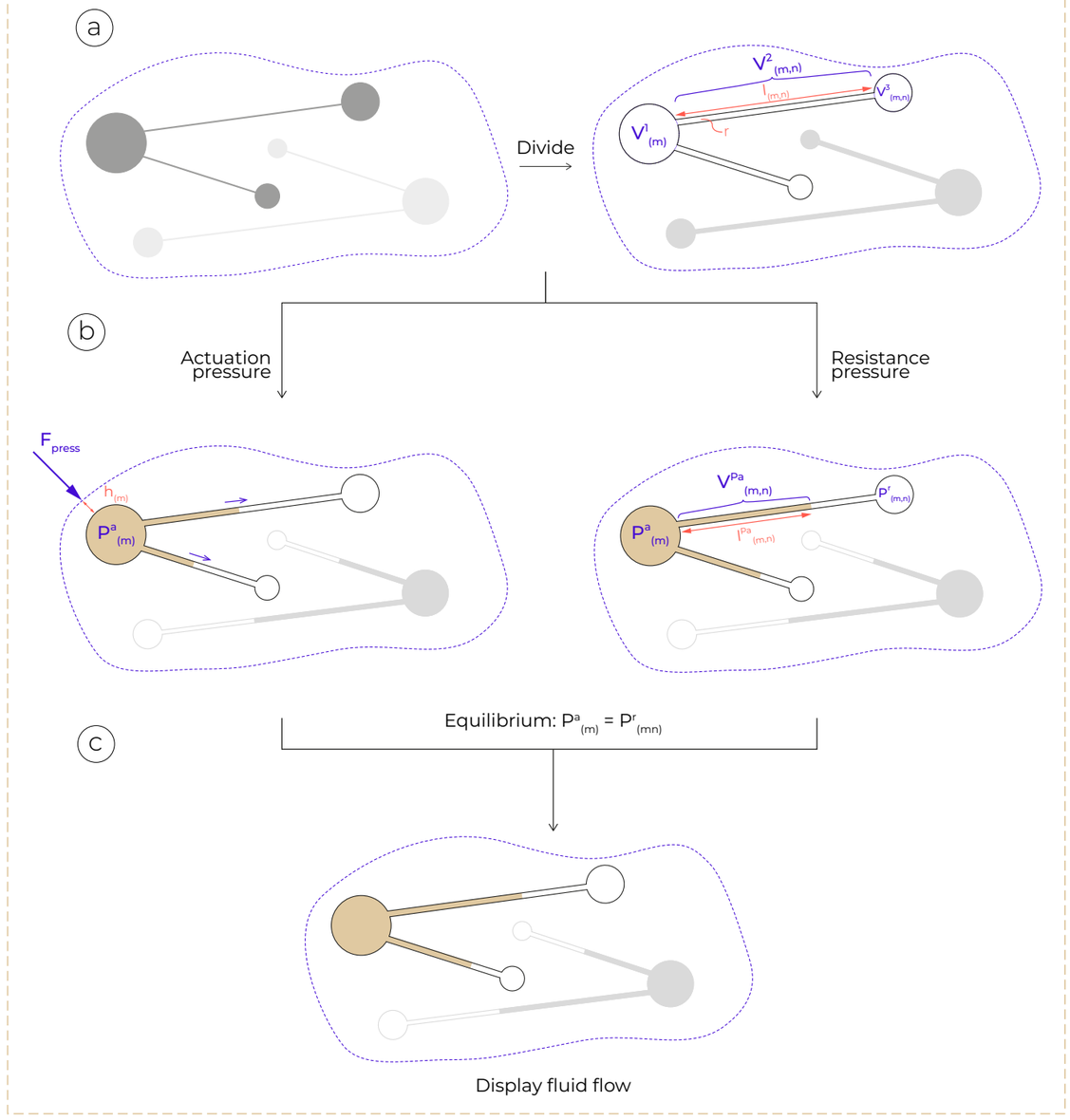

Figure 23: Simulation workflow. (a) Division into volumes with corresponding lengths. (b) Calculation of actuation pressure and resistance pressure. (c) Calculate flow map based on equilibrium.

Division of repositories and channels

First, the fluid repositories, fluid channels and air repositories are divided and stored in multiple lists. The fluid repositories are described by (m); the index of the list. Each of the channels and corresponding air repositories are described by (m,n): in which m is the index of the list, and n is the index of the list item, as shown in Figure 23 (a).

Calculation of actuation pressure

Next, the actuation pressure Pa is defined to evaluate the increment in internal pressure caused by the applied pressing force Fpress (Figure 23(b)). For calculating Pa the following assumptions are made:

Since the actuation of the fluid interfaces is caused by pressing the liquid repository, it is assumed that in most cases the pressing force Fpress is applied at the surface of the part, at the closest point from the liquid repository and normal to its centre point. It is assumed the internal pressure throughout the fluid in the repository and the channels is equal, as they are connected and the liquid material is an incompressible substance.

A computational model is used to characterise the relation between Pa and Fpress. First, the proportional relation of Pa to Fpress is inferred. Then, a Gaussian factor is introduced to describe the decay of the applied pressing force due to the plasticity of the substrate material (Agillus30). The integrated computational model is shown in Equation (1), in which kp is the proportional coefficient, h(m) is the distance from the point of applied pressing force to the liquid repository and is the decay coefficient.

$$P^a_{(m)} = k_p F_{press} e^{-\sigma h_{(m)}} + P_0 \quad (1)$$

Define resistance pressure

Then, the resistance of the fluidic structure to the fluid flow is evaluated by defining the resistance pressure P(m,n)r. This resistance is caused by an increase of internal pressure when the fluid flows into the structure, compressing the encapsulated air inside the air repository and the remaining channel(Figure 23 (b). The internal pressure Pr(m,n) is defined using Boyle's Law (2). By substitution of V2(m,n) (3), V3(m,n) (4) and VPa(m,n) (5), equation (6) is obtained. Within this equation, R is the volume ratio factor V2(m,n): V3(m,n), l is the total length of the channel and lPa is the length of the displaced fluid (fluid flow).

$$P_0(V^2_{(m,n)} + V^3_{(m,n)}) = P^r_{(m,n)}(V^2_{(m,n)} + V^3_{(m,n)} - V^{Pa}_{(m,n)}) \quad (2)$$

$$V^2_{(m,n)} = \pi l_{(m,n)} r^2 \quad (3)$$

$$V^3_{(m,n)} = R\ V_2 \quad (4)$$

$$V^{Pa}_{(m,n)} = \pi l^{Pa}_{(m,n)} r^2 \quad (5)$$

$$P^r_{(m,n)} = \frac{P_0 l_{(m,n)}(R+1)}{R l_{(m,n)} - l^{Pa}_{(m,n)} + l_{(m,n)}} \quad (6)$$

Calculation of liquid flow

The final goal of the simulation is to determine the magnitude of fluid flow in relation to the applied actuation force (Figure 23 (c)). Therefore it is assumed the fluid will continue to displace until the internal pressure within the system reaches an equilibrium state as described in Equations (7) . Therefore Pr(m,n) can be substituted for Pa(m) in equation (5), resulting in equation (8). Finally, this equation is rewritten for lPa(m,n).

$$P^r_{(m,n)} = P^a_{(m)} \quad (7)$$

$$P^a_{(m)} = \frac{P_0 l_{(m,n)}(R_{(m)}+1)}{R_{(m)} l_{(m,n)} - l^{Pa}_{(m,n)} + l_{(m,n)}} \quad (8)$$

$$\begin{cases} l^{Pa}_{(m,n)} = \frac{-l_{(m,n)}(P_0 R_{(m)} - P^a_{(m)} R_{(m)} + P_0 - P^a_{(m)})}{P^a_{(m)}} \\ P^a_{(m)} = k_p F_{press} e^{-\sigma h_{(m)}} + P_0 \end{cases} \quad (9)$$

The final calculation of the fluid flow is shown in Equation (9). It calculates the fluid displacement lPa(m,n) for variables R(m), h(m) and the actuation force Fpress. Based on this equation, it can be concluded that the critical parameters affecting the magnitude of the fluid flow are: R(m)and h(m). This means that the magnitude of fluid flow is independent of the channel radius. However, it must be pointed out that this simulation is limited to displaying the final fluid displacement, neglecting latency (response time) and temporal behaviour of the interface. Based on the Hagen-Poiseuille law it is assumed the channel radius r and viscosity of the fluid η are indeed important parameters, as they affect the flow resistance.

Experimental validation

Experiments on actuation pressure

A quantitative experiment has been performed to validate the computational model for P(m) as presented in Equation (1) and estimate the undetermined coefficients kp and σ.

To test the actuation force, the sample is placed on a scale, underneath a cylinder which is held in place so it can move freely along the z-axis, as shown in Figure 24. By gradually placing weights on the cylinder, the pressing force is increased. A pressure gauge (Greisinger GMH 3100) is connected to a fluid repository in the sample using a needle. Through recorded video, the actuation force Fpress and internal pressure Pa have been noted for each instance of adding weight. This process is conducted and repeated two times for 4 samples with h(m)ranging from 5 to 20 mm with 5mm increments.

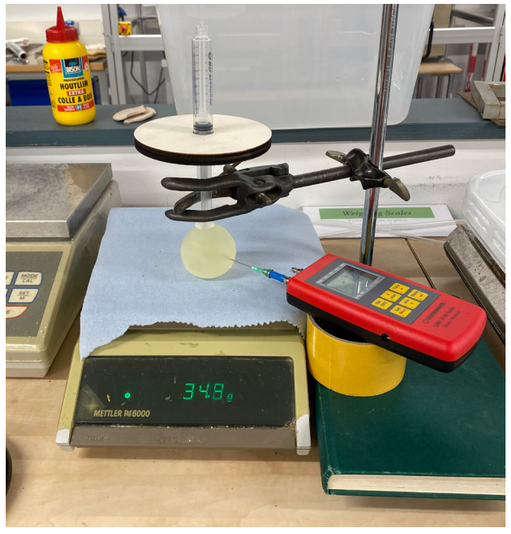

Figure 24: Test setup for the experiment on Pa.

ⓐ

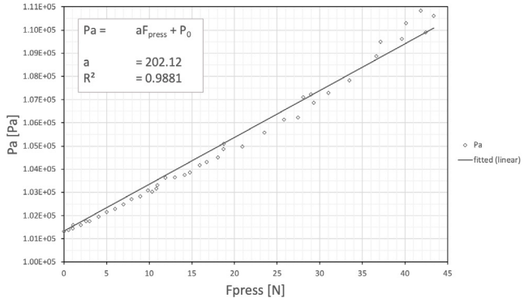

ⓑ

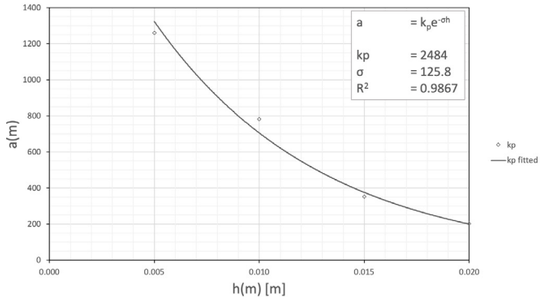

ⓒ

Coefficient estimate results

	Value	R^2
Proportional coefficient k_p	2484	0.9867
Decay coefficient σ	125.8	0.9867

R-squared values for experimental values fitted to model

Sample	R^2
Sample 1: h = 5[mm]	0.988
Sample 2: h = 10[mm]	0.990
Sample 3: h = 15[mm]	0.986
Sample 4: h = 20[mm]	0.973

Figure 25: (a) Fitting results for Pa - Fpress curve, from one of the samples with h=20 [mm]. (b) Fitting result for a(m)-h(m) curve for all of the samples. (c) Estimated results for undetermined coefficients in the computational model and R-square values for fitting with experimental values.

ⓐ

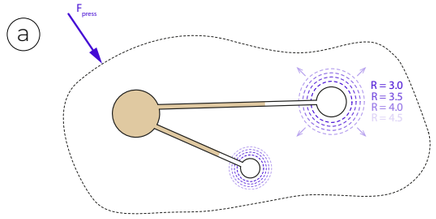

ⓑ

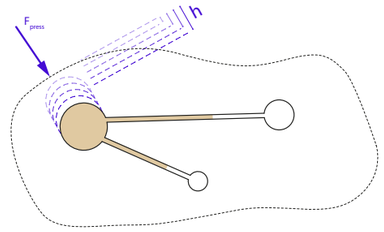

ⓒ

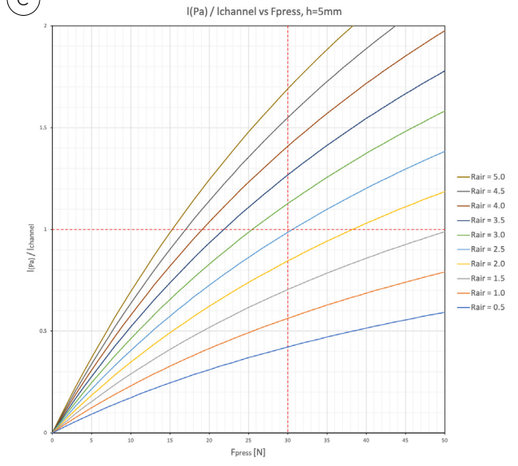

ⓓ

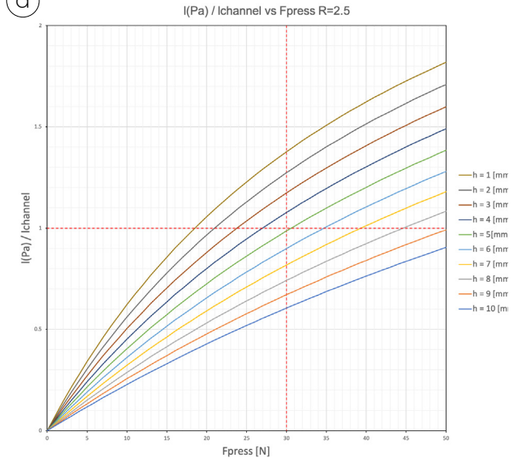

Figure 26: Plotted results. (a) Increasing R. (b) Increasing h. (c) Plotted results for increasing R. (d) Plotted results for increasing h.

For data analysis, two Pa(m)-Fpress curves have been obtained for each sample. To minimise error, the average of the two curves is calculated. This averaged curve is then fitted with a linear proportion model to estimate a for each sample within Pa(m)=a(m)Fpress+P0. Figure 25 (a) shows this process for one of the sample samples with h(m)=20 [mm].

Next, a continues a(m)-h(m)curve is obtained by combining the results of each sample. Finally, this curve is fitted with a exponential regression model, to estimate kp and in equation (1) as shown in Figure 25 (b).

A quick validation of the model shows that all of the experimental curves fit well with the computational model, with a high R-square, the results of the experiment are shown in Figure 25(c) .

Evaluation of the effect of of R(m) and h(m) on fluid flow

A tool within Excel is created to plot the effect of R(m)and h(m) for fluid displacement (Appendix E). This tool helps designers to determine the initial values of the dependent variables when designing and simulating 3D printed fluidic interfaces. The tool is adjustable for the parameters Fpress (max) and h(m). For typical applications in which the actuation force is applied with a fingertip, Fmax is advised between 15-35 [N], within the range for maximum voluntary (comfortable) fingertip force [44].

To showcase the amount of displacement, a displacement factor is used on the y-axis; dividing the displacement length by the total channel length. The plotted results are shown in Figure 26. It can be concluded the fluid flow has a nonlinear relation with Fpress, with decreasing sensitivity over Fpress. This means that the further a fluid flows within a fluidic interface, the more pressure must be applied to generate the same fluid displacement.

Designers can iterate on their designs by tuning the sensitivity of a fluid interface. Interpreting the plotted results, it can be concluded that to to increase the sensitivity of a fluidic interfaces one should increase R(m) or decrease h(m). Which of the two approaches is more suitable, depends on the variations and requirements of the design of that specific fluidic interface.

Evaluation of pressure sensor sensitivity

3 individual Interlink Electronics FSR 402 force-sensitive resistors (FSR) are used to measure pressing force to interact with the simulation. The FSRs are connected to an Arduino Uno which is implemented in Grasshopper using the plugin Firefly. The connection circuit of a single FSR is shown in Figure 27. The data sheet of the FSR is available in Appendix F. For the implementation of the sensor the integration guide [31] provided by the manufacturer is used.

The FSR has a force sensitivity range of 0.1-100 [N]. Since the pressure force of a fingertip ranges from 0-35 [N][44], the pressure sensor is used in combination with a 10KΩ measuring resistor to provide for the right sensitivity range, according to Figure 28.

For characterisation of the sensor, the relation for Fpress and the SerialRead [V] value of the Arduino must be determined.

Within the datasheet of the sensor the Vout value is given as the following equation, in which Vin = 5V (operating voltage of the arduino), and Rm=10k (as described) (10):

$$V_{out} = \frac{R_m V_{in}}{(R_m + R_s)} \quad (10)$$

Within literature the relation for Rs and Fpress has been characterised for this specific brand FSR based on a set of data points taken from the datasheet [19]. When rewritten for Fpress in [N] instead of [g], it is given as equation (11):

Substituting equation (11) in equation (10), and

$$R_s = 22388.89470 * F^{-0.9585} \quad (11)$$

solving equation (10) for Fpress gives the final equation (12), which is used in the simulation to determine Fpress based on the SerialRead [V] value of the arduino.

By characterisation of the FSR, it can be used

$$F_{Press} = 34544.20686 * \left(\frac{V_{out}}{R_m(V_{in} - 1 * V_{out})}\right)^{\frac{2000}{1917}} \quad (12)$$

within the simulation tool with an accuracy of +-10% [31]. For this application, this is within acceptable boundaries. However, for increased accuracy up to approximately 1% , a calibration process on the specific set of sensors used within this research can be performed as described in [19] and [31].

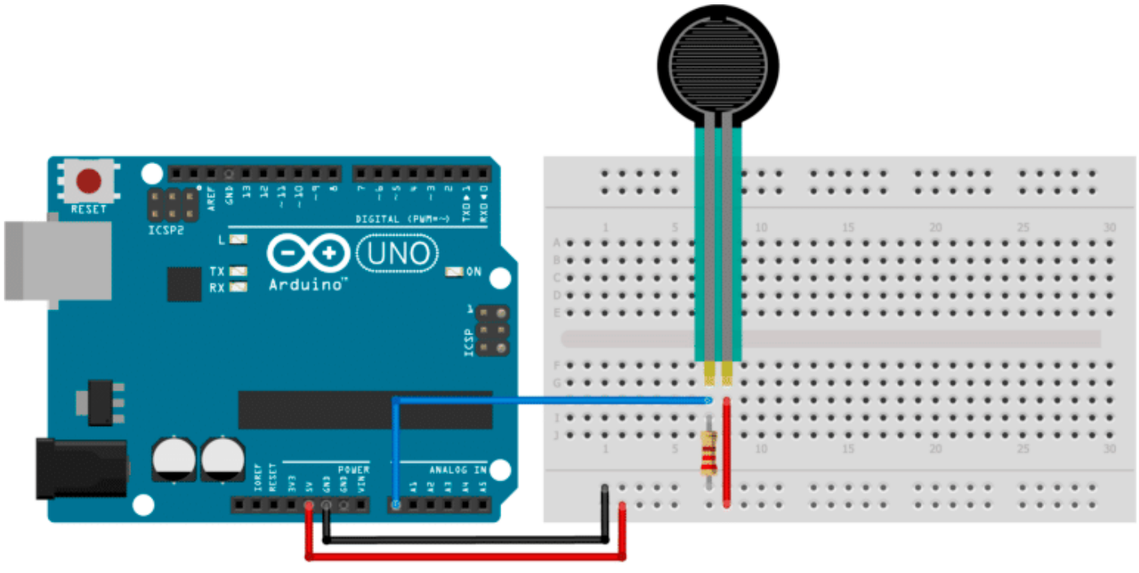

Figure 27 :Arduino connection circuit for a single FSR [11].

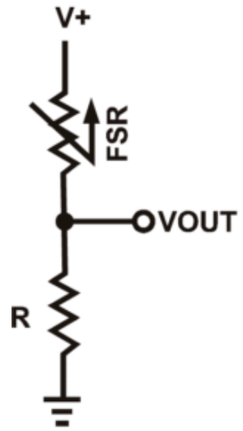

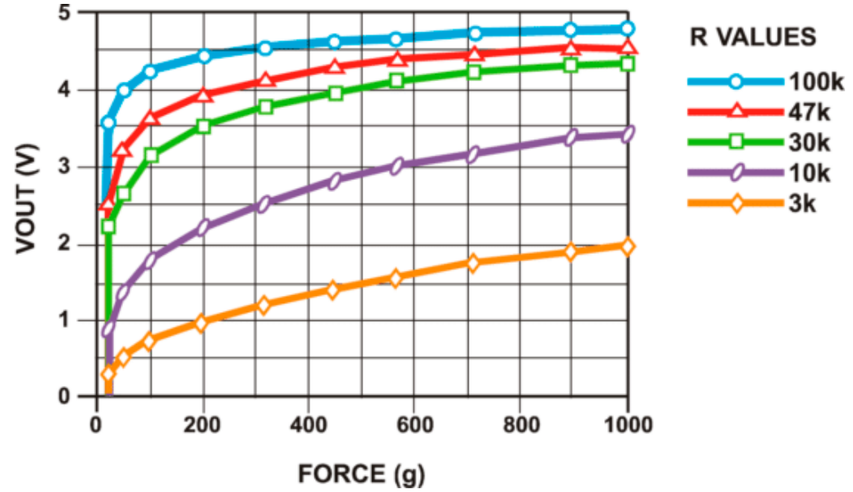

Figure 28: Vout vs Force graph for FSR in combination with different measuring resistors, obtained from Appendix F.

07

Fabrication

7 Fabrication

Voxel slicing

3D Fluidic interface geometries must be printed using the Voxel Print Utility within the Grabcad print environment of Stratasys [77]. A Matlab script based on a halftoning principle as presented by Doubrovski et al. [18] is used within this research to generate the .BMP as input for the Voxel Print Utility.

Polyjet 3D printing

Within the scope of this project the AM process PolyJet 3D printing is researched and validated as a technique for manufacturing fluidic interfaces. PolyJet 3D printing is developed by Stratasys and categorised as "Material Jetting" following the ASTM terminology [37]. All of the prints within this research have been printed on the Stratasys J750 PolyJet printer (29).

PolyJet utilises inkjet technology to deposit layers of a liquid photopolymer. These layers are cured by an ultraviolet lamp directly after deposition. Similar to traditional colour-inkjet processes, PolyJet utilises arrays of multiple inkjet heads in order to deposit up to 6 different materials during a single run. Combined with its microscopic layer resolution and accuracy down to 0.014mm this enables the fabrication of single meta-material components, with variable and graded properties: such as stiffness, transparency, and colour. For an overview of the Polyjet process see Figure 30.

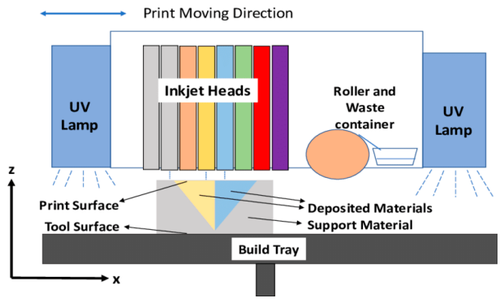

Figure 30: Polyjet 3D printing process.

Opportunities: Why Polyjet 3D printing for fluidic interfaces?

Apart from the ability to create fluidic interfaces in 3D, PolyJet's unique capability to print materials with graded properties opens up a new field of design possibilities. The specific features and relevance for manufacturing fluidic interfaces are shown in Table 1.

Figure 29: Stratasys J750 PolyJet printer

Limitations: Polyjet 3D printing fluidic interfaces

As described, Polyjet 3D printing is a suitable and promising manufacturing technique for fluidic interfaces. However, it also has some limitations which are displayed in Table 2.

Polyjet printing is significantly more expensive as opposed to other commercially available 3D printing techniques. [14]. Besides, flexible material (Agilus30) is reported to have poor mechanical and optical durability. However, since the novelty and goal of this research, the optimisation of these limitations are left out of the scope.

A more important limitation of Polyjet 3D printing is that it can not print overhang without support material. Due to the nature of the Material jetting technique each of the droplets deposited within a layer needs to rest on an underlying layer as can be seen in Figure 30. Therefore, a badly soluble support material (SUP706) is printed within every cavity or underneath every overhang modelled within a part. Previous research has reported this support material can not be removed from tiny or complex internal cavities [5], [43].

As a solution to this, multiple printing workflows can be used which are available in the Research Package of Stratasys as: Liquid, Air, and Pause Printing [76]. the following section describes the validation of these workflows for 3D printing fluidic interfaces.

PolyJet Feature	**Relevance for Fluidic interfaces**
Microscopic layer resolution and 0.014mm accuracy	- Tiny geometries - Tiny features within substrate meta-material
Liquid-, Air, and Pause printing provided in Research Package	- Enables to print internal cavities, which form the fluidic structures
Varying local material stiffness	- Substrate mechanical meta-material
Local full colour and transparent printing	- Substrate optical meta-material

Table 1: Most important features of PolyJet 3D-printing for printing fluidic interfaces

PolyJet limitation	**Relevance for Fluidic interfaces**
High costs	- Expensive parts and prototyping (left out of scope)
Poor mechanical and optical durability for flexible material (Agilus 30)	- Short lifetime for parts including flexible material (left out of scope)
Can't print overhang and cavities without support material	- Badly soluble SUP796 is difficult to remove - Alternative solutions show poor printing properties [48], [74], [5]

Table 2: PolyJet limitations and their relevance for fluidic interfaces

3D printing workflow for fluidic interfaces

Initial exploration of different printing workflows

An initial exploration and validation of two promising workflows available through the research package of Stratasys [76] has been performed for creating complex internal cavities.

The workflows include:
- Air printing
- Liquid printing

Each of the workflows has been validated for their capabilities to manufacture the main components of the 3D printed Fluidic Interface Architecture as presented in section 3; Fluid Repositories, Fluid channels, and Air repositories. The conclusions drawn from the initial research are presented in table 3. The complete research on and explanation of these printing workflows is available in Appendix B.

Based on this initial validation, Liquid Printing is considered the most suitable printing workflow for manufacturing 3D Printed Fluidic Interfaces. The main reason is the form freedom it provides for fluidic geometries.

Voxel-based support structure

As described, Liquid Printing is a suitable manufacturing workflow to create complex internal geometries for 3D printed Fluidic Interfaces. However, Liquid Printing results in poor printing properties, which heavily affects the performance of 3D printed fluidic interfaces. Maccurdy and Speijer [48], [74], [73] present a set of guidelines to take into account when 3D printing with liquid material to reduce these effects. The most important ones for 3D printing fluidic interfaces are shown in Table 4.

Figure 32: (a) layer collapse on top liquid material, (b) poor interface quality, (c) Delamination in layers surrounding liquid material [74].

The guidelines presented by Maccurdy and Speijer result in better printing quality to some extent. However, during the initial exploration of liquid printing, it has been found that support pillars and walls are still difficult to remove from tiny channels and complex internal cavities. Additionally, poor interface surface quality and delamination were still present and therefore affecting the optical performance of different samples as shown in Figure 31.

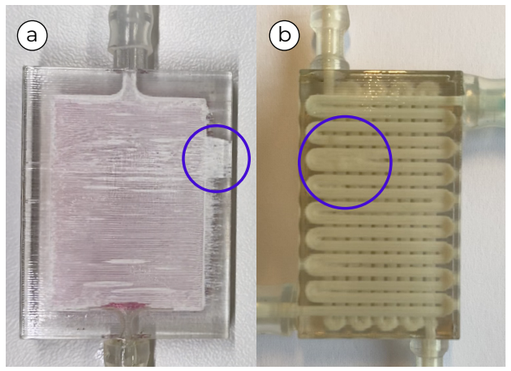

Figure 31: (a) Poor surface quality and delamination in a liquid surface sample, (b) Poor surface quality and delamination in a channel sample.

Printing workflow	Pro	Con
Liquid printing	- Large form freedom for fluidic geometries - Can print closed-off integrated fluidic geometries. - Refraction index of liquid material is close to substrate material	- Poor interface surface quality between liquid and substrate material. - Delamination due to spillage of fluid by roller - Top layer collapse for printing over liquid repositories - Limited to cleanser liquid
Air printing	- Good interface surface quality between air and substrate material - No draining needed	- Limited form freedom of fluidic structures - Can not print surfaces or repositories (only channels) - Needs thick walls (>1mm) - Post printing injection of liquid (and sealing)

Table 3: Exploration of Liquid and Air printing as a possible workflow for 3D printing fluidic interfaces

Limitation (challenge)	Cause	Guideline presented by Maccurdy & Speijer [48], [74]
Top layer collapse for printing over Liquid repositories exceeding 20x20 mm. Shown in Figure 32 (a)FIXME	Sinking of uncured deposited droplets *Substrate Material* on top of the printed *Liquid Material*	Integration of support pillars within liquid volumes providing structural support for top layers.
Poor interface surface quality between Liquid and substrate material. Shown in Figure 32 (b) FIXME.	Mixing of (cured) substrate material particles and uncured liquid material at the surface interface.	Integration of thin support walls (0.2 mm) surrounding liquid repositories.
Delamination of printed layers surrounding large liquid areas, substantially along the y-axis. Shown in Figure 32 (c) FIXME.	Spillage of liquid material due to ‘waving’. Caused by roller movement and print bed shaking.	Minimum wall thickness of 2.11mm, combined with the addition of support walls along the y-axis to reduce the ‘waving’ effect.

Table 4: Limitations, cause and guidelines found by Maccurdy and Speijer [48], [74]

The development and validation of the voxel based support structure is available in Appendix xx FIMXE. The voxel based support structure has been optimised to provide the best printing quality, without surpassing the ability to be drained from complex internal cavities. The difference in approach for using a CAD bases support structure as presented by Maccurdy and Speijer [48], [74] and a voxel-based approach is shown in Figure 33.

Based on empirical data available in Appendx C the optimum voxel based support structure for 3D printing fluidic interfaces is determined at a 55% Cleanser to 45% SUP706 ratio, see Figure 35. The support structure is characterised as a homogeneous shear thinning liquid as shown in the semi-log plot in Figure 36.

The gain in print quality for using a voxel-based support structure of 55% liquid to 45% support material vs liquid printing is shown in Figure 34. It shows a significant gain in printing results for delamination and surface interface quality. Therefore this voxel-based support structure is used within the continuation of the research for 3D printing fluidic interfaces.

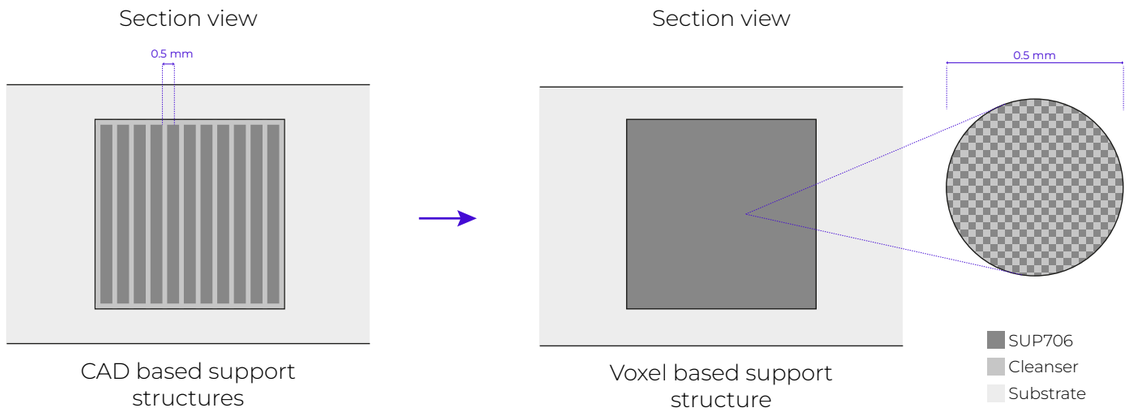

Figure 33: Difference between CAD based support (walls and pillars) [48], [74] and voxel based support structure.

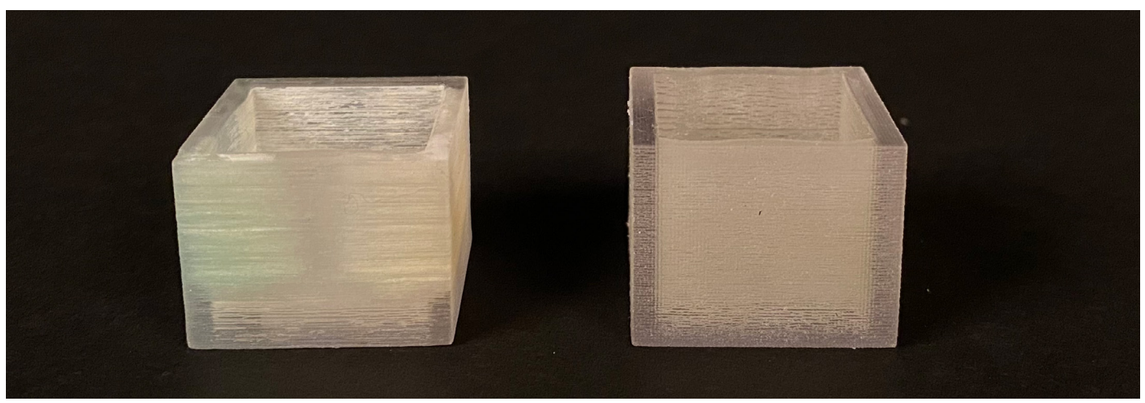

Figure 34: Gain in printing quality for 20x20mm cube using a voxel-based support structure of 55% liquid to 45% support. (left) A sample printed with 100% liquid support. (right) A sample printed with voxel-based 55% liquid to 45% support structure.

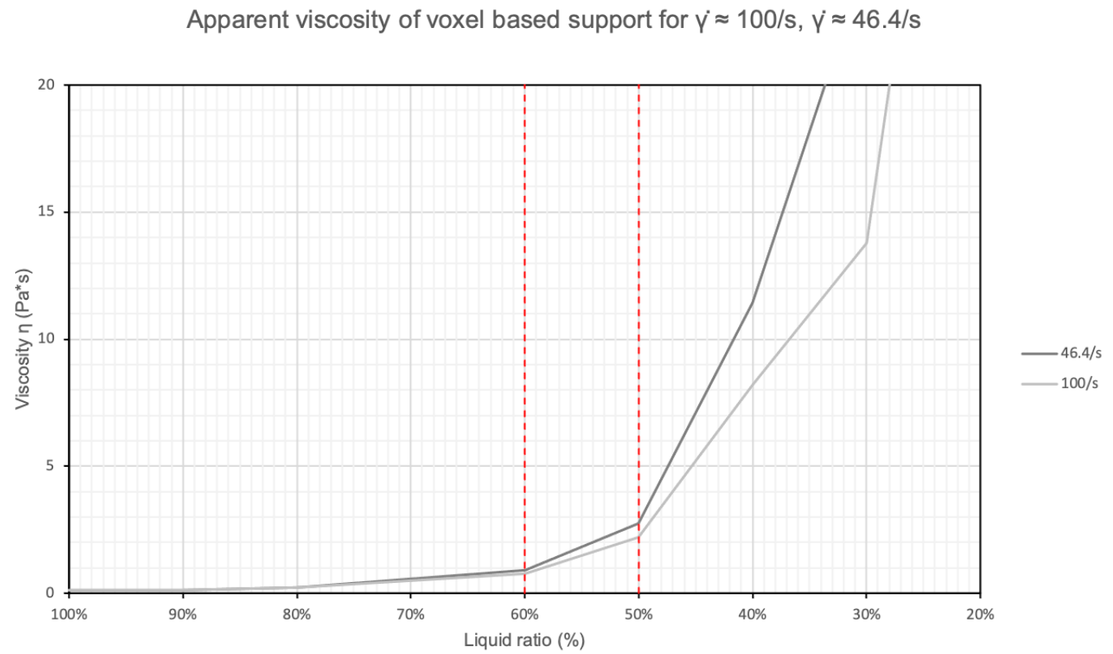

Figure 35: Optimum ratio is determined at 55% liquid to 45% support. Below 50% liquid, voxel support material increases heavily in viscosity.

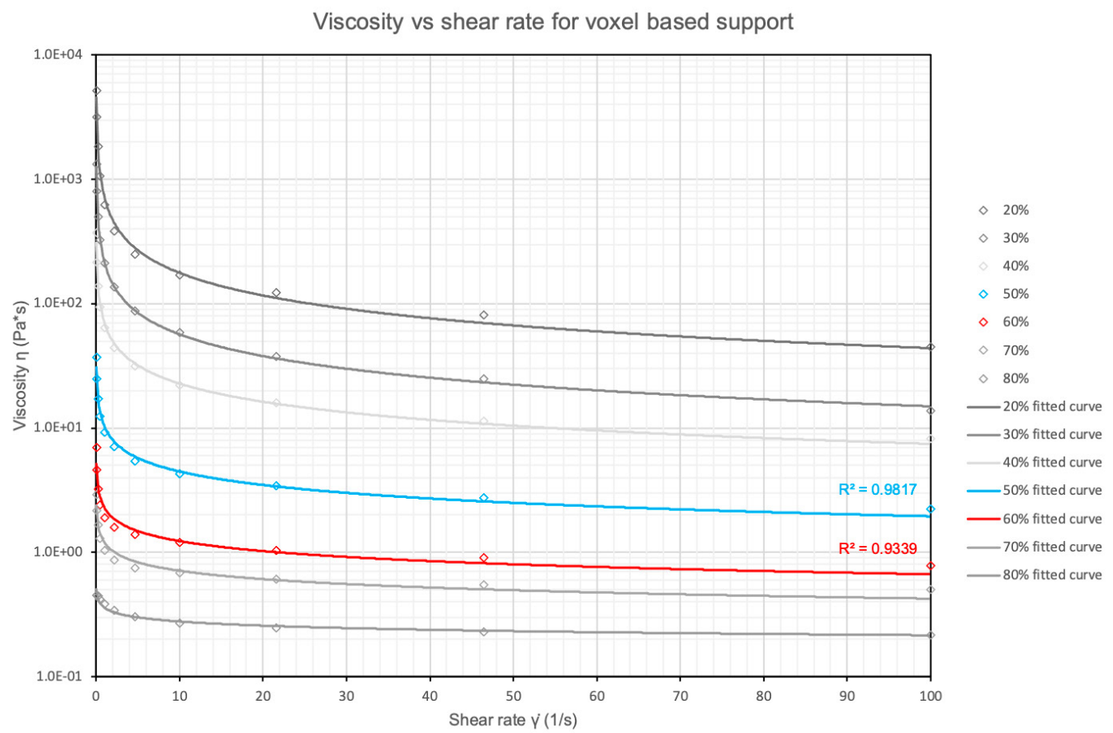

Figure 36: Voxel based support acts as a shear thinning fluid. Apparent viscosity for voxel support at 60% liquid to 40% support, $\dot{\gamma}$=100, 0.78 Pa.s, 50% liquid to 50% support, $\dot{\gamma}$=100, 2.22 Pa.s

08

Post-processing

8 Post-processing

As shown in Figure 21, the post-printing process of the design and fabrication pipeline includes: cleaning the part, draining of printed fluid, injecting of liquid material and sealing of the geometry.

During the continuation of this research, multiple insights have been gathered for this operations.

Cleaning parts

Cleaning the parts can be done by using a water-jet. The waterjet can be operated on high pressure for parts printed in VeroClear, and medium pressure for parts printed in Agillus30. For parts with tiny features (<3m), it is advised to clean parts using a toothbrush and water.

Draining printed liquid

Fluidic structures are printed using a 55% liquid to 45% support voxel-based support structure. Draining the geometries can be done with a vacuum pump. To accelerate the process, water can be injected using a syringe on the opposite side. After draining the fluidic structure, the internal cavities must be rinsed with water using a syringe. Finally, the parts must be dried before proceeding to the injection of liquid material. The drying process can be accelerated by putting the parts in a dehydration oven at 45 degrees Celsius.

Injecting liquid material

A wide variety of liquid materials can be used for fluidic interfaces. However, it has been reported different liquids have varying optical performances in fluidic interfaces due to light refraction at the substrate-liquid material interface. This effect occurs as a white blur situated at the materials interface as shown in Figure 38..

To overcome this effect a liquid must be selected with a refractive index close to the refractive index of the substrate material. In this way scattering of light due to refraction at the material interface is minimised. Veroclear has a refractive index of 1.52 at 589 nm [90]. Within this research, cleanser material has been used as liquid material for fluidic interfaces, which showed good optical performance. For coloured liquid material, the cleanser material is dyed with Avis Colerex universele mengkleur.

Sealing geometry

Parts printed with inlets for liquid material should be capped off. For parts with encapsulated fluid structure, transparent UV-glue can be used to seal the part. Using a needle, the UV-glue is applied within the hole which is used to drain the part as shown in Figure 37.

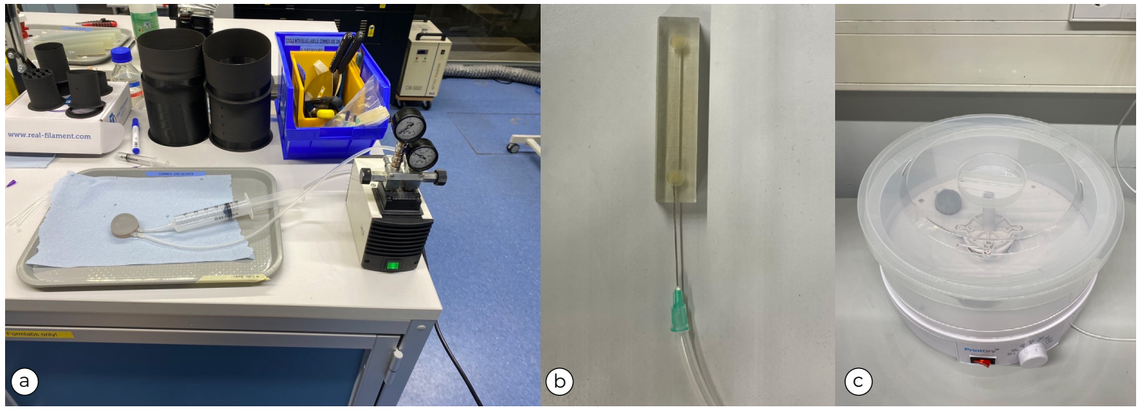

Figure 37: (a) Draining a fluidic structure with a vacuum pump and water injection from the opposite side. (b) for encapsulated fluidic structures a needle can be used for draining. (c) part in a dehydration oven at 45 degrees Celsius.

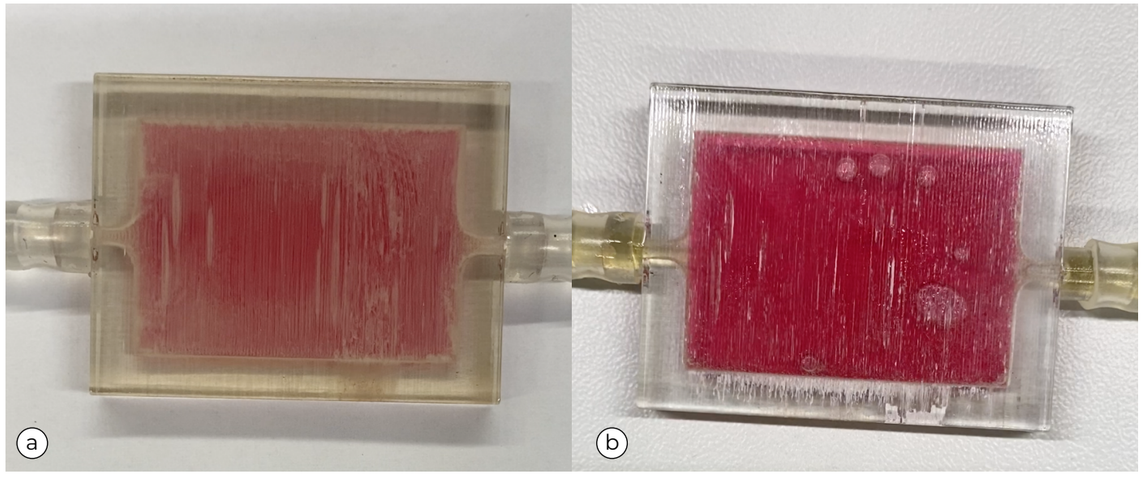

Figure 38: Gain in printing quality for 20x20mm cube using a voxel-based support structure of 55% liquid to 45% support. (left) A sample printed with 100% liquid support. (right) A sample printed with voxel-based 55% liquid to 45% support structure.

09

Characterisation and applications

9 Characterisation and applications

Karana et al. [42] have developed the Material Driven Design method (MDD). This method facilitates designers and material scientists to design for specific material experiences. The key principle of this method is that in order to design for meaningful interactions and applications, (novel) materials should not be characterised and developed for their functionality only (technical properties) but also for the experience it can evoke when interacting with it (experiential qualities).

As described in section 2 fluidic interfaces are a novel concept, which is only scarcely explored. Precedent research is mainly focused on the manufacturing of such interfaces, and only a handful of applications are proposed [54], [5], [69], [73]. In section 3 the requirements and architecture defines the design space for 3D printed fluidic interfaces in terms of configurations and technical possibilities. It expands on previous characterisations of Mor et. al [54] and Speijer [73]. Therefore, it can be concluded fluidic interfaces are well-characterised for their technical properties. However, a knowledge gap remains for the experiential and sensorial characterisation of 3D printed fluidic interfaces, in order to design for meaningful interactions and future applications.

The MDD [42] consists of four steps as shown in Figure 39, starting with the characterisation of the material in step one. Although the MDD is not fully applied within this project, several steps have been obtained from the method in order to provide some first insights on the experiential value of 3D printed fluidic interfaces. The interfaces are characterised for their experiential qualities (step 1) using the material experience framework as presented by Giaccardi & Karana [27]. This framework includes four experiential levels; the sensorial, the interpretive, the affective and the performative level. The characterisation was done via tinkering with the material and a set of user studies. Five experts in different fields of research and design closely related to 3D printed fluidic interfaces have been interviewed. Secondly, a material experience vision is created (step two) which is ued to design a demonstration concept which is presented in section 10.

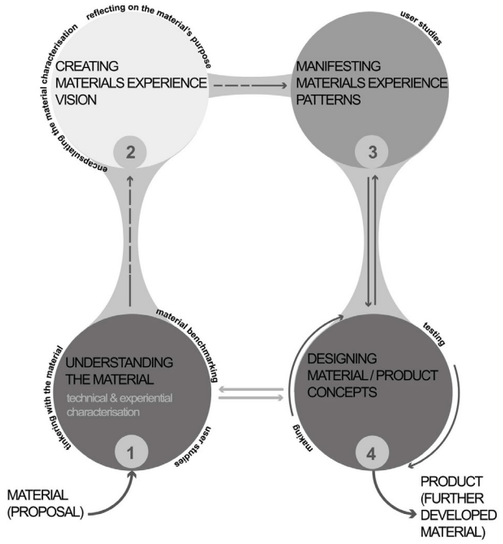

Figure 39: Overview of MDD method of which step 1 and 2 are performed as an initial experiential characterisation of 3D printed fluidic interfaces, obtained from [42].

Expert interviews

Qualitative interviews have been held with five experts from multiple design fields related to 3D printed fluidic interfaces. The interviews consist of two parts: the first part functioned as a user study for the initial characterisation of the experiential qualities of 3D printed fluidic interfaces. The second part included an exploration of possible application areas, Thirdly, some overall recommendations on the presented samples and concept as a whole were gathered. During the interviews, participants were exposed to a series of samples shown in Figure 40, varying in channel geometry, surface finish and use of coloured liquid.

The argument for choosing experts as participants is that their phenomenal field is broader than a layperson's [79], [51]. They are better equipped to reflect upon and articulate what they see, especially for the conceptual stage in which the samples are presented. Additionally, it is assumed that the experts can easily relate specific experiential qualities of the interface to applications within their field of operation. Thirdly, by selecting experts from multiple areas, a broader field of applications can be explored within the limited time frame and more differentiated recommendations will be obtained for the samples. In later stages of the characterisation, it is recommended to perform user studies, especially on laypersons, to validate the obtained results for experiential characterisation.

A total of five experts were invited, of which one lecturer, two professors, one assistant professor and one associate professor at the Faculty Of Industrial Design Engineering at the Delft University of Technology. Respectively with expertise in (1)(embodied) interaction design, and human-computer interactions, (2)materials experience, (3) perceptual intelligence and visual communication of light, material and space, (4) Embodied interactions and haptic experiences and (5) materials, manufacturing and design. They are referred to as IxD 1-5 in the analysis of the results presented in Appendix G.

The interview insights are presented in 4 categories: the Experiential qualities of fluidic interfaces, Future applications, Recommendations on the presented samples, and Overall recommendations.

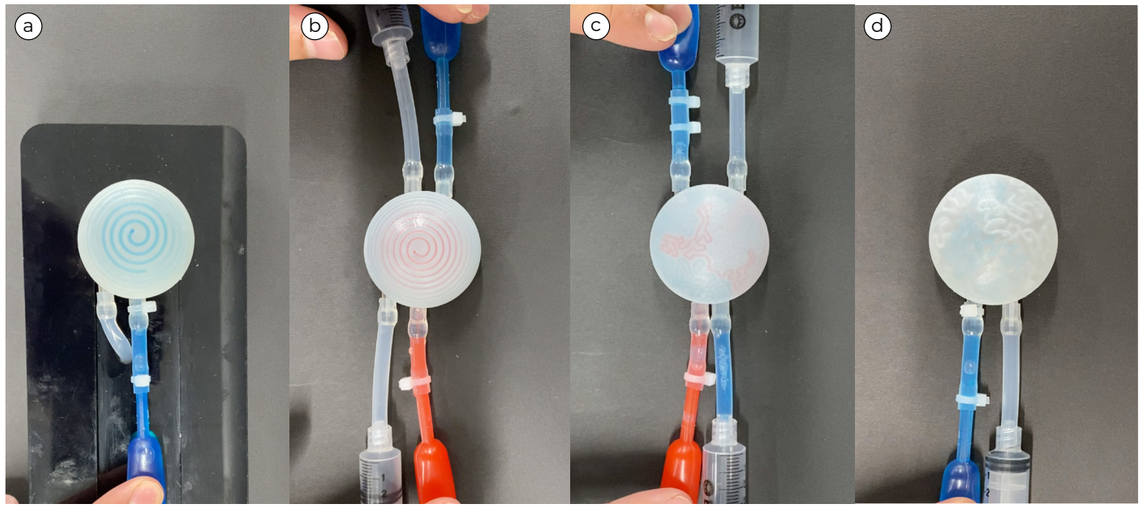

Figure 40: Samples used during interviews. (a) Spiral pattern, one colour (b) Spiral pattern, 2 colours, (c) Surface growth pattern, 2 colours. (d) Volumetric growth pattern, 1 colour

Experiential qualities of 3D printed fluidic interfaces

The experiential qualities have been categorised at four levels: the sensorial, interpretive, affective and performative level [27]. The results are shown in Figure 41.

The pre-settled meanings playful, intriguing, aesthetically (beautifull), direct and novel were detected at the interpretive level. For a subset of the samples (with growth patterns) the meaning 'organical' was also found. Colour contrast (in pattern and geomtries), haptic feel, sensitivity and response time of the interfaces were identified as four important qualities at the sensorial level to elicit these meanings. It was found people were particularly drawn to the sense of control between in- and output, and continued to explore this as expressed by one of the participants (IxD 4): "You have a very direct sense of control, I like to see how hard I have to push to get to a certain level".

All of the samples are found to be very performative. Multiple participants described them as "very inviting to touch". Besides touching the samples participants continue to play with it for a while to discover and explore the in-output relation. As described the sample were also identified as very controllable. Additionally, it was found that the samples had a certain amount of ephemerality, users perform an action for which data exists for a small moment after it fades away. The process of touching and exploring the interfaces generally elicited emotions of happiness, excitement, amasement and satisfaction at the affective level. In some cases, in which it was hard to displace the fluid, the samples also elicited feelings of annoyance. Besides, for a more simple channel pattern (spiral) it was found that the samples were easily explored, which weakened the effect of excitement.

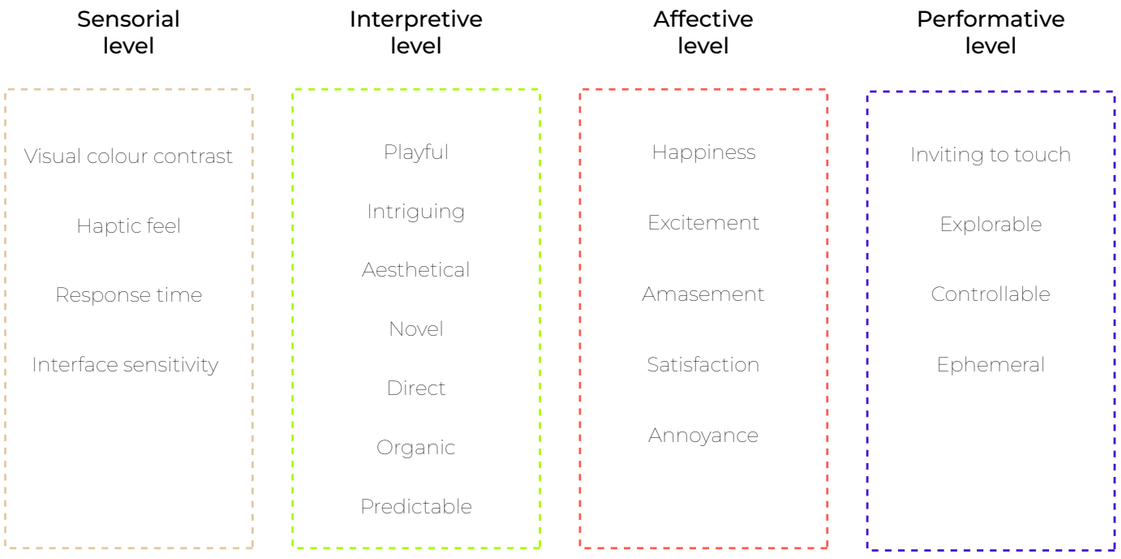

Figure 41: Experiental qualities of 3D printed fluidic interfaces.

Future applications areas for 3D printed fluidic interfaces

It has been found that the design space for 3D printed fluidic interfaces is very broad. Various participants explicitly expressed this, and a wide variety of applications has been obtained from the interviews. The founded application areas are presented in nine domains: Healthcare, Living organisms, Toys, Wearables, Art and fashion, Lighting, Social design, (Soft), robotics and data display. Specific application concept ideas which arise during the interview are present in the interview results in Appendix G.

Figure 42 shows an overview of future applications for 3D-printed fluidic interfaces which were identified and explore during the expert interviews. Although there is no proof for one-on-one underlying relationships, it was noticed that various application areas hold strong relationships with specific qualities or capabilities of 3D-printed fluidic interfaces during the interviews. For example, applications in need of direct and accurate feedback, such as pressure-sensing wearables and soft-robotics are assumed to be more dependent on sensitivity and response time, whereas toys and lighting applications can be more dependent on colour contrast.

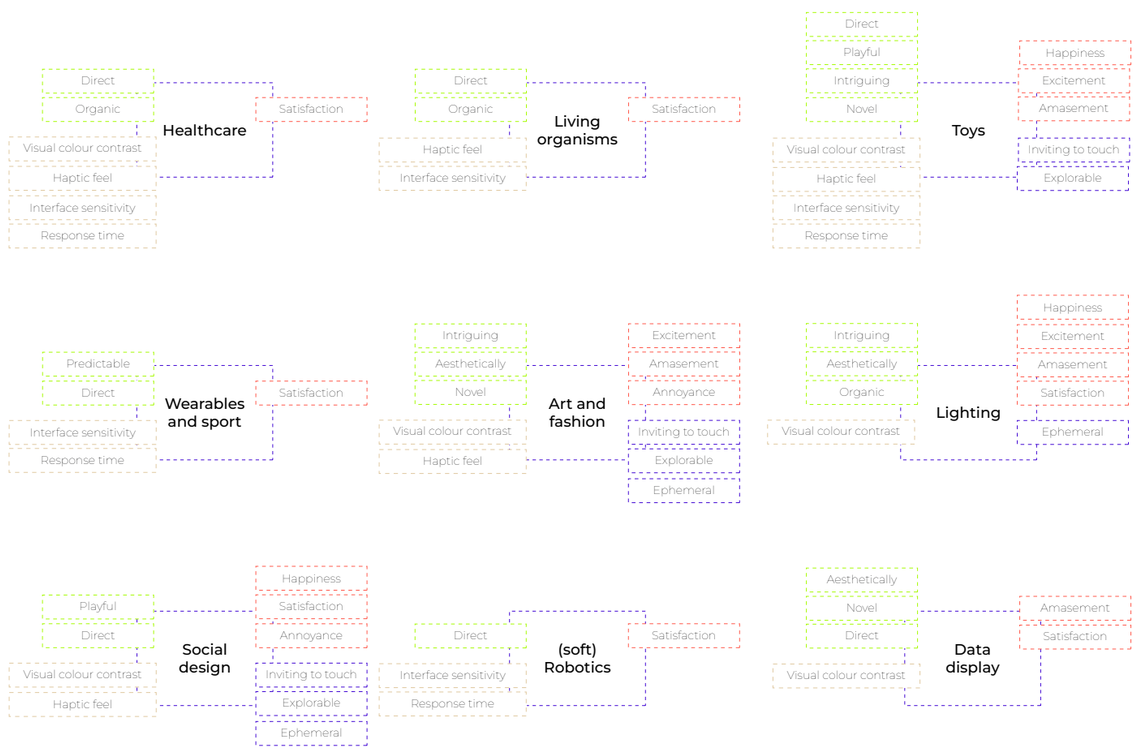

Figure 42: Application areas and affecting experital qualities of 3D printed fluidic interfaces.

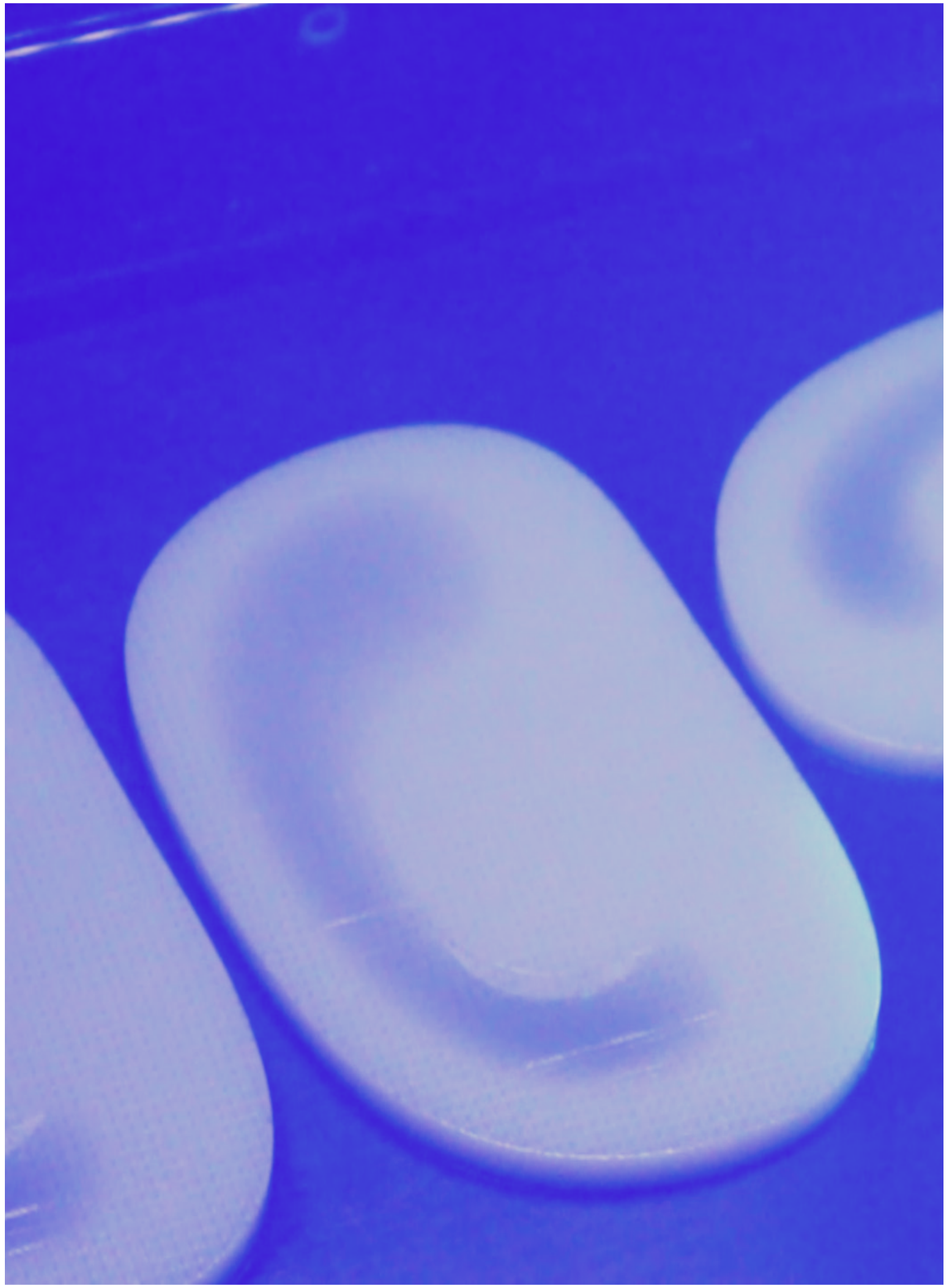

Recommendations on the 3D printed samples

As described the interviews also gain insight as recommendations on the printed samples. The recommendations primarily included feedback on the appearance (output) and haptic feel (input) of the samples which can be taken into account for future prototyping.

Appearance (output) of the samples

- The samples were printed in rigid VeroClear material, but non-polished samples visually appeared to be soft and flexible.
- The colour contrast within the samples is too low.
- Due to the lack of transparency you can't see the full 3D effect inside the samples.
- Light reflection can interfere with the data display of the channels.
- Perfect curvature does not exist in nature, therefore the domes seem artificial, weakening the organic expression of the growth patterns.
- The geometry does not show full 3D potential, it should have a more embodied holistic shape.
- The spiral shape can express more precise data than the growth patterns.
- Air bubbles are present in the system, they could be an enemy and a friend.

Haptic feel (input) of the samples

- For some samples, you have to push too hard to display the fluid, the sensitivity is too low.
- The material of the sample should be flexible, so in- and output could have the same location.
- The response time of the interface is very slow in some of the samples.

Overall recommendations

Next to these results, a few general remarks came to rise during the interviews. Multiple participants implied further research on the temporal form of the 3D printed fluidic interfaces. Besides, 3 out of 5 participants opted to perform such, or other research in an art and science project. The main reason for this recommendation is the novelty, and aesthetic value of the 3D printed fluidic interfaces. Another interesting suggestion was to further research the ability of 3D printed fluidic interfaces to contribute to skill-based learning through embodied interactions. It was hypothesised that the direct link between in- and output can provide very interesting results in this domain.

10

Validation by demonstration

10 Validation by demonstration

To validate and demonstrate the concept of 3D-printed fluidic interface, a set of final demonstration concepts have been designed and manufactured using the fabrication pipeline and design and simulation tool, as presented in section 5. By undergoing this complete process, each of the phases from the fabrication pipeline can be validated and provide insights for future research on designing and manufacturing 3D printed fluidic interfaces.

Design goal for the demonstration concept

The experiential characterisation of 3D printed fluidic interfaces presented in the previous section found a variety of experiential qualities on the sensorial, interpretive affective and performative level.

Although these findings can not be completely grounded by the first exploration and interviews for experiential characterisation, it is interpreted that specific experiences on the interpretive level, such as direct and controllable or playful and intriguing respectively hold strong relationships with different material experiences on the affective level such as satisfaction or excitement, amasement and happiness. Besides, it is interpreted that variations in the interpretation which were evoked by different samples are driven by the difference in temporal form and flow patterns and geometries within the presented samples.

It can be concluded that by varying the temporal form and fluidic structure patterns or geometries, the concept of 3D printed fluidic interfaces has promising capabilities to be tuned and programmed towards specific material experiences. To showcase this quality of 3D printed fluidic interfaces and the findings of the experiential characterisation, three demonstrating concepts are developed which are individually tuned to showcase the most predominant material experiences found in the characterisation process. Tuning towards this experience is done by variations in channel geometry and temporal form (defined by sensitivity and response time).

Therefore, the main design goal of this demonstration concept as a whole is:

To showcase:..
1) the capabilities of multi-material 3D printing as a manufacturing technique for fluidic interfaces, 2) the experiential qualities of 3D printed fluidic interfaces and 3) the promising capabilities of tuning a 3D printed fluidic interface for specific material experiences.

Material expression vision for demonstration concept

A playful and explorable interface called: Wow!

Based on the experiential characterisation it is assumed that 3D printed fluidic interfaces which are interpreted as novel, playful, aesthetical and organic on the interpretive level can evoke happiness, excitement and amasement on the affective meaning. Combined with the performative qualities of being inviting to touch and explorable, this resulted in the following material experience vision for a playful and explorable interface:

My vision is to program colour contrast, sensitivity and response time in such a way that interacting with the interface feels playful, intriguing, aesthetical and novel to evoke emotions of happiness, excitement and amasement whilst being inviting to touch and explorable.

A direct and controllable interface called: scale

3D-printed fluidic interfaces which were very controllable on the performative hold strong relationships with interpretations of direct and predictable on the interpretive level. It is assumed these interfaces can elicit satisfactory experiences on the affective level. This resulted in the following vision for a direct and controllable interface:

My vision is to program sensitivity, response time and colour contrast in such a way that the interface feels very controllable, to elicit direct and predictable interpretations which evoke a satisfactory experience.

An aesthetic and ephemeral interface called: Hhhelloooooo...

During the interviews, multiple participants specifically identified the performative quality of ephemerality for 3D printed fluidic interfaces. It was also suggested to make use of this quality for social design applications, in which users can leave a trace of presence over time. Based on this idea the following vision was created for an aesthetic and ephemeral interface:

My vision is to program colour contrast and response time in such a way that the interface elicits aesthetical and intriguing experiences to evoke feelings of happiness and satisfaction for being inviting to touch and ephemeral.

Design and simulation of the demonstration concept

To showcase the full potential for 3D fluidic structures and geometries by using PolyJet 3D-printing, a set of organic-shaped blobs is chosen as a final object for the demonstration concept(s). The blobs are conceptual shapes which are able to showcase the capabilities of the concept of 3D printed fluidic interface in isolation of specific user contexts. Additionally, the feedback on presented samples being too geometrical in shape and therefore not showcasing the full potential of the 3D design space has been taken into account. After a quick form-finding process the final blob shape was found which felt nice to the hand and was inviting to touch, shown in figure 43.

Figure 43: Formstudy for demonstrator blob shape..

The three different blobs have been designed in such a way the encoded responsive behaviour is programmed towards the material expression vision. This was done by variations in the fluidic flow patterns, sensitivity and response time. All of the blobs are responsive to applied actuation pressure. Flexible Agilus material regions have been used at the pressure points, which allows for the deformation of the substrate material to increase the internal pressure in the liquid repository of the interface. A brief overview of the important design choices is presented for each of the demonstrating blobs:

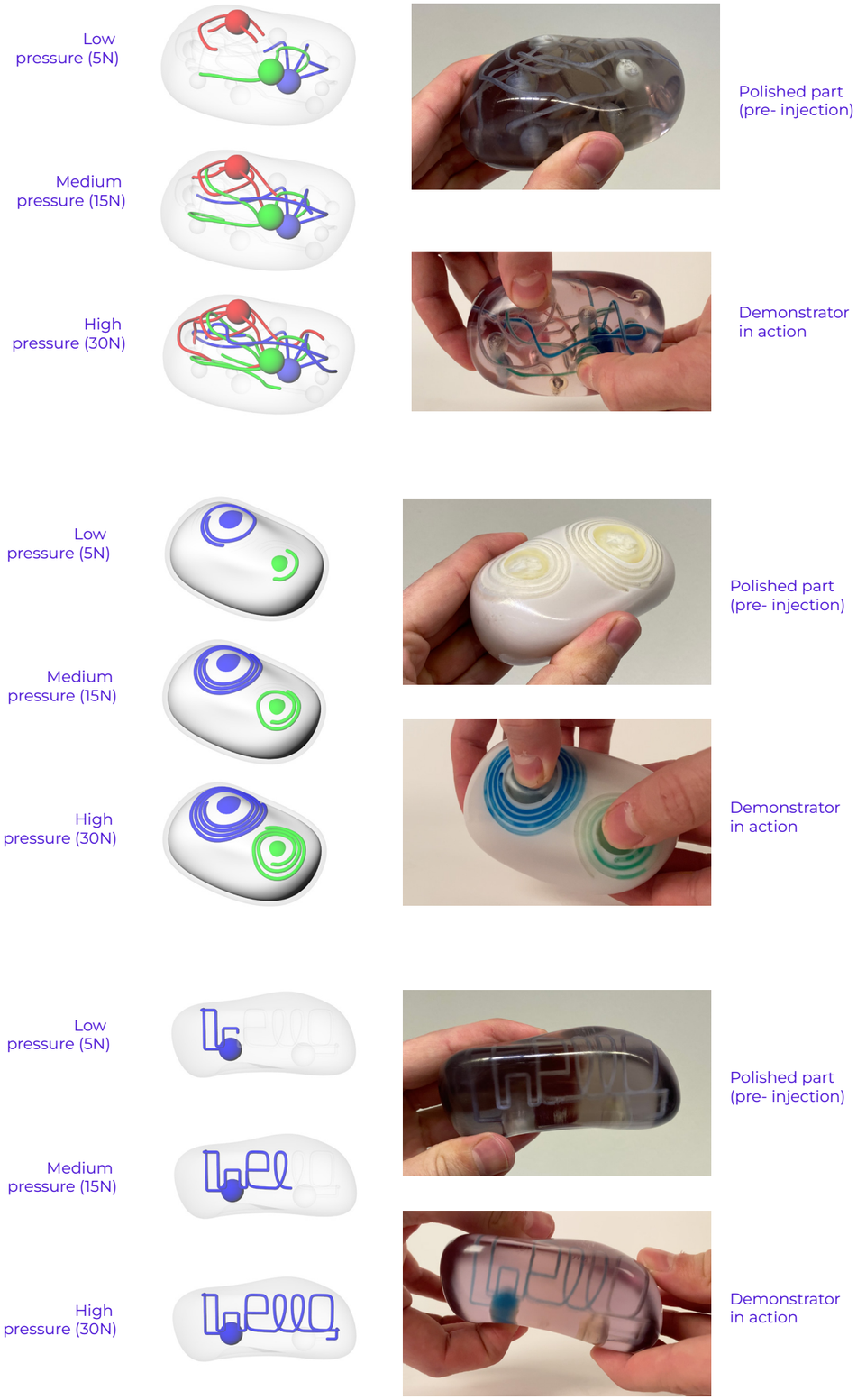

Figure 44: Design, inteded sensitivty and final result for (top) Wow!, (middle) Scale and (botom) Hhhelloooooo...

Wow!

Vallgårda et al. found that complexity, unpredictability and asynchronous rhythms in temporal form can lead to entertainment in interaction design [82]. Additionally, they found that working against the anticipation can evoke a feeling of surprise. Using these insights, Wow! has been designed to evoke playful and intriguing interactions as a multi-colour fluidic interface with intertwined channels which are modelled hand-free as curves in Rhinoceres and linked to the design tool in the Grasshopper environment. Some channels share the same colour and liquid repository, which means they are responsive to the same pressure point for actuation. Additionally, variable radii along the length of the channel are used to program for inconsistent response time, creating a more asynchronous rhythm in temporal form. Overall, Wow! is tuned for medium sensitivity using the computational design and simulation tool and design parameters (Air repositoy ratio R(m) and wall thickness h(m) as presented in section 6 .

scale

Vallgårda et al also found that working with the anticipation can lead to smooth and satisfactory experiences [82]. Using this principle scale is tuned for direct and controllable responsive behaviour. Scale displaces two separate coloured liquids in a spiral flow pattern for two pressure points. The spiral pattern is intended for easy interpretable and predictable visual data display. Scale is tuned for fast response time by maximising channel radius. The separate pressure points are tuned for different sensitivities using the computational design and simulation tool to showcase and validate this possibility for 3D-printed fluidic interfaces. The blue pattern is tuned for high sensitivity and the green pattern is tuned for low sensitivity.

Hhhelloooooo...

To demonstrate the ephemeral qualities of 3D-printed fluidic interfaces, Hhhelloooooo... has been tuned for low sensitivity using the design and simulation tool. More importantly, it is intended for very low response time by making use of a small channel radius. The channel pattern is designed to express a simple message, to allow for social expression.

An overview of the design, intended sensitivity and fabricated result of Wow!, Scale and Hhhelloooooo... is shown in Figure 44.

Fabrication of the demonstration concept

The demonstration blobs were fabricated using the fabrication pipeline presented in this research. After the design and simulation of the blobs, each of the blobs was prepared for 3D-printed using the voxel slicer and voxel print utility. 3D printing of the blobs was done using the 55% liquid to 45% support voxel-based support structure for internal fluidic structures. After printing, the blobs were cleaned, emptied, injected through the filling holes and finally sealed. Several steps of this procs are shownin Figure 45.

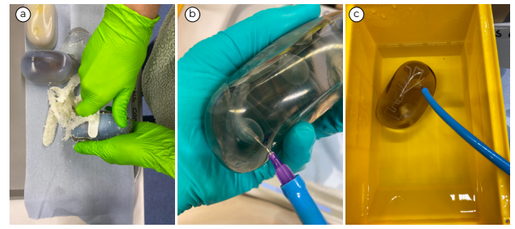

Figure 45: Different post-processing operations. (a) cleaing part, (b) emptying with vacuum, (c) rinsing by vacuum underwater.

Validation of demonstration concepts

Reflecting on the design process for the demonstration bobs it can be concluded the design and manufacturing pipeline allows to design and manufacture of Multi-material 3D printed responsive fluidic interfaces with programmable dynamic appearance. All of the demonstration blobs were successfully fabricated with distinct internal cavities, and no leaks appeared after sealing. However, some printing imperfections were identified within the blobs (see dots in bottom image of Figure 48) . Overall, it was experienced that the complete pipeline for fabrication is very time-consuming and takes up to multiple days.

The design workflow in Rhinoceros and Grasshopper was found to be successful for the design and preparation of 3D-printed fluidic interfaces. However, it was found that for exporting the STL files of interfaces which house more than two materials (which was the case for all of the blobs), the STL files can have slight overlap due to the mesh boolean operations in the design tool. This resulted in overlapping pixels in the bitmap files which causes an error within the voxel print utility. This was fixed by manually deleting the overlapping pixels which is a labour-intensive task. Investigating other workflows for the mesh boolean operation can solve this problem in future work.

A comparison of the real-life sensitivity with the simulated responsiveness showcases that the simulation tool is capable of simulating the responsive behaviour with reasonable accuracy. Although the simulation can be optimised in future work it was found to be sufficient for pre-fabrication validation of the interface sensitivity and determining the design parameters, for each of the interfaces, intended liquid displacement was within comfortable boundaries for applying actuation pressure. Additionally, the intended variations in sensitivity for different channel geometries (Scale and Hhhelloooooo...) were notable when interacting with the blobs. However, due to air bubbles in the system, the specific liquid displacement could not be compared with the simulation model for these samples. Variations in response time (Hhhelloooooo...) were less noticeable within the interface.

It was found that clearing the liquid repositories of voxel-based support material through a single filling hole remains difficult due to the spherical shape. Rinsing it with water, a path with the least resistance occurs in the centre of the sphere. Each of the repositories and interconnecting channels was rinsed and shaken multiple times for 5-10min each, to get rid of the internal support structure.

Injecting the liquid repositories through a single filling hole without encapsulating air bubbles in the systems remains difficult, especially for liquid repositories which share multiple channels (Wow!). Additionally, it was noticed that when injecting a liquid repository that shares multiple channels, some of the channels are filling up with liquid before the liquid repository itself is completely full. This resulted in various channels being unusable for liquid displacement by mechanical actuation. To avoid this, some of the repositories are not completely filled, leaving a large air bubble in the system (Wow!).

Besides, it was found that after interacting with the interface for the first time, liquid material remains in the channels which does not retract to the liquid repository. This effect could occur because of imperfection in the internal channel surface. The non-retracted liquid appears as fractions of liquid with air bubbles in between. The fragmented liquid distorts the output signal, leading to less predictive and controllable behaviour. Explorations of using this effect can possibly lead to more entertaining and intriguing experiences [82].

Figure 48: Final demonstrator results, (top) Wow!, (middle) Scale and (bottom) Hhhelloooooo...

11

Limitations and future work

11 Limitations and future work

Fabrication and scalability

The fabrication pipeline presented in this research allows for the manufacturing of embedded responsive fluidic interfaces using Polyjet 3D printing technology. The demonstration concept showcased a feasible concept of a 3D-printed fluidic interface. However, limitations for this workflow include the fragility and long-term optical properties of flexible Agilus material, high-costs, manual post-processing and scale (printer dimensions). Additionally, printing imperfections were still present in the fabricated samples.

For long-term use of the interfaces more robust solutions should be explored to increase lifespan which allows for more viable future product applications. For large-scale interfaces such as dynamic installations or wearable suits, it can be investigated to divide fluidic interfaces into separate 3D-printed parts, as showcased by Bader et al. [5]. Additionally, scalability and mass production of these interfaces is still heavily subject to high production costs and time-consuming manual task in the fabrication pipeline (Cleaning, draining, injection and sealing of geometry). A pause printing workflow for Polyjet 3D printing as presented by Andre et al. [13] shows a possible workflow for the manufacturing of complex embedded fluidic structures, without the need for manual post-processing tasks. Additional to cutting down on post-processing steps, this could also provide a solution towards the difficulties in draining, rinsing and injecting of liquid material as experienced and described in section 10. A proposed design & fabrication pipeline using this workflow is shown in Figure 49. Another proposal to allow for a more automated fabrication pipeline is to investigate the possibilities deposit other types of (coloured) liquid materials than the Cleanser material by Polyjet 3D printing, possibly in collaboration with Stratasys.

The voxel-based support material developed for printing complex internal geometries has been optimised via validation with empirical and Rheological data. However, The rheological measurements for the dynamic viscosity have been performed at shear rates ranging from 0-100 1/s. The voxel-based support material acts as a shear-thinning liquid and can be characterised as a power-law fluid, for which the shear rates for pressure-driven flow are dependent on the channel radius. Due to the small channel radii in the fluidic interface, it is assumed that shear rates within fluidic interfaces exceed 1/100s. To fully understand the shear thinning behaviour of voxel-based support material for manufacturing fluidic interfaces, rheological measurements should be taken at higher shear rates. This can ultimately lead to the optimisation of the voxel-based support material, allowing for better printing quality.

Another workflow which can possibly allow for the creation of complex internal geometries using Polyjet 3D printing is using WSS150 [78] water-soluble support material. This material has recently (during this research) been presented by Stratasys on a series of printers (excluding the printer used within this project (PolyJet J750)).

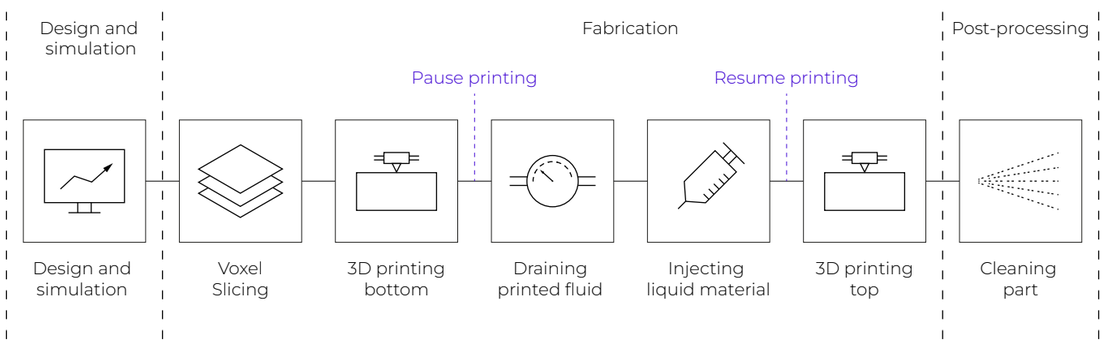

Figure 49: Proposed fabircation pipeline for using pause printing as a manufacturing workflow.

Design and simulation tool

The computational design and simulation tool presented in this research provide a relatively accurate simulation of liquid displacement triggered by mechanical pressure for 3D printed fluidic interfaces. However, there is room for improvement and expansion of the simulation tool to allow designers to better validate their designs before manufacturing.

The tool can only simulate liquid displacement for actuation pressure and can be expanded for other deformation inputs like bending, twisting or stretching the interface. The simulation tool makes use of an FSR to sense input pressure with an accuracy of +/- 10%. Performing a calibration process as described in [19] and [31] on the specific set of sensors used within the research the accuracy can be optimised to be approximately 1%.

Besides, the simulation tool can only simulate tunable sensitivity but as showcased within the demonstration concepts, fluidic systems can also be tuned for response time. Further research into the underlying principles and affecting parameters such as the viscosity of the liquid, radii of the channels and elasticity of meta-material structure should be performed to allow accurate simulation and a better understanding of response time and temporality of 3D printed fluidic interfaces.

Embedded computation and in-output configurations

Within this research multiple patterns, geometries and optical principles have been explored for 3D printed fluidic interfaces. To extend de design space and possibilities in computational logic and visual output further exploration can be performed. This includes using different liquid materials such as photochromic, thermochromic or bioluminescent liquid materials [8] to create different inputs. Besides, liquids with different viscosities can be explored [90]. Using various viscosities can possibly allow for different response-time and temporal form in 3D-printed fluidic interfaces.

Various optical principles have been explored within this research to create dynamic visual output. Further, explore of optical principles such as subsurface light scattering [29] can expand the possibilities for dynamic visual output of 3D-printed fluidic interfaces. In addition, other types of dynamic output, such as deformation [63] or dynamic (haptic) texture [73] can be explored to extend the design space for 3D printed fluidic interfaces.

Material experience of fluidic interfaces in HCI

A first exploration of the performative experiential qualities and temporal form for 3D printed fluidic interfaces has been performed, together with an investigation of the underlying parameters to tune for specific temporal form and material experiences. 3D-printed fluidic has shown to be tuneable for specific sensitivity with reasonable accuracy using the presented fabrication pipeline. However, tuning for specific response time remains still limited and the defining parameters and their relationship remain unclear. Further research can lead towards a better understanding of the defining parameters for temporal form in 3D printed fluidic interfaces. For example, the use of intended or non-intended air bubbles within the system can be investigated for their possibility to define and distort rhythm in the responsive behaviour, leading toward various experiences in HCI.

Further exploration, using the the MDD [42] can lead to better characterisation of experimental qualities and more meaningful material experiences which expand the application areas for 3D printed fluidic interfaces in HCI.

12

Conlusion

12 Conclusion

In conclusion, this research contributes to the field of HCI and digital manufacturing by presenting a concept for multi-material 3D printed responsive fluidic interfaces with programmable dynamic appearance. The interfaces utilise internal fluidic mechanisms in a 3D-printed meta-material structure, which can output visual information through the internal displacement of coloured liquid triggered by mechanical deformation input. A basic architecture is presented that expands the design space for fluidic interfaces with new possibilities and configurations by introducing multi-material 3D printing as a manufacturing workflow. A design and fabrication pipeline, including a computational design and simulation tool and a novel voxel-based support material for 3D-printing complex internal cavities, has been developed. Technical evaluation validated a similar behaviour of the simulation tool and a set of fabricated samples. Additionally, a first characterisation of the performative experiential and sensorial qualities of responsive fluidic interfaces has been performed to allow for designing more meaningful material experiences together with various promising future application directions for 3D printed fluidic interfaces. Finally, a series of demonstrating blobs with embedded and encoded responsive behaviour for specific material experiences have been developed to showcase the unique capabilities of 3D printed fluidic interfaces.

Fluidic interfaces have interesting capabilities, and many future challenges and design possibilities still exist. The exploration of multi-material 3D printed fluidic interfaces within this research showcases the rich potential of programmable fluidic structures and opens up new design paradigms for the design space of fluidic interfaces.

13

References

13 References

[1] Edward H. Adelson. 2001. On seeing stuff: the perception of materials by humans and machines. In Human Vision and Electronic Imaging VI, Photonics West 2001 - Electronic Imaging, SPIE, 1–12. DOI:https://doi.org/10.1117/12.429489

[2] Anthony K Au, Nirveek Bhattacharjee, Lisa F Horowitz, Tim C Chang, and Albert Folch. 2015. 3D-printed microfluidic automation. Lab Chip 15, 8 (April 2015), 1934–1941. DOI:https://doi.org/10.1039/c5lc00126a

[3] Moritz Bächer, Emily Whiting, Bernd Bickel, and Olga Sorkine-Hornung. 2014. Spin-it. ACM Trans. Graph. 33, 4 (July 2014), 1–10. DOI:https://doi.org/10.1145/2601097.2601157

[4] Daniel Bachmann, Frank Weichert, and Gerhard Rinkenauer. 2018. Review of Three-Dimensional Human-Computer Interaction with Focus on the Leap Motion Controller. Sensors 18, 7 (July 2018). DOI:https://doi.org/10.3390/s18072194

[5] Christoph Bader, William G. Patrick, Dominik Kolb, Stephanie G. Hays, Steven Keating, Sunanda Sharma, Daniel Dikovsky, Boris Belocon, James C. Weaver, Pamela A. Silver, and Neri Oxman. 2016. Grown, printed, and biologically augmented: an additively manufactured microfluidic wearable, functionally templated for synthetic microbes. 3D Printing and Additive Manufacturing 3, 2 (June 2016), 79–89. DOI:https://doi.org/10.1089/3dp.2016.0027

[6] S. Sandra Bae and Mary Etta West. 2021. Cyborg crafts: second SKIN (soft keen interaction). In Proceedings of the Fifteenth International Conference on Tangible, Embedded, and Embodied Interaction, TEI '21: Fifteenth International Conference on Tangible, Embedded, and Embodied Interaction, ACM, New York, NY, USA, 1–3. DOI:https://doi.org/10.1145/3430524.3444705

[7] Bahareh Barati, Elvin Karana, and Paul Hekkert. 2020. Understanding Experiential Qualities of Light-Touch-Matters: Towards a Tool Kit. JDT 1, 1 (May 2020), 1–20.

[8] Bahareh Barati, Elvin Karana, Sylvia Pont, and Tim van Dortmont. 2021. Living light interfaces — an exploration of bioluminescence aesthetics. In Designing Interactive Systems Conference 2021, DIS '21: Designing Interactive Systems Conference 2021, ACM, New York, NY, USA, 1215–1229. DOI:https://doi.org/10.1145/3461778.3462038

[9] Laurent Belcour, Romain Pacanowski, Marion Delahaie, Aude Laville-Geay, and Laure Eupherte. 2014. Bidirectional reflectance distribution function measurements and analysis of retroreflective materials. J. Opt. Soc. Am. A Opt. Image Sci. Vis. 31, 12 (December 2014), 2561–2572. DOI:https://doi.org/10.1364/JOSAA.31.002561

[10] Peter N Belhumeur, David J Kriegman, and Alan L Yuille. 1997. The Bas-Relief Ambiguity.

[11] Benne. 2019. Force Sensing Resistor (FSR) with Arduino Tutorial. (February 2019). Retrieved October 27, 2022 from https://www.makerguides.com/fsr-arduino-tutorial/

[12] Claus-Christian Carbon. 2014. Understanding human perception by human-made illusions. Front. Hum. Neurosci. 8, (July 2014), 566. DOI:https://doi.org/10.3389/fnhum.2014.00566

[13] Andre D Castiaux, Cody W Pinger, Elizabeth A Hayter, Marcus E Bunn, R Scott Martin, and Dana M Spence. 2019. PolyJet 3D-Printed Enclosed Microfluidic Channels without Photocurable Supports. Anal. Chem. 91, 10 (May 2019), 6910–6917. DOI:https://doi.org/10.1021/acs.analchem.9b01302

[14] Joshua V Chen, Alan B C Dang, and Alexis Dang. 2021. Comparing cost and print time estimates for six commercially-available 3D printers obtained through slicing software for clinically relevant anatomical models. 3D Print. Med. 7, 1 (January 2021), 1. DOI:https://doi.org/10.1186/s41205-020-00091-4

[15] B Choudhury and R M Jha. 2013. A review of metamaterial invisibility cloaks. Computers, Materials & Continua 33, 3 (2013), 275–303.

[16] Steven A. Cummer, Johan Christensen, and Andrea Alù. 2016. Controlling sound with acoustic metamaterials. Nat. Rev. Mater. 1, 3 (March 2016), 16001. DOI:https://doi.org/10.1038/natrevmats.2016.

[17] Elvan Dogan, Anant Bhusal, Berivan Cecen, and Amir K Miri. 2020. 3D Printing metamaterials towards tissue engineering. Applied Materials Today 20, (September 2020). DOI:https://doi.org/10.1016/j.apmt.2020.100752

[18] E L Doubrovski, E Y Tsai, D Dikovsky, J M P Geraedts, H Herr, and N Oxman. 2015. Voxel-based fabrication through material property mapping: A design method for bitmap printing. Computer-Aided Design 60, (March 2015), 3–13. DOI:https://doi.org/10.1016/j.cad.2014.05.010

[19] Jorge Duarte Forero, Guillermo E. Valencia, and Luis G. Obregón. 2018. Methodology of calibration of FSR sensor for seat occupancy detection in vehicles. Indian J. Sci. Technol. 11, 23 (June 2018), 1–7. DOI:https://doi.org/10.17485/ijst/2018/v11i23/126554

[20] Willemijn S. Elkhuizen, Boris A. J. Lenseigne, Teun Baar, Wim Verhofstad, Erik Tempelman, Jo M. P. Geraedts, and Joris Dik. 2015. Reproducing oil paint gloss in print for the purpose of creating reproductions of Old Masters. In Measuring, Modeling, and Reproducing Material Appearance 2015, IS&T/SPIE Electronic Imaging, SPIE, 93980W. DOI:https://doi.org/10.1117/12.2082918

[21] Tolga Ergin, Nicolas Stenger, Patrice Brenner, John B Pendry, and Martin Wegener. 2010. Three-dimensional invisibility cloak at optical wavelengths. Science 328, 5976 (April 2010), 337–339. DOI:https://doi.org/10.1126/science.1186351

[22] Roland W Fleming. 2014. Visual perception of materials and their properties. Vision Res. 94, (January 2014), 62–75. DOI:https://doi.org/10.1016/j.visres.2013.11.004 Roland W Fleming. 2017. Material Perception. Annu. Rev. Vis. Sci. 3, (September 2017), 365–388. DOI:https://doi.org/10.1146/annurev-vision-102016-061429

[23] Juri Fujii, Takuya Matsunobu, and Yasuaki Kakehi. 2018. COLORISE: Shape- and Color-Changing Pixels with Inflatable Elastomers and Interactions. In Proceedings of the Twelfth International Conference on Tangible, Embedded, and Embodied Interaction - TEI '18, the Twelfth International Conference, ACM Press, New York, New York, USA, 199–204. DOI:https://doi.org/10.1145/3173225.3173228

[24] Juri Fujii, Satoshi Nakamaru, and Yasuaki Kakehi. 2021. LayerPump: Rapid Prototyping of Functional 3D Objects with Built-in Electrohydrodynamics Pumps Based on Layered Plates. In Proceedings of the Fifteenth International Conference on Tangible, Embedded, and Embodied Interaction, TEI '21: Fifteenth International Conference on Tangible, Embedded, and Embodied Interaction, ACM, New York, NY, USA, 1–7. DOI:https://doi.org/10.1145/3430524.3442453

[25] Rüdiger Ganslandt and Harald Hofmann. 1992. Handbook of Lighting Design.

[26] Elisa Giaccardi and Elvin Karana. 2015. Foundations of materials experience: an approach for HCI. In Proceedings of the 33rd Annual ACM Conference on Human Factors in Computing Systems - CHI '15, the 33rd Annual ACM Conference, ACM Press, New York, New York, USA, 2447–2456. DOI:https://doi.org/10.1145/2702123.2702337

[27] Eduard Georges Groutars, Carmen Clarice Risseeuw, Colin Ingham, Raditijo Hamidjaja, Willemijn S. Elkhuizen, Sylvia C. Pont, and Elvin Karana. 2022. Flavorium: an exploration of flavobacteria's living aesthetics for living color interfaces. In CHI Conference on Human Factors in Computing Systems, CHI '22: CHI Conference on Human Factors in Computing Systems, ACM, New York, NY, USA, 1–19. DOI:https://doi.org/10.1145/3491102.3517713

[28] Miloš Hašan, Martin Fuchs, Wojciech Matusik, Hanspeter Pfister, and Szymon Rusinkiewicz. 2010. Physical reproduction of materials with specified subsurface scattering. ACM Trans. Graph. 29, 4 (July 2010), 1–10. DOI:https://doi.org/10.1145/1778765.1778798

[29] Tomoko Hashida, Yasuaki Kakehi, and Takeshi Naemura. 2011. Photochromic sculpture: Volumetric color-forming pixels. In ACM SIGGRAPH 2011 Emerging Technologies on - SIGGRAPH '11, ACM SIGGRAPH 2011 Emerging Technologies, ACM Press, New York, New York, USA, 1–1. DOI:https://doi.org/10.1145/2048259.2048270

[30] Interlink Electronics. FSR400 Series Integration Guide. Interlink Electronics.

[31] Alexandra Ion, Johannes Frohnhofen, Ludwig Wall, Robert Kovacs, Mirela Alistar, Jack Lindsay, Pedro Lopes, Hsiang-Ting Chen, and Patrick Baudisch. 2016. Metamaterial Mechanisms. In Proceedings of the 29th Annual Symposium on User Interface Software and Technology - UIST '16, the 29th Annual Symposium, ACM Press, New York, New York, USA, 529–539. DOI:https://doi.org/10.1145/2984511.2984540

[32] Alexandra Ion, Robert Kovacs, Oliver S. Schneider, Pedro Lopes, and Patrick Baudisch. 2018. Metamaterial Textures. In Proceedings of the 2018 CHI Conference on Human Factors in Computing Systems - CHI '18, the 2018 CHI Conference, ACM Press, New York, New York, USA, 1–12. DOI:https://doi.org/10.1145/3173574.3173910

[33] [Alexandra Ion, Ludwig Wall, Robert Kovacs, and Patrick Baudisch. 2017. Digital Mechanical Metamaterials. In Proceedings of the 2017 CHI Conference on Human Factors in Computing Systems, CHI '17: CHI Conference on Human Factors in Computing Systems, ACM, New York, NY, USA, 977–988. DOI:https://doi.org/10.1145/3025453.3025624

[34] Hiroshi Ishii, Dávid Lakatos, Leonardo Bonanni, and Jean-Baptiste Labrune. 2012. Radical atoms. interactions 19, 1 (January 2012), 38. DOI:https://doi.org/10.1145/2065327.2065337

[35] Hiroshi Ishii and Brygg Ullmer. 1997. Tangible bits. In Proceedings of the SIGCHI conference on Human factors in computing systems - CHI '97, the SIGCHI conference, ACM Press, New York, New York, USA, 234–241. DOI:https://doi.org/10.1145/258549.258715

[36] ISO/TC 261. 2021. ISO/ASTM 52900:2021.

[37] Hoon Yeub Jeong, Eunsongyi Lee, Soo-Chan An, Yeonsoo Lim, and Young Chul Jun. 2020. 3D and 4D printing for optics and metaphotonics. Nanophotonics 9, 5 (February 2020), 1139–1160. DOI:https://doi.org/10.1515/nanoph-2019-0483

[38] Yuhua Jin, Isabel Qamar, Michael Wessely, and Stefanie Mueller. 2020. Photo-Chromeleon: Re-Programmable Multi-Color Textures Using Photochromic Dyes. In ACM SIGGRAPH 2020 Emerging Technologies, SIGGRAPH '20: Special Interest Group on Computer Graphics and Interactive Techniques Conference, ACM, New York, NY, USA, 1–2. DOI:https://doi.org/10.1145/3388534.3407296

[39] R. Barry Johnson and Gary A. Jacobsen. 2005. Advances in lenticular lens arrays for visual display. In Current Developments in Lens Design and Optical Engineering VI, Optics & Photonics 2005, SPIE, 587406. DOI:https://doi.org/10.1117/12.618082

[40] Hsin-Liu (Cindy) Kao, Manisha Mohan, Chris Schmandt, Joseph A. Paradiso, and Katia Vega. 2016. Chromoskin: towards interactive cosmetics using thermochromic pigments. In Proceedings of the 2016 CHI Conference Extended Abstracts on Human Factors in Computing Systems - CHI EA '16, the 2016 CHI Conference Extended Abstracts, ACM Press, New York, New York, USA, 3703–3706. DOI:https://doi.org/10.1145/2851581.2890270

[41] Elvin Karana, Bahar Barati, Valentina Rognoli, and Anouk Zeeuw van der Laan. 2015. Material Driven Design (MDD): A Method to Design for Material Experiences. International Journal of Design in press, (May 2015).

[42] Steven J Keating, Maria Isabella Gariboldi, William G Patrick, Sunanda Sharma, David S Kong, and Neri Oxman. 2016. 3D printed multimaterial microfluidic valve. PLoS ONE 11, 8 (August 2016), e0160624. DOI:https://doi.org/10.1371/journal.pone.0160624

[43] Kevin G Keenan, Veronica J Santos, Madhusudhan Venkadesan, and Francisco J Valero-Cuevas. 2009. Maximal voluntary fingertip force production is not limited by movement speed in combined motion and force tasks. J. Neurosci. 29, 27 (July 2009), 8784–8789. DOI:https://doi.org/10.1523/JNEUROSCI.0853-09.2009

[44] Johnny C. Lee, Scott E. Hudson, and Edward Tse. 2008. Foldable interactive displays. In Proceedings of the 21st annual ACM symposium on User interface software and technology - UIST '08, the 21st annual ACM symposium, ACM Press, New York, New York, USA, 287. DOI:https://doi.org/10.1145/1449715.1449763

[45] Guanhong Liu, Haiqing Xu, Xianghua(Sharon) Ding, Mingyue Gao, Bowen Li, Fushen Ruan, and Haipeng Mi. 2022. "It Puts Life into My Creations": Understanding Fluid Fiber as a Media for Expressive Display. In CHI Conference on Human Factors in Computing Systems, CHI '22: CHI Conference on Human Factors in Computing Systems, ACM, New York, NY, USA, 1–15. DOI:https://doi.org/10.1145/3491102.3501990

[46] Francisco López Jiménez, Shanmugam Kumar, and Pedro Miguel Reis. 2016. Soft Color Composites with Tunable Optical Transmittance. Adv. Opt. Mater 4, 4 (April 2016), 620–626. DOI:https://doi.org/10.1002/adom.201500617

[47] Robert MacCurdy, Robert Katzschmann, Youbin Kim, and Daniela Rus. 2016. Printable hydraulics: A method for fabricating robots by 3D co-printing solids and liquids. In 2016 IEEE International Conference on Robotics and Automation (ICRA), 2016 IEEE International Conference on Robotics and Automation (ICRA), IEEE, 3878–3885. DOI:https://doi.org/10.1109/ICRA.2016.7487576

[48] Miodownik Mark and Tempelman Erik. Light Touch Matters the product is the interface.

[49] Yancheng Meng, Xue Gong, Yinan Huang, and Liqiang Li. 2019. Mechanically tunable opacity effect in transparent bilayer film: Accurate interpretation and rational applications. Applied Materials Today 16, (September 2019), 474–481. DOI:https://doi.org/10.1016/j.apmt.2019.07.013

[50] Maurice Merleau-Ponty. 1945. Phenomenology of Perception. Routledge, London and New York. DOI:https://doi.org/10.4324/9780203720714

[51] Benjamin Harvey Miller, Helen Liu, and Mathias Kolle. 2022. Scalable optical manufacture of dynamic structural colour in stretchable materials. Nat. Mater. 21, 9 (September 2022), 1014–1018. DOI:https://doi.org/10.1038/s41563-022-01318-x

[52] Stephen A Morin, Robert F Shepherd, Sen Wai Kwok, Adam A Stokes, Alex Nemiroski, and George M Whitesides. 2012. Camouflage and display for soft machines. Science 337, 6096 (August 2012), 828–832. DOI:https://doi.org/10.1126/science.1222149

[53] Hila Mor, Tianyu Yu, Ken Nakagaki, Benjamin Harvey Miller, Yichen Jia, and Hiroshi Ishii. 2020. Venous materials: towards interactive fluidic mechanisms. In Proceedings of the 2020 CHI Conference on Human Factors in Computing Systems, CHI '20: CHI Conference on Human Factors in Computing Systems, ACM, New York, NY, USA, 1–14. DOI:https://doi.org/10.1145/3313831.3376129

[54] Gregory Murphy. 2002. The Big Book of Concepts. (January 2002).

[55] Harold T. Nefs. 2008. On the visual appearance of objects. In Product Experience. Elsevier, 11–39. DOI:https://doi.org/10.1016/B978-008045089-6.50004-6

[56] Jifei Ou, Mélina Skouras, Nikolaos Vlavianos, Felix Heibeck, Chin-Yi Cheng, Jannik Peters, and Hiroshi Ishii. 2016. aeroMorph - Heat-sealing Inflatable Shape-change Materials for Interaction Design. In Proceedings of the 29th Annual Symposium on User Interface Software and Technology - UIST '16, the 29th Annual Symposium, ACM Press, New York, New York, USA, 121–132. DOI:https://doi.org/10.1145/2984511.2984520

[57] Jifei Ou, Lining Yao, Daniel Tauber, Jürgen Steimle, Ryuma Niiyama, and Hiroshi Ishii. 2013. jamSheets: Thin interfaces with tunable stiffness enabled by layer jamming. In Proceedings of the 8th International Conference on Tangible, Embedded and Embodied Interaction - TEI '14, the 8th International Conference, ACM Press, New York, New York, USA, 65–72. DOI:https://doi.org/10.1145/2540930.2540971

[58] Amanda Parkes and Hiroshi Ishii. 2010. Bosu: a physical programmable design tool for transformability with soft mechanics. In Proceedings of the 8th ACM Conference on Designing Interactive Systems - DIS '10, the 8th ACM Conference, ACM Press, New York, New York, USA, 189. DOI:https://doi.org/10.1145/1858171.1858205

[59] Jayson Paulose, Anne S Meeussen, and Vincenzo Vitelli. 2015. Selective buckling via states of self-stress in topological metamaterials. Proc Natl Acad Sci USA 112, 25 (June 2015), 7639–7644. DOI:https://doi.org/10.1073/pnas.1502939112

[60] Sylvia C Pont and Susan F te Pas. 2006. Material-illumination ambiguities and the perception of solid objects. Perception 35, 10 (2006), 1331–1350. DOI:https://doi.org/10.1068/p5440

[61] S C Pont, J J Koenderink, A J van Doorn, M W A Wijntjes, and S F te Pas. 2012. Mixing material modes. In Human Vision and Electronic Imaging XVII, IS&T/SPIE Electronic Imaging, SPIE, 82910D. DOI:https://doi.org/10.1117/12.916450

[62] Isabel P. S. Qamar, Rainer Groh, David Holman, and Anne Roudaut. 2018. HCI meets Material Science: A Literature Review of Morphing Materials for the Design of Shape-Changing Interfaces. In Proceedings of the 2018 CHI Conference on Human Factors in Computing Systems - CHI '18, the 2018 CHI Conference, ACM Press, New York, New York, USA, 1–23. DOI:https://doi.org/10.1145/3173574.3173948

[63] Tommaso Ranzani, Sheila Russo, Nicholas W Bartlett, Michael Wehner, and Robert J Wood. 2018. Increasing the Dimensionality of Soft Microstructures through Injection-Induced Self-Folding. Adv. Mater. 30, 38 (September 2018), e1802739. DOI:https://doi.org/10.1002/adma.201802739

[64] Majken K. Rasmussen, Esben W. Pedersen, Marianne G. Petersen, and Kasper Hornbæk. 2012. Shape-changing interfaces: A review of the design space and open research questions. In Proceedings of the 2012 ACM annual conference on Human Factors in Computing Systems - CHI '12, the 2012 ACM annual conference, ACM Press, New York, New York, USA, 735. DOI:https://doi.org/10.1145/2207676.2207781

[65] Christian Rendl, David Kim, Patrick Parzer, Sean Fanello, Martin Zirkl, Gregor Scheipl, Michael Haller, and Shahram Izadi. 2016. FlexCase: Enhancing Mobile Interaction with a Flexible Sensing and Display Cover. In Proceedings of the 2016 CHI Conference on Human Factors in Computing Systems - CHI '16, the 2016 CHI Conference, ACM Press, New York, New York, USA, 5138–5150. DOI:https://doi.org/10.1145/2858036.2858314

[66] Daniela K. Rosner, Miwa Ikemiya, Diana Kim, and Kristin Koch. 2013. Designing with traces. In Proceedings of the SIGCHI Conference on Human Factors in Computing Systems, CHI '13: CHI Conference on Human Factors in Computing Systems, ACM, New York, NY, USA, 1649–1658. DOI:https://doi.org/10.1145/2470654.2466218

[67] Daniel Saakes, Masahiko Inami, Takeo Igarashi, Naoya Koizumi, and Ramesh Raskar. 2012. Shader printer. In ACM SIGGRAPH 2012 Emerging Technologies on - SIGGRAPH '12, ACM SIGGRAPH 2012 Emerging Technologies, ACM Press, New York, New York, USA, 1–1. DOI:https://doi.org/10.1145/2343456.2343474

[68] [Ge Shi, Andrea Palombi, Zara Lim, Anna Astolfi, Andrea Burani, Silvia Campagnini, Federica G C Loizzo, Matteo Lo Preti, Alessandro Marin Vargas, Emanuele Peperoni, Calogero Maria Oddo, M Li, Joseph Hardwicke, Matthew Venus, Shervanthi Homer-Vanniasinkam, and Helge Arne Wurdemann. 2020. Fluidic Haptic Interface for Mechano-Tactile Feedback. IEEE Trans. Haptics 13, 1 (March 2020), 204–210. DOI:https://doi.org/10.1109/TOH.2020.2970056

[69] Ralph C. Smith. 2005. Smart material systems: model development. Society for Industrial and Applied Mathematics. DOI:https://doi.org/10.1137/1.9780898717471

[70] R D Sochol, E Sweet, C C Glick, S Venkatesh, A Avetisyan, K F Ekman, A Raulinaitis, A Tsai, A Wienkers, K Korner, K Hanson, A Long, B J Hightower, G Slatton, D C Burnett, T L Massey, K Iwai, L P Lee, K S J Pister, and L Lin. 2016. 3D printed microfluidic circuitry via multijet-based additive manufacturing. Lab Chip 16, 4 (February 2016), 668–678. DOI:https://doi.org/10.1039/c5lc01389e

[71] Gabor Soter, Martin Garrad, Andrew T. Conn, Helmut Hauser, and Jonathan Rossiter. 2019. Skinflow: A soft robotic skin based on fluidic transmission. In 2019 2nd IEEE International Conference on Soft Robotics (RoboSoft), 2019 2nd IEEE International Conference on Soft Robotics (RoboSoft), IEEE, 355–360. DOI:https://doi.org/10.1109/ROBOSOFT.2019.8722744

[72] P Speijer Diez. 2022. 3D printing with fluid analysis and guidelines Pablo Speijer-2021.

[73] Pablo Speijer Diez. 2022. 3D printed Fluidic systems. Delft University of Technology, Delft. Retrieved April 3, 2022 from http://resolver.tudelft.nl/uuid:708a9c8c-a1e6-49d7-9a1f-835b174265cd

[74] Stratasys. Polishing Coated Parts - PolyJet Printers. Retrieved November 29, 2022 from http://Polishing Coated Parts - PolyJet Printers

[75] Stratasys. 2021. Research Package Best Practice Guide. Stratasys.

[76] Stratasys. 2021. Voxel Printing Guide with GrabCAD Print - English.pdf. Stratasys.

[77] Stratasys. 2022. WSS150 Water Soluble Support - EN PolyJet Best Practice.pdf. Stratasys.

[78] Dag Svanæs. 2013. Interaction design for and withthe lived body. ACM Trans. Comput.-Hum. Interact. 20, 1 (March 2013), 1–30. DOI:https://doi.org/10.1145/2442106.2442114

[79] Skylar Tibbits. 2014. 4D Printing: Multi-Material Shape Change. Archit. Design 84, 1 (January 2014), 116–121. DOI:https://doi.org/10.1002/ad.1710

[80] Udayan Umapathi, Patrick Shin, Ken Nakagaki, Daniel Leithinger, and Hiroshi Ishii. 2018. Programmable droplets for interaction. In Extended Abstracts of the 2018 CHI Conference on Human Factors in Computing Systems - CHI '18, Extended Abstracts of the 2018 CHI Conference, ACM Press, New York, New York, USA, 1–1. DOI:https://doi.org/10.1145/3170427.3186607

[81] A Vallgårda, M Winther, N Mørch, and E Vizer. 2015. Temporal Form in Interaction Design. IJDesign 9, 3 (December 2015).

[82] Anna Vallgårda and Johan Redström. 2007. Computational composites. In Proceedings of the SIGCHI Conference on Human Factors in Computing Systems, CHI07: CHI Conference on Human Factors in Computing Systems, ACM, New York, NY, USA, 513–522. DOI:https://doi.org/10.1145/1240624.1240706

[83] Dhaval Vyas, Wim Poelman, Anton Nijholt, and Arnout De Bruijn. 2012. Smart material interfaces: A new form of physical interaction. In CHI '12 Extended Abstracts on Human Factors in Computing Systems, CHI '12: CHI Conference on Human Factors in Computing Systems, ACM, New York, NY, USA, 1721–1726. DOI:https://doi.org/10.1145/2212776.2223699

[84] Akira Wakita and Midori Shibutani. 2006. Mosaic textile: Wearable ambient display with non-emissive color-changing modules. In Proceedings of the 2006 ACM SIGCHI international conference on Advances in computer entertainment technology - ACE '06, the 2006 ACM SIGCHI international conference, ACM Press, New York, New York, USA, 48. DOI:https://doi.org/10.1145/1178823.1178880

[85] Guanyun Wang, Lining Yao, Wen Wang, Jifei Ou, Chin-Yi Cheng, and Hiroshi Ishii. 2016. xPrint: A Modularized Liquid Printer for Smart Materials Deposition. In Proceedings of the 2016 CHI Conference on Human Factors in Computing Systems - CHI '16, the 2016 CHI Conference, ACM Press, New York, New York, USA, 5743–5752. DOI:https://doi.org/10.1145/2858036.2858281

[86] L Wang and E Whiting. 2016. Buoyancy optimization for computational fabrication. Computer Graphics Forum 35, 2 (May 2016), 49–58. DOI:https://doi.org/10.1111/cgf.12810

[87] George M Whitesides. 2006. The origins and the future of microfluidics. Nature 442, 7101 (July 2006), 368–373. DOI:https://doi.org/10.1038/nature05058

[88] Karl Willis, Eric Brockmeyer, Scott Hudson, and Ivan Poupyrev. 2012. Printed optics: 3D printing of embedded optical elements for interactive devices. In Proceedings of the 25th annual ACM symposium on User interface software and technology - UIST '12, the 25th annual ACM symposium, ACM Press, New York, New York, USA, 589. DOI:https://doi.org/10.1145/2380116.2380190

[89] Daniel Wolfe and K W Goossen. 2018. Evaluation of 3D printed optofluidic smart glass prototypes. Opt. Express 26, 2 (January 2018), A85–A98. DOI:https://doi.org/10.1364/OE.26.000A85

[90] Lining Yao, Jifei Ou, Chin-Yi Cheng, Helene Steiner, Wen Wang, Guanyun Wang, and Hiroshi Ishii. 2015. bioLogic. In Proceedings of the 33rd Annual ACM Conference on Human Factors in Computing Systems - CHI '15, the 33rd Annual ACM Conference, ACM Press, New York, New York, USA, 1–10. DOI:https://doi.org/10.1145/2702123.2702611

[91] Jiani Zeng, Honghao Deng, Yunyi Zhu, Michael Wessely, Axel Kilian, and Stefanie Mueller. 2021. Lenticular Objects: 3D Printed Objects with Lenticular Lens Surfaces That Can Change their Appearance Depending on the Viewpoint. In The 34th Annual ACM Symposium on User Interface Software and Technology, UIST '21: The 34th Annual ACM Symposium on User Interface Software and Technology, ACM, New York, NY, USA, 1184–1196. DOI:https://doi.org/10.1145/3472749.3474815

[92] Fan Zhang, Huib de Ridder, Pascal Barla, and Sylvia Pont. 2019. A systematic approach to testing and predicting light-material interactions. J. Vis. 19, 4 (April 2019), 11. DOI:https://doi.org/10.1167/19.4.11

14

Appendices

Appendix A: Initial graduation Design brief

Personal Project Brief - IDE Master Graduation

TU Delft

Designing 3D printed fluidic systems for influencing human perception — project title

Please state the title of your graduation project (above) and the start date and end date (below). Keep the title compact and simple. Do not use abbreviations. The remainder of this document allows you to define and clarify your graduation project.

start date 24 - 01 - 2022 — 04 - 07 - 2022 end date

INTRODUCTION **

Please describe, the context of your project, and address the main stakeholders (interests) within this context in a concise yet complete manner. Who are involved, what do they value and how do they currently operate within the given context? What are the main opportunities and limitations you are currently aware of (cultural- and social norms, resources (time, money,...), technology, ...).

Multi-material 3D printing is a novel additive manufacturing (AM) technique that enables the creation of single 3d printed parts with a variety of different materials and properties. This technique allows for unprecedented possibilities in shape complexity, custom geometry and meta-material structures for material design. It greatly enhances the possibilities to alter properties, mechanical, and perceptual behavior of 3d printed objects [1]. Due to these unique characteristics, multi-material AM opens up a variety of possibilities for new product design applications, and human-product interactions.

A recent development of multi-material AM is the possibility to combine solid with liquid materials in one printed part, allowing the development of novel meta-material concepts that include interactive fluidic structures. Using non-3d printing methods, tangible interfaces with fluidic-structures were presented by the Tangible Media group at MIT. [2]. Within these interfaces, fluids simultaneously function as a sensor and display of tangible information. The concept of these interfaces is yet explored as a set of 2D venous structures that respond to mechanical inputs of the user. The fluid acts as an embedded analog fluidic sensor, dynamically displaying flow and color change (Figure 1) [3].

Based on the principle of these venous structures, another approach using a novel evolution in Polyjet 3D-printing: printable hydraulics [4], is carried out by Pablo Speijer as a graduation project at the faculty of IDE at the TU Delft [5]. The goal of this research is to create 3D fluidic structures rather than only 2D, whilst exploring different design applications. The (yet to be completed) result of this research presents a 3D fluidic structure in which the fluid acts as a medium to trigger dynamic material surface properties for corresponding mechanical inputs (Figure 2) [5], focusing on creating interactive, haptic interfaces

The unique properties of novel meta-materials in general and its ability to react and/ or manipulate in preprogrammed ways to external stimuli have shown to open up a wide variety of possibilities for dynamic human-product interactions, e.g. dynamic visual appearance [6],[7]. However the exploration of different design applications in which such materials are used to alter, influence or manipulate sensory perception is yet scarcely or close to completely unexplored.

[1] Dogan, E., Bhusal, A., Cecen, B., & Miri, A. K. (2020). 3D Printing metamaterials towards tissue engineering. Applied Materials Today, 20, 100752. https://doi.org/10.1016/j.apmt.2020.100752
[2] Mor, H., Yu, T., Nakagaki, K., Miller, B. H., Jia, Y., & Ishii, H. (2020). Venous Materials: Towards Interactive Fluidic Mechanisms. Proceedings of the 2020 CHI Conference on Human Factors in Computing Systems. https://doi.org/10.1145/3313831.3376129
[3] Mor, H., Nakagaki, K., Tianyu, Y., Miller, B. H., Jia, Y., & Ishii, H. (2020). Prototyping Interactive Fluidic Mechanisms. Proceedings of the Fourteenth International Conference on Tangible, Embedded, and Embodied Interaction. https://doi.org/10.1145/3374920.3374967
[4] MacCurdy, R., Katzschmann, R., Youbin Kim, & Rus, D. (2016). Printable hydraulics: A method for fabricating robots by 3D co-printing solids and liquids. 2016 IEEE International Conference on Robotics and Automation (ICRA). https://doi.org/10.1109/icra.2016.7487576
[5] Speijer, P. (2020). Graduation project TO BE COMPLETED
[6] Illusory Material. (2020). Illusory Material. Retrieved 26 January 2022, from https://www.illusorymaterial.com/

space available for images / figures on next page

introduction (continued): space for images

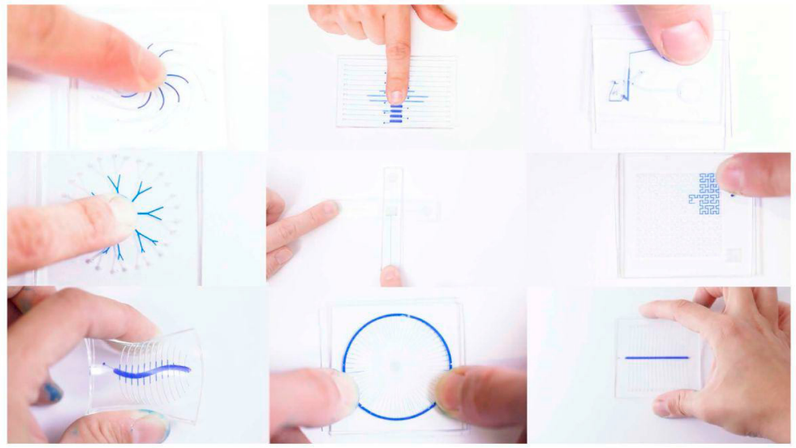

image / figure 1: 2D venous structures responding to human mechanical input. Mor, H et al. (2020).

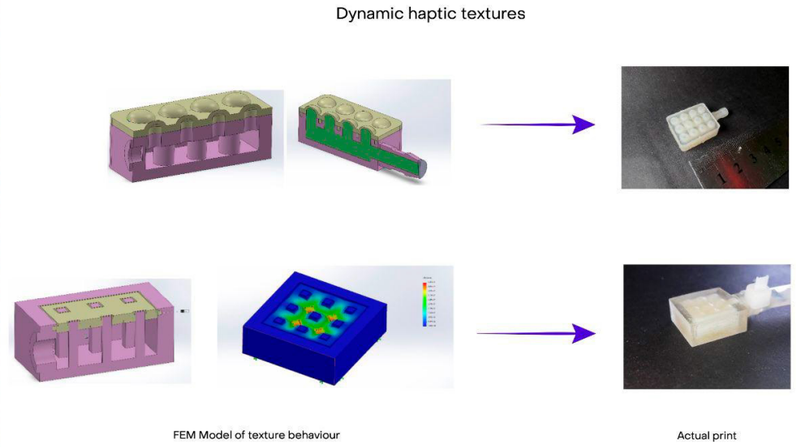

image / figure 2: Examples of 3D printed multi-material fluidic-structures for dynamic haptic texture. Speijer, P. (2022)

PROBLEM DEFINITION **

Limit and define the scope and solution space of your project to one that is manageable within one Master Graduation Project of 30 EC (= 20 full time weeks or 100 working days) and clearly indicate what issue(s) should be addressed in this project.

The current progress made with 3D printed fluidic-structures shows promising and unique possibilities. Preceding research has shown applications for mechanical triggering of different actuators using fluidics [1],[2]. However, further design applications and human-product interactions are still scarcely, close to completely unexplored. Especially from a human perception perspective, in which the unique dynamic sensory properties of such materials as color, shape, texture, or sound which could result in material qualities for new human-product interactions remain unexposed.

Furthermore, there is a need for research into the manufacturing process of 3D printable hydraulics for creating such fluidic interfaces. To date, few design guidelines and parameters have been defined [1], [2]. A better understanding of the manufacturing opportunities and limitations is needed in order to prototype and design for future applications.

The scope of this project is to discover new human-product interaction value, and explore perceptive performances and design applications of 3D printed fluidic interfaces. Whilst simultaneously creating new knowledge on the opportunities, limitations, guidelines, and parameters of using printable hydraulics as a manufacturing tool for fluidic-structures.

[1] MacCurdy, R., Katzschmann, R., Youbin Kim, & Rus, D. (2016). Printable hydraulics: A method for fabricating robots by 3D co-printing solids and liquids. 2016 IEEE International Conference on Robotics and Automation (ICRA). https://doi.org/10.1109/icra.2016.7487576
[2] Speijer, P. (2020). Graduation project TO BE COMPLETED

ASSIGNMENT **

State in 2 or 3 sentences what you are going to research, design, create and / or generate, that will solve (part of) the issue(s) pointed out in "problem definition". Then illustrate this assignment by indicating what kind of solution you expect and / or aim to deliver, for instance: a product, a product-service combination, a strategy illustrated through product or product-service combination ideas, ... In case of a Specialisation and/or Annotation, make sure the assignment reflects this/these.

The assignment is to deliver a product concept design and physical prototype which showcases and inspires designers for new design application(s) of fluidic-interfaces.

A new type of fluidic material and possible design applications will be designed using hydraulic printables through a hands-on, learning-by-doing approach, and an investigation into the state-of-the-art. The ultimate result of this process will be a product concept design, materialized in a newly developed material based on fluidic-structures, showcasing the possibilities of this material in a (future) design application.

The goal is to create value for new human-product interactions and showcase design applications for this novel material/ concept, whilst gaining new knowledge on the design guidelines, design parameters and material limitations when using printable hydraulics as a manufacturing process.

PLANNING AND APPROACH **

Include a Gantt Chart (replace the example below - more examples can be found in Manual 2) that shows the different phases of your project, deliverables you have in mind, meetings, and how you plan to spend your time. Please note that all activities should fit within the given net time of 30 EC = 20 full time weeks or 100 working days, and your planning should include a kick-off meeting, mid-term meeting, green light meeting and graduation ceremony. Illustrate your Gantt Chart by, for instance, explaining your approach, and please indicate periods of part-time activities and/or periods of not spending time on your graduation project, if any, for instance because of holidays or parallel activities.

start date 24 - 1 - 2022 4 - 7 - 2022 end date

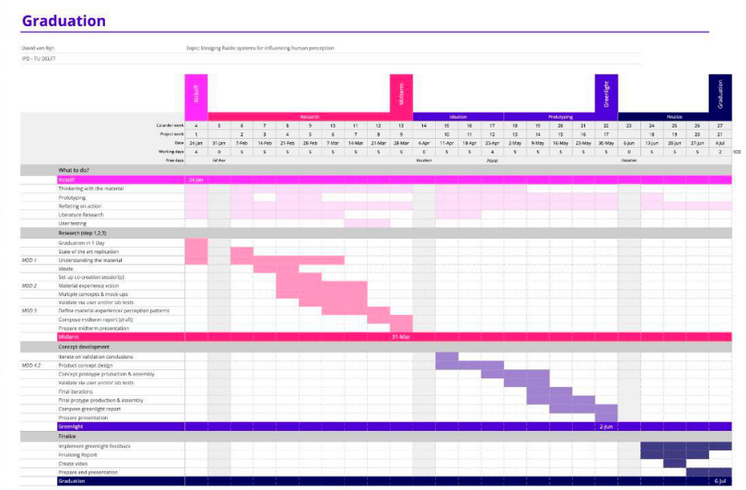

Personal Project Brief - IDE Master Graduation

TU Delft

MOTIVATION AND PERSONAL AMBITIONS

Explain why you set up this project, what competences you want to prove and learn. For example: acquired competences from your MSc programme, the elective semester, extra-curricular activities (etc.) and point out the competences you have yet developed. Optionally, describe which personal learning ambitions you explicitly want to address in this project, on top of the learning objectives of the Graduation Project, such as: in depth knowledge a on specific subject, broadening your competences or experimenting with a specific tool and/or methodology, ... Stick to no more than five ambitions.

Motivation and personal ambitions
During my masters (IPD) I discovered a great interest in digital manufacturing processes and generative design. Applying basic knowledge on these subjects within the course AED, I experienced myself the endless possibilities of these novel design approaches, and that it heavenly influences the way we can design and make as of today and in the future. Currently my AED team and I are still involved in the development of a football goalkeeper wrist guard, applying basic digital manufacturing and generative modeling techniques. I would like to extend my knowledge on these 2 subjects, as I foresee myself working in an environment using these techniques in my professional career after my graduation.

Besides, I highly enjoyed the course Lighting Design. Within this course I discovered the basic knowledge on how humans receive visual stimuli, enabling me as a designer to design for different visual experiences. This reflects and complemented with my activities as a DJ and stage designer within my personal life, in which I partly use sound and light as stimuli for visitors to perceive, enjoy and experience their surroundings. The end-result of the course was a dynamic interactive light installation which was envisioned to be present at a future party (>300 visitors).

Only recently I came across a fascinating topic: meta-materials. Using (future) digital manufacturing tools and generative design approaches we are constantly pushing the possibilities to design, manufacture (on a small scale) and predict the behavior of materials which are able to adapt and complement their surroundings in a dynamic way. This creates the possibility to design for human- product interactions we've never experienced before. The unique properties of meta-materials to manipulate and alter (natural) stimuli fascinates me most, since we as humans perceive these same stimuli activating such materials through our senses, ultimately resulting in the human umwelt, or "our reality". What if we could expand, change or manipulate these stimuli in such a way, so we can perceive things we've never experienced before? Like seeing in X-ray or hearing in ultrasonic sound? Would that result in a new human umwelt?

Yet developed:
- Interest & basic knowledge on digital manufacturing processes during AED.
- Interest & basic knowledge on generative modeling (grasshopper) during AED.
- Interest & basic knowledge on visual perception (light) during Lighting Design.
- Experience & knowledge in creating interactive experiences & installations using sound & light as a DJ and stage designer in personal life.

Learning ambitions
- Extend in depth knowledge on Human perception.
- Extend in depth knowledge on Metamaterials & fluidic-structures.

- Experiment with digital manufacturing tools and multi-material printing.
- Experiment with generative modeling (grasshopper)

FINAL COMMENTS

In case your project brief needs final comments, please add any information you think is relevant.

Prof. dr. Sylvia Pont (Perceptual Intelligence) will also be partly involved in this project as a (3rd) advising expert on human perception and visual appearance.

Initials & Name D van Rijn 5501 Student number 4457951

Title of Project Designing 3D printed fluidic systems for influencing human perception

Appendix B: Initial explorative research on 3D printing workflows

Following an iterative research and design approach, three promising workflows are explored and validated for the manufacturing of a fluidic interface:

- Air printing
- Hydraulic printing
- Pause print (only studied in literature)

Each of the workflows has been validated and optimised for their capabilities to manufacture the main components of the *Fluidic Interface Architecture* as presented in chapter 5; *Liquid Channels*, *Liquid Repositories* and *Liquid Surfaces*. An overview of the different workflows and the results for printing different Fluidic components is presented in Table 1.

	Fluidic cavities			Overall	
	Channels	Repositories	Surfaces	Pro	Con
Liquid printing					
Agilus 30	- 0.32 > 2.1mm - x/y > 0.4mm [26] - z > 0.2mm [26] - Print along x-axis	- x/y/z < 20mm [2] [26] - Print long sides along x-axis [26]	- x/y > 20mm [26] - z > 0.2mm [26]	- Form freedom in channel geometry - Can print closed off integrated liquid geometries (no draining) - Refraction index of liquid material is close to substrate material	- Poor fluid/ substrate interface - Delamination due to liquid spillage oby roller - Top layer collapse for printing on top of liquid material - Limited to Cleanser fluid
VeroClear	- Equals Agilus 30 - Print along x-axis	- x/y/z < 20mm [[26] - Print long sides along x [26]	- x/y > 20mm [26] - z > 0.2mm [26]	- Equals Agilus 30	- Equals Aglius 30, with slightly better fluid/ substrate interface
Air printing					
Agilus 30	-3° < ∠ < 23° - Cone or diamond section [42] - Print along x/y-axis 45°	- Not possible	- Not possible	- Good air/ substrate interface - No draining needed	- Limited form freedom of liquid structures - Can not print surfaces or repositories - Needs thick walls > 1mm - Needs injection of liquid material

VeroClear	-4° < ∠ < 9° - Cone or diamond section [[42] - Print at x/y 45°	- Not possible	- Not possible	- Equals Aglius 30	- Equals Aglius 30 - Limited top corner
Pause printing Glycol					
Agilus 30	- Unknown	- Unknown	- Unknown	- Unknown	- Unknown
VeroClear	- 0.2 x 0.2mm with liquid [8]	- Unknown	- Unknow - Shows possibilities	- Shows promising liquid/ substrate interface [8] - Small >0.2mm channeling [8]	- Limited form freedom for liquid geometries - Only suitable for cavities with open top (in z-direction) - Print needs to be paused
Pause printing Membrane					
Agilus 30	- Unknown	- Unknown	- Unknown	- Unknown	- Unknown
VeroClear	- 0.125 x 0.054mm with membrane [8]	- 6x15x35mm shows good result [8]	- Unknow - Seems possible	- Shows promising liquid/ substrate interface [8] - Small >1.26mm channelling [8]	- Limited form freedom for liquid geomtries - Only suitable for cavities with open top (in z-direction) - Print needs to be paused - Membrane placement is critical and needs training
Support printing					
Agilus 30	- Unknown	- Maximum printer dimensions	- >0.05mm	- Form freedom in cavity design - Good surface interface quality	- Support material is difficult/ impossible to remove - No long channels possible - Complex geometries not possible due to support removal
VeroClear	- > 0.7mm [6]	- Maximum printer dimensions	- >0.05mm	- Equals Agilus 30	- Equals Agilus 30

Table 1: An overview of the printing workflows and corresponding results based on literature or findings within this research.

Air printing

Air printing is a novel feature within the digital GrabCad Print environment of Stratasys, which enables users to select 'air' as a printing material for PolyJet printing. It is presented in the Research Package of Stratasys [42] and only available for selected research partners..

Capabilities of air printing

Within the typical workflow of PolyJet printing, it is not possible to print 'overhangs'. When cavities are modelled as empty space inside a body, these are filled with support material during the printing process. The support provides a base layer for the photopolymer droplets which are deposited on top of the cavity. In fact, every 'empty' space within a 3D-model is completely filled with support material during printing.

The workflow of *Air Printing* enables printing empty cavities in a body which are not filled with PolyJet support material. However, due to the process of PolyJet, printing overhangs is still very limited. Droplets of uncured resin seem to displace before curing when no sufficient support layer is present. To overcome this effect, Stratasys presented the limitations of air printing for air cavities, with a top corner ranging from 6 to 9 degrees [42] (Figure 1).

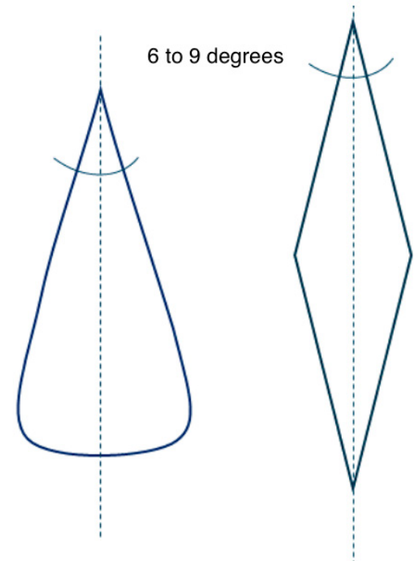

Figure 1: cross sections of Air Repositories as presented by Stratasys in the Research package.

To manufacture fluidic interfaces, *Air Printing* is researched for its ability to create *Liquid Channels* and *Air Repositories* with a cross section as shown on the left in Figure 1. Since *Air Printing* is limited to geometries with sharp top corners, the height to width ratio of *Liquid Repositories* is very high. Consequently, the validation of *Air Printing* to manufacture large *Liquid Repositories* and *Surfaces* is left out of this research.

It must be pointed out that all of the *Liquid Channels* produced using *Air printing* are printed as 'empty' channels. Dyed water is injected in the *Air Channels* after printing as a *Liquid Material* to validate the samples on its flow performance. *Liquid Channels* printed using this workflow will be referred to as *Air Channels*.

Main challenges of air printing

- Channel collapse for printing larger top corners than listed by Stratasys, resulting in a high height to width ratio.
- Channel collapse for channels printed close to each other.
- Channel or repository orientation; top corner must always point in the direction of the +Z-axis.

A typical collapse of a 3D printed *Air Channel* is shown in Figure 2. *Substrate Material* creeps down during printing, resulting in an 'open' channel at the top. Possible causes and parameters of this behaviour ar are the wetting and viscosity of 3D printed resin (Vero™ or Agilus™)

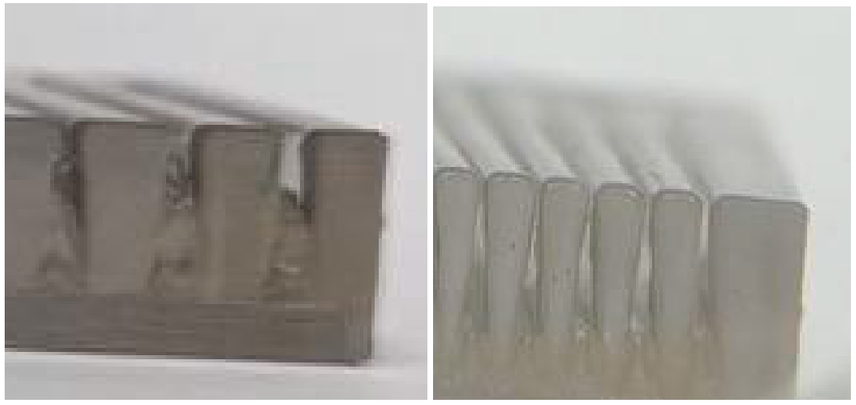

Figure 2: two typical air channels collapsed. Top of the channel is open and Substrate material flows down in the channel.

Air printing results

Air repositories

Air Printing allows for small encapsulated air repositories as designed and oriented in Figure 3 with top corners ranging from 5 to 12 degrees (Table 2). No visible difference has been reported between VeroClear™ and Agilus30™. Print orientation should be designed in such a way, the top of the repositories points in the +Z axis. X-Y orientation does not affect printed parts, since the *Air Repositories* are modelled having full rotational symmetry.

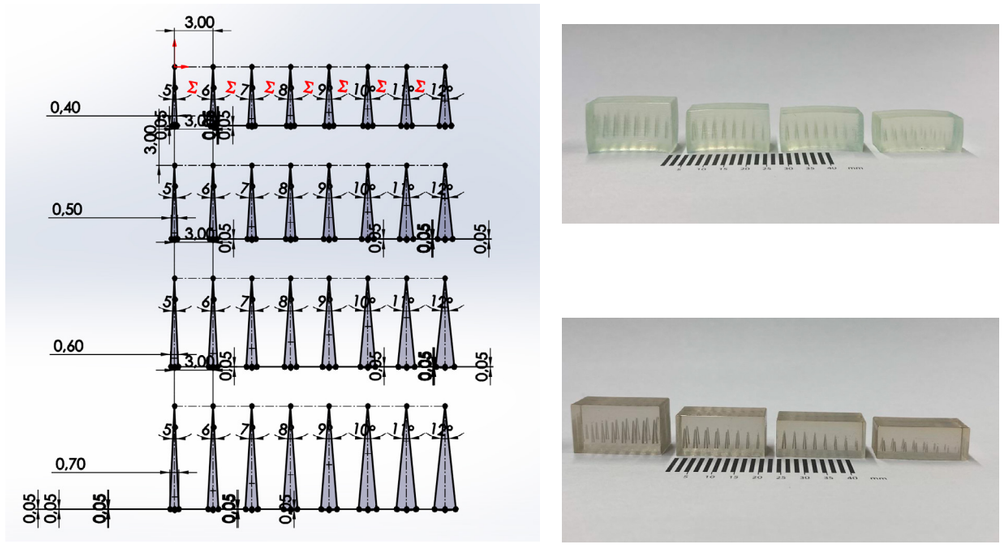

Figure 3: Design en results of Air repositories. Sections revolve around the centre axis resulting in rotational symmetry.

Top corner (°)	0.4mm height	0.5mm height	0.6mm height	0.7mm height
	Vero material			
5				
6				
7				
8				
9				
10				
11				
12				
	Agilus			
5				
6				
7				
8				
9				
10				
11				
12				
	Printed succeed			
	Printed did not succeed			

Table 2: Results for air repository printing.

Air Channels

Using *Air Printing as* a manufacturing tool for *Air Channels* shows different results for VeroClear™ and Agilus30™. *Air Channels* as modelled in Figure 4 allow flow of liquid as presented in Table 3. Parts orientated with *Air Channels* running at 45 degrees in the X- and Y-axis show less collapsing (Figure 5).

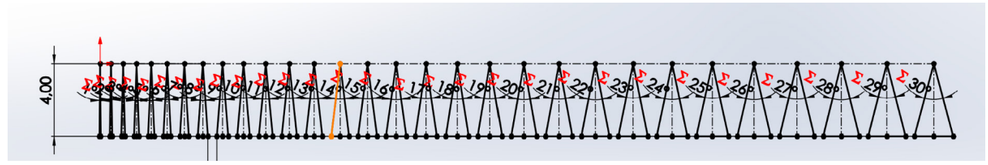

Figure 4: Design of test sample for validation of Air Channel printing on liquid flow.

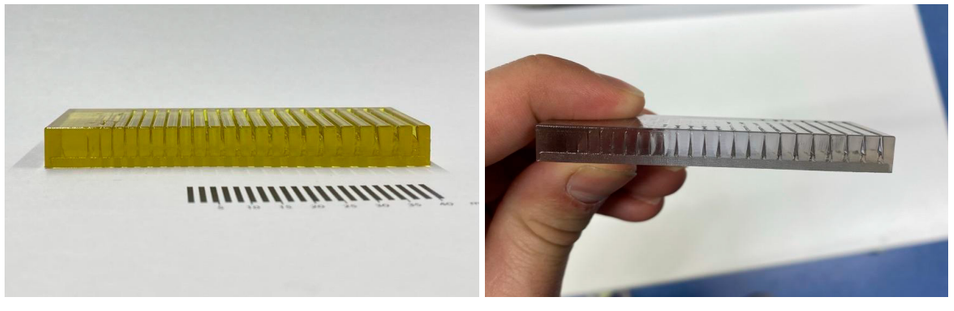

Figure5: sample printed at 45 degrees along x- and y-axis (right) shows less collapsing of air channels than when channels are printed along x-axis(left).

Top corner (°)	Aglius	Vero	Vero 45°
1			
2			
3			
4			
5			
6			
7			
8			
9			
10			
11			
12			
13			
14			
15			
16			
17			
18			
19			
20			
21			
22			
23			
24			
25			
26			
27			
28			
29			
30			
	Liquid flows		
	Liquid doen not t flow		
	Print failed		

Table 3: Flow of liquid through Air channels

The minimum separation of *Air Channels* within VeroClear™ and Agilus30™ is validated using test samples as shown in Figure 6 . It was reported all of the channel prints failed as shown in figure 7. Therefore Minimum separation of *Air Channels* for Agilus30™ and VeroClear™ could not be determined. Test samples are printed orientated with channels running along the X-axis. It is likely printing *Air Channels* running at 45 degrees in the X- and Y-axis results in a lower minimum separation.

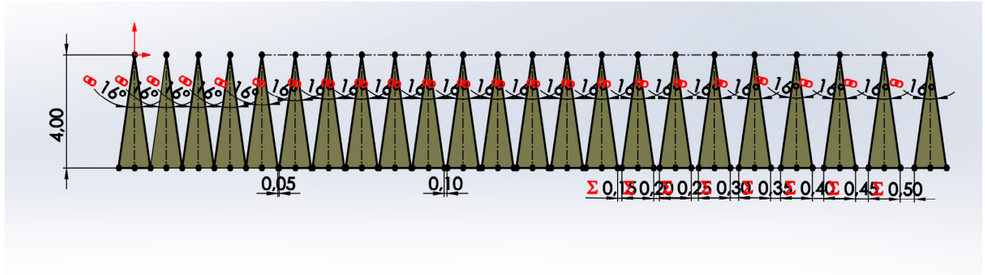

Figure 6: Cross section of design for testing air channel separation.

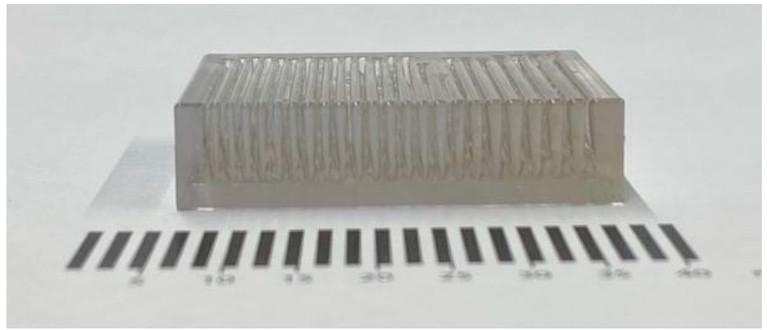

Figure7: result for Air channel separation print.

Conclusions for air printing

Air Printing is a suitable workflow for creating small *Fluidic Channels*, but only for a small range of dimensions. Besides, it has to be taken into account that channels are always subject to injection of *Liquid Material* after printing. Therefore parts printed with this technique are always in need of one or multiple inlets or a workflow which allows to inject and seal the 3D printed parts..

Furthermore, *Air Channel* geometries are very limited in design freedom. Due to the sharp top corner, which in any case should point towards the +Z axis. Finally, *Air Printing* does not allow for *Air Channels* printed close to each other as channels are likely to collapse.

Hence the result of this validation, *Air Printing* is not considered as a suitable solution for the creation of *Liquid Channels* of *Fluidic Interfaces*. This is due to its limited freedom in channel geometries and limitations regarding minimum channel separation and top corners.

However, it does show promising results for tiny *Air Repositories*, with top corners ranging beyond the limitations known in literature. Such Repositories have been used for optical 3D printed mechanisms before [46]. To conclude, *Air printing* will not be the main focus for the continuation of this research, but will be taken into account for possible future configurations in which tiny air repositories are needed.

Recommendations for air printing

Air Channel printing performs best, when parts are orientated in such a way channels are running at 45 degrees along the X- an Y-axis. The results also point out Aglius30 performs better than VeroClear™ for printing *Air Channels*. This effect is hypothetically subjective to its wetting and viscosity properties. However further determination and validation on wetting and visceral behaviour of different PolyJet materials should be performed to validate this difference. A proposal to overcome this effect is to model thin walls surrounding the *Air Channels* within VeroClear™ parts. These walls should be composed of Agilus30 material, or a voxel based mix of Agilus30 and VeroClear™. Another approach could be to design 'self supporting' geometries for *Air Channels* as presented in [45], [43].

In this research it is proven rotational symmetrical *Air Repositories* can be printed for top corners extending the limitations as provided by Stratatsys, up to 12 degrees. For specific applications such as 3D printed optics as presented in [46], *Air Printing* shows promising capabilities. Further research could be performed to determine the boundaries of printing rotational symmetrical air repositories.

Liquid printing

Liquid printing is a novel approach for PolyJet 3D printing, which simultaneously prints typical PolyJet materials and a liquid material in a single part. *Liquid printing* was first introduced as *Hydraulic printing* by Robert MacCurdy et al. in 2016 [26] as an approach to manufacture functional robotics in a single printing run. Stratasys provided this workflow as *Liquid Printing* later on in their research package in 2021 [42].

Liquid Printing enables one to directly select the Cleanser material, a cleaning fluid for PolyJet systems, as a printer material within the GrabCad Print digital environment. The cleanser material droplets are deposited layer by layer through the printer head as a normal polymer resin (like Vero™ or Agilus™), yet does not cure when exposed to UV Light. By combining the Cleanser with typical PolyJet materials, encapsulated liquid bodies can be printed in a single component, in a single run.

Capabilities of liquid printing

Liquid printing offers several opportunities for manufacturing fluidic interfaces:

- No additional assembly or injection is needed because liquid droplets are deposited simultaneously with the *Substrate Material [26]*, [40].
- The liquid can be used as an incompressible hydraulic fluid, for actuation of *Substrate Mechanical Actuators* within a fluidic network [26], [40].
- The liquid can be used as a liquid support material. This enables complex structures such as capillary-like structures which are typically impossible to clear using PolyJet support material [26], [2].

For these capabilities *Liquid Printing* is promising as a manufacturing workflow for *Fluidic Interfaces*. Theoretically, it enables printing of all of the *Fluidic Cavities* in the *Fluidic Architecture*.

Within this research *Liquid Printing* has been used for manufacturing *Liquid Channels, Liquid Repositories and Liquid surfaces*. A variety of test samples has been produced and analysed within an iterative research and design process. The ultimate goal of this approach is to find the limitations, critical parameters and design guidelines for designing *Fluidic Interfaces* which are printed using *Liquid Printing*.

Maccurdy presents a set of *Liquid Printing* guidelines which are shown in Table 4 [26]. Combined with the recommendations found by Speijer in [40], [39] these form the guidelines which are taken into account for designing the test samples in this research.

1	Separation (minimum along X/Y-axis):	0.4 mm
2	Separation (minimum along Z-axis):	0.2 mm
3	Feature thickness (minimum along X/Y-axis):	0.325 mm
4	Feature thickness (minimum along Z-axis):	0.2 mm
5	Feature growth (perpendicular to Y/Z-axis)	0.150 mm
6	Feature growth (perpendicular to X-axis)	0.2 mm
7	Solid-solid clearance at rotational joint	0.3 mm
8	Solid-over-liquid support thickness	0.2 mm
9	Solid-next-to-liquid support thickness	0.5 mm
10	Largest segment of liquid (dist in X or Y)	20 mm
11	Recommended width of support “pillars” inserted to connect model layers otherwise isolated by liquid; see Fig. 8 (X/Y-axis):	0.5 mm
12	Recommended solid feature thickness when adjacent to largest liquid segment (X/Y-axis):	2.11 mm

Table 4: Design guidelines for Liquid printing as presented by Maccurdy [26].

Main challenges of liquid printing

Maccurdy and Speijer [26], [40], [39] describe a set of challenges to overcome when printing with *Liquid Material*. During the iterative process of designing and producing the *Liquid Print* samples for this research the same challenges were identified:

- Top layers collapse for *Liquid Repositories* Figure 8.
- Poor interface surface quality between *Liquid* and *Substrate Material* Figure 10.
- Delamination of printed layers surrounding large Liquid area’s Figure 12.

Top layer collapse

Maccurdy [26] found *Liquid Repositories* with a surface area exceeding 20mm in one axis (X- or Y-axis) are subject to top layer collapse, as shown in Figure 8. This effect is caused by sinking of the deposited droplets *Substrate Material* on top of the printed *Liquid Material*. Maccurdy defines a solution for this effect by: integrated support pillars or walls within the *Liquid Material* as defined in Figure 9. These support structures can provide structural support for the top layers of a *Liquid Repository*.

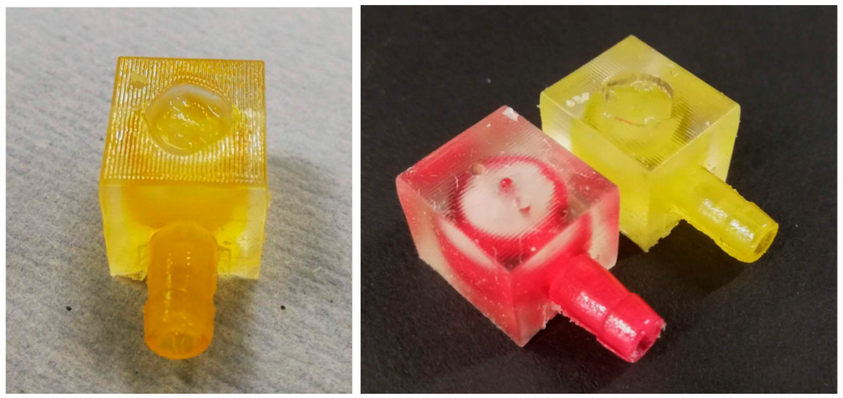

Figure 8: Collapsed top layers printed on Liquid Repository appear in the left (yellow) part [39].

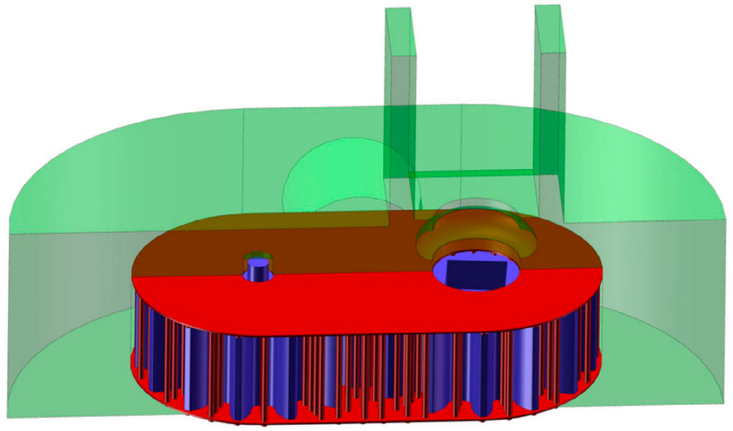

Figure 9: Support pillars modelled in a Liquid area (red pillars in between two layers) [26].

Poor interface surface quality

Liquid printed parts show poor surface qualities at the interface of Liquid and Substrate Material Figure 10. It is strongest for the top surface of Liquid Cavities. The sides of Liquid Cavities show a slightly better surface quality [39]. The poor qualities do not occur at the bottom surface, since the *Substrate Material* of the base layer is already cured when *Liquid Material* droplets are deposited on top. It is known [39] poor surfaces occur stronger for Agilus™ materials than for Vero™ materials.

Figure 10: Poor surface interface quality.

Possible solutions for poor surface quality are presented by Maccurdy and Speijer [26], [39], by modelling a thin wall of support material between *Liquid* and *Substrate material* of approximately 0.2mm thick [26].

Delamination

Delamination of printed layers occurs for walls surrounding *Liquid Reposities*. This effect is also reported by Speijer [39], named as *improperly cured resin*. Figure 11 shows delamination occurs mostly in walls parallel to the Y-axis. Walls running along the X-axis are less subject to delamination. This is due to the print direction and roller of the printer.

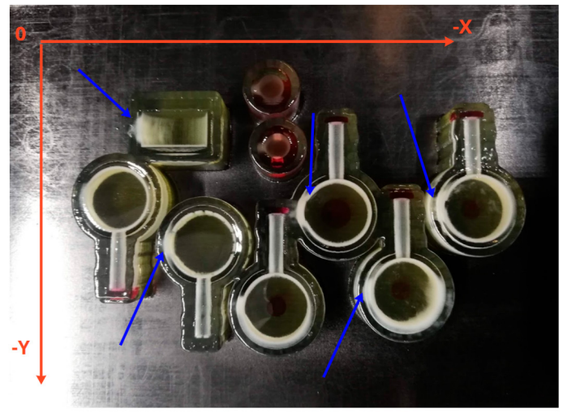

Figure 11: Walls along the Y-axis are more subject to delamination [39].

Delamination is caused by spillage of *Liquid Material* during printing. The liquid can be seen ‘waving’ during printing, especially along the X-axis.. Liquid ‘spills’ over its surrounding layers of cured *Substrate Material* before a new layer of photopolymer droplets are deposited. This causes a bad layer adhesive of the *Substrate Material* as shown in Figure 12.

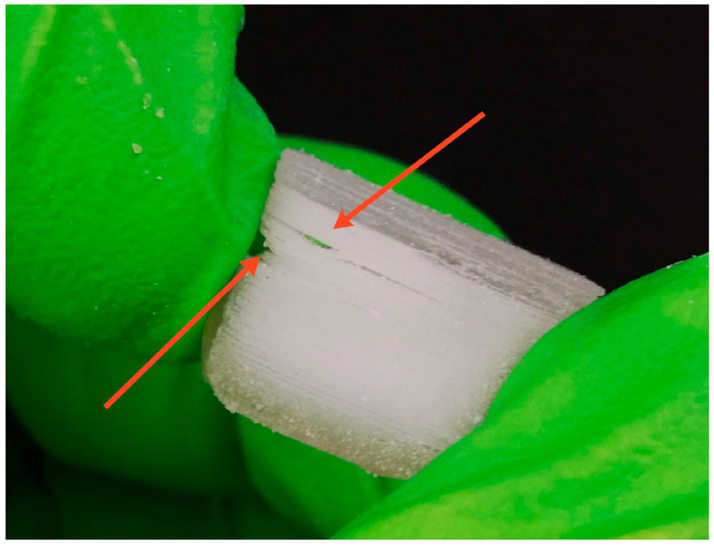

Figure 12: Delamination of layers printed next to liquid repositories.

Causes for ‘waving’ of Liquid Material are:

- The roller: during printing a roller sweep over the printed layers, to scrape off excess material. As an effect Liquid Material waves appear in the direction of the roller’s movement.
- Print bed shake: the printhead moves along the X-axis back and forth during printing. When it comes to a stop, this causes a slight shake to the print bed. However, *Liquid Material* movement seems to be marginally due to this effect.

Possible solutions for delamination presented in [26] and [39] are a minimum wall thickness of 2.11mm for walls adjacent to large *Liquid Repositories*. Additional support walls along the Y-axis within liquid repositories can be added to reduce ‘waving’ of the liquid material during printing.

Liquid printing results

Liquid Channels

Small *Liquid Channels* channels have been printed to validate flow resistance for *Liquid Material*. The channels are designed as presented in Figure 13 To overcome the effect of poor surface quality, thin support membranes are printed surrounding the liquid material (0.105 and 0.210mm). The parametric results of the flow resistance are presented in Table 5. Poor interface surface qualities were still present, yet slightly better than no support membranes. No visible difference is found for 0.105mm or 0.210mm support membranes. Two samples were printed for each validation; one along the X-axis and one 45 degrees along X- and Y-axis. No difference in flow resistance, surface quality or delamination is reported.

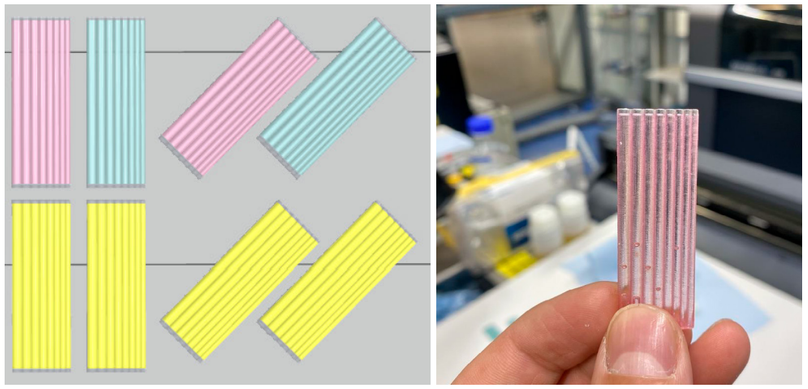

Figure 13: design and result of liquid channel test. Liquid channels diameter: 0.21 to 2.1mm with intervals of 0.315mm, channel length 50mm.

Channel diameter (mm)	Vero 0.105mm support Along y-axis	Vero 0.210mm support Along y-axis	Vero 0.105mm support 45°	Vero 0.210mm support 45°	Aglius 0.105mm support Along y-axis	Aglius 0.210mm support Along y-axis	Agilus 0.105mm support 45°	Aglius 0.210mm support 45°
0.210								
0.525								
0.840								
1.155								
1.470								
1.785								
2.100								
	Did not flow							
	Flow							

Table 5: Results of flow test for liquid channels.

For better observation of surface quality and delamination effects, larger *Liquid Channels* are printed Figure 14. Again, thin support membranes are printed, with the addition of support pillars or support walls. Again, poor surface quality is visible for all of the test samples. Large channels printed along the X-axis are less subject to top layer collapse, however show more delamination. Large channels printed 45 degrees along the X- an Y-axis show more collapse, yet less delamination. For the two support structures tested, walls show the best results to prevent both collapse as delamination.

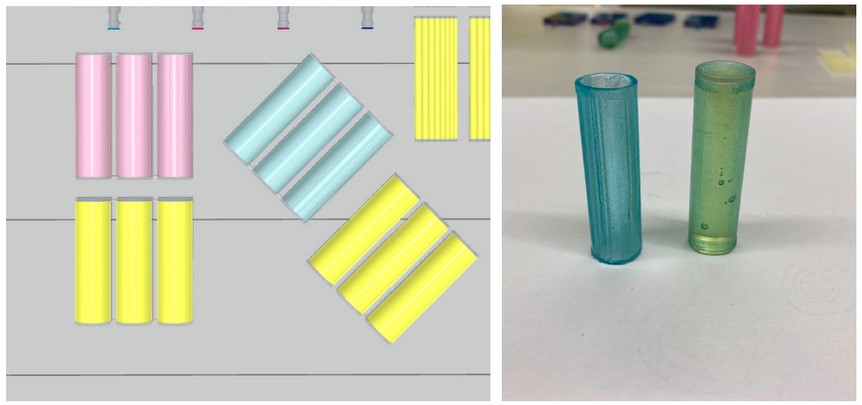

Figure 14: Design and result of large channels test. On the left: a channel without and with Cleanser liquid inside.

Liquid Surfaces

Liquid Surfaces surpassing 20mm in both the X- and Y-axis have been printed Figure 15. The *Liquid Surfaces* were modelled as 0.21 and 0.42mm thick and with and without support membrane on top. For Liquid surfaces of 0.42mm thick, it is reported Liquid is able to be flushed out. Top and bottom layers of *Substrate Material* were separated throughout the whole surface. Delamination is reported for *Substrate Material* surrounding the *Liquid Surface* along the X-axis. However, this effect occurs less than for Liquid Repositories (>0.5mm thick).

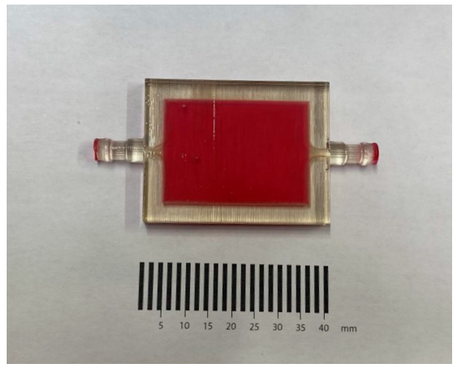

Figure 15: Printed Liquid surface surpassing 20x20mm in X- and Y- direction.

Liquid Repositories

Liquid Repositories have shown to be highly subject to collapse and delamination as presented in [39]. Within his research ‘waving’ of liquid repositories has been reported for larger volumes. During printing.

Conclusions

After the first iterations on Liquid printing the following can be concluded:

- Small Liquid channels can be printed and flushed for diameters ranging between 0.32mm to 2.1mm.
- Adding support membranes (0.105mm) does improve poor surface quality.
- Using Cleanser as a liquid material conceals poor surface quality. It is assumed this is due to the refraction index of the fluid, further research can be performed to identify the specific cause of this effect and possibility to use other liquids.
- Liquid surfaces are less subject to delamination and collapse, further research can be performed to find the limitations in X-, Y- and Z-axis.
- The optimum orientation for larger liquid repositories is 45 degrees along X- and Y-axis in addition with support walls.
- Voxel based Liquid and support material is yet to be validated.

Pause printing

Pause printing allows for pausing and resuming a print operation at a specific layer or slice height. Within the pause one can insert electronics, components, membranes or most importantly: inject a fluid. The print can then resume to encapsulate these components into the 3D printed body. It shows promising capabilities for printing *Fluidic Interfaces,* as it has been used for the manufacturing of several microfluidic devices [8]. It enables the injection and encapsulation of different liquids than the printed Cleanser material.

Within this research pause printing has not been validated, but based on the findings in literature it shows promising opportunities for 3D printing fluidic interfaces.

Most important insights

- *Air Printing* can print rotational symmetrical *Air Repositories* which extend the limitations given by Stratasys.
- Small *Liquid Channels* can be printed and flushed for diameters ranging between 0.32mm to 2.1mm.
- *Liquid Surfaces* appear to be less subject to collapse and delamination effects.
- Liquid printing is most suitable for 3D printing fluidic interfaces, however it still has limitations in terms of:
    - Poor interface surface quality between liquid and substrate material.
    - Delamination of substrate material layers surrounding liquid material.
    - Top player collapse for printing on top of liquid area's exceeding 20x20mm.

Bibliography

1. MacCurdy R, Katzschmann R, Youbin Kim, Rus D. Printable hydraulics: A method for fabricating robots by 3D co-printing solids and liquids. 2016 IEEE International Conference on Robotics and Automation (ICRA). IEEE; 2016. p. 3878–85.
2. Stratasys. Research Package Best Practice Guide. Stratasys; 2021.
3. Castiaux AD, Pinger CW, Hayter EA, Bunn ME, Martin RS, Spence DM. PolyJet 3D-Printed Enclosed Microfluidic Channels without Photocurable Supports. Anal Chem. 2019 May 21;91(10):6910–7.
4. Willis K, Brockmeyer E, Hudson S, Poupyrev I. Printed optics: 3D printing of embedded optical elements for interactive devices. Proceedings of the 25th annual ACM symposium on User interface software and technology - UIST '12. New York, New York, USA: ACM Press; 2012. p. 589.
5. Vouga E, Höbinger M, Wallner J, Pottmann H. Design of self-supporting surfaces. ACM Trans Graph. 2012 Aug 5;31(4):1–11.
6. Su R, Wen J, Su Q, Wiederoder MS, Koester SJ, Uzarski JR, et al. 3D printed self-supporting elastomeric structures for multifunctional microfluidics. Sci Adv. 2020 Oct 9;6(41).
7. Speijer Diez P. 3D printed Fluidic systems [Internet]. Delft: Delft University of Technology; 2022 Mar [cited 2022 Apr 3]. Available from: http://resolver.tudelft.nl/uuid:708a9c8c-a1e6-49d7-9a1f-835b174265cd
8. Bader C, Patrick WG, Kolb D, Hays SG, Keating S, Sharma S, et al. Grown, printed, and biologically augmented: an additively manufactured microfluidic wearable, functionally templated for synthetic microbes. 3D Printing and Additive Manufacturing. 2016 Jun;3(2):79–89.
9. Speijer Diez P. 3D printing with fluid analysis and guidelines Pablo Speijer-2021. 2022.

Appendix C: Development of voxel-based support structure

In addition to previous printing guidelines founded by Maccurdy et al. and Speijer [26], [39] a new 3D printing workflow using a voxel-based support structure is introduced to overcome the challenges of Liquid Printing fluidic cavities.

The main challenges and guidelines for 3d printing fluidic interfaces are presented in Table 1.

Limitation (challenge)	**Cause**	**Guideline presented by Maccurdy & Speijer [26], [40]**
Top layer collapse for printing over Liquid repositories exceeding 20x20 mm. Shown in Figure xx FIXME	Sinking of uncured deposited droplets *Substrate Material* on top of the printed *Liquid Material*	Integration of support pillars within liquid volumes providing structural support for top layers.
Poor interface surface quality between Liquid and substrate material. Shown in Figure xx FIXME.	Mixing of (cured) substrate material particles and uncured liquid material at surface interface.	Integration of thin support walls (0.2 mm) surrounding liquid repositories.
Delamination of printed layers surrounding large liquid areas, substantially along the y-axis. Shown in Figure xx FIXME.	Spillage of liquid material due to 'waving'. Caused by roller movement and print bed shaking.	Minimum wall thickness of 2.11mm, combined with the addition of support walls along the y-axis to reduce 'waving' effect.

Table 1: Limitations, cause and guidelines found by Maccurdy and Speijer [26], [40] FIXME

Maccurdy and Speijer use a CAD-based workflow for the integration of support material within liquid structures. This means that components are imported as separate STL files within the Grabcad Print environment, with individual mesh bodies assigned to each material. The downside of this approach is that support walls and pillars result in discrete 'solid' bodies with sharp edges of transition between SUP706 and Cleanser material. The solid bodies solve the effects to some extent, but still poor printing qualities are reported. Besides, they remain very difficult to remove when draining complex internal structures.

Making use of a process called ‘bitmap printing’, graded heterogeneous components can be created as described by Doubrovski et al. in [11]. Using this workflow, a voxel based support structure is developed by mixing SUP706 and Cleanser droplets on a halftoning principal. To showcase the haltoning principle, the difference between the CAD based workflow as used by Maccurdy and Speijer and the Voxel based workflow is shown in Figure 1.

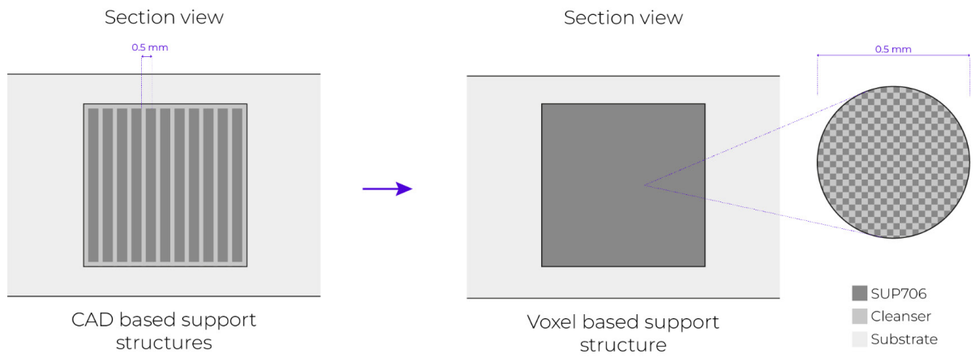

Figure 1: Difference between CAD based support and Voxel based support structure.

The goal for the voxel based support structure is to achieve better printing quality, whilst still being easily removable from complex internal structures.

Validation of voxel based support structure

It is hypothesised that the voxel based support structure acts as a homogeneous substance, which allows it to be drained from complex structures. Besides it is hypothesised the voxel based support structure is less subjective to: sinking of top layer substrate material droplets, resulting in top layer collapse, ‘waving’ resulting in delamination in adjacent layers of substrate material, and poor material surface interfaces between support structures and substrate material.

To validate these hypotheses on voxel based support material, a set of samples have been printed and visually observed for delamination, interface surface quality, top layer collapse and the viscosity of support material. In addition to the visual observance viscosity measurements have been performed on a subset of the samples using a rheological measurement device (TA Instruments GR-G2).

The samples vary in Cleanser to SUP706 ratio; from 0-100% with increments of 10%. The overall design and dimensions of the samples is shown in Figure 2. To showcase the variations in ratio, corresponding bitmap images for increased deposition of Cleasner material for different samples is shown in Figure 3.

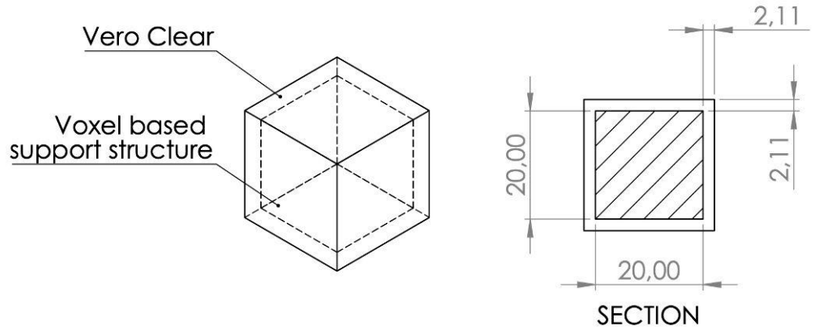

Figure 2: Design and dimensions of the encapsulated sample. Following Macurdy guidelines [26].

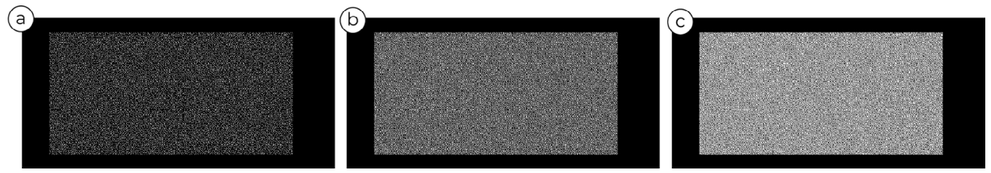

Figure 3: Bitmap image describing Cleanser material deposition of a central layer for printed samples. Printed with voxel-based support material of (a) 20% Cleanser to 80% SUP706, (b) 40% Cleasner to 60% SUP706, (c) 60% Cleanser to 40% SUP706. (x : y = 2 : 1).

Results

Figure 4 shows the results of the 3D printed samples. 2 series of samples have been printed: a series without a top enclosure to observe the support structures viscosity, delamination and surface interface quality, and an encapsulated series to observe top layer collapse.

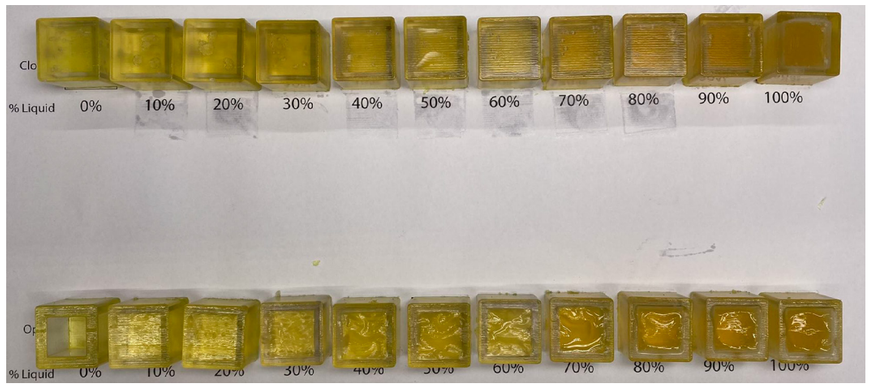

Figure: 2 series of samples printed with voxel based support. Encapsulated (above) and open top (below)

The resulting support structures appear as an homogeneous substance. The viscosity varies from a solid gel-like substance (0% Cleanser) to a fully liquid substance (100% Cleanser). A tip over point from solid (gel-like) to fluidic properties can be visually determined in between 50% and 60% cleanser material, shown in Figure 5.

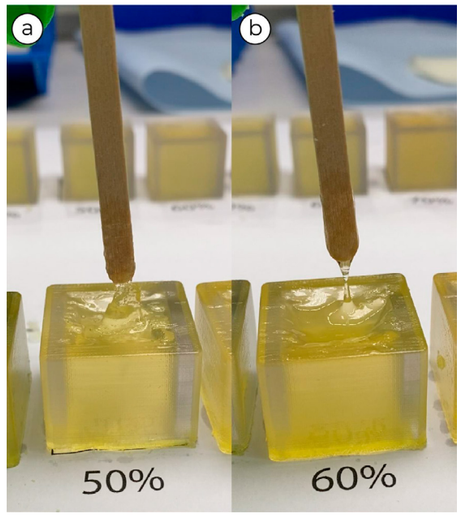

Figure 5: (a) 50% liquid support structure (b) 60% liquid support structure , tip over point from gel-like to liquid support structure.

The results of the rheological measurements are presented in Figure xx FIXME and the semi-log plot in Figure6.

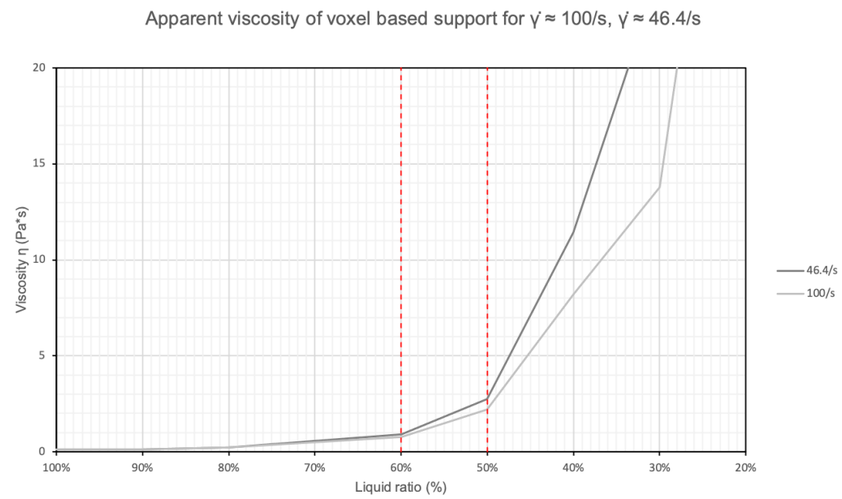

Figure 6: Below 50% liquid, voxel support material increases heavily in viscosity.

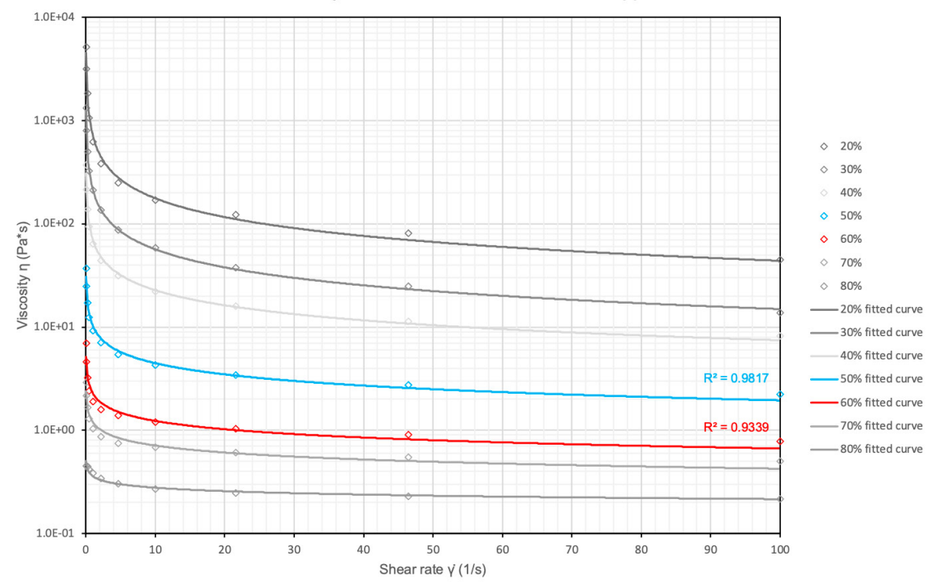

Figure 6: Semi-log plot: voxel based support acts as a shear thinning fluid. Apparent viscosity for 60% voxel support at $\dot{\gamma}$=100, 0.78 Pa.s.

Conclusion

Interpreting the results, the following conclusion can be drawn:

What is the effect of the ratio on delamination?
The ratio Cleanser to SUP706 has a positive effect on delamination; this means that if more cleanser material is present in the voxel based support structure, more delamination has been reported within the samples..

What is the effect of the ratio on surface interface quality?
The ratio Cleanser to SUP706 has a negative effect on surface interface quality; this means that if more cleanser material is present in the voxel based support structure, surface interface quality decreases within the samples.

What is the effect of the ratio on top layer collapse?
Due to the dimensions of the printed samples (not exceeding 20x20x20mm, limitation provided by Maccurdy [26]) no significance effect of the ratio on the top layer collapse could be determined. However, few top layer imperfections can be identified on multiple samples.

What is the effect of the ratio on the viscosity of the support structure?
BY visually observing the samples it can be concluded that the ratio Cleanser to SUP706 has a negative effect on viscosity; this means that if more cleanser material is present in the voxel based support structure, the viscosity of the support structure decreases.

Figure xx FIXME shows a significant strong increase in viscosity for voxel based support structures below 50% Cleanser ratio. Combining these results with the visual observance of the samples it can be concluded the optimum ratio is in between 60% and 50%.

Combining experimental and empirical research the **optimum support structure for 3D printing fluidic interfaces is determined as voxel based support structure with a 55% SUP706 cleaner, generated using a haltoning principle. The support structure can be characterised as a homogeneous shear thinning liquid.**

The gain in print quality for using a 55% support : 45% liquid voxel-based support structure in comparison to a fully liquid print is shown in Figure 7:

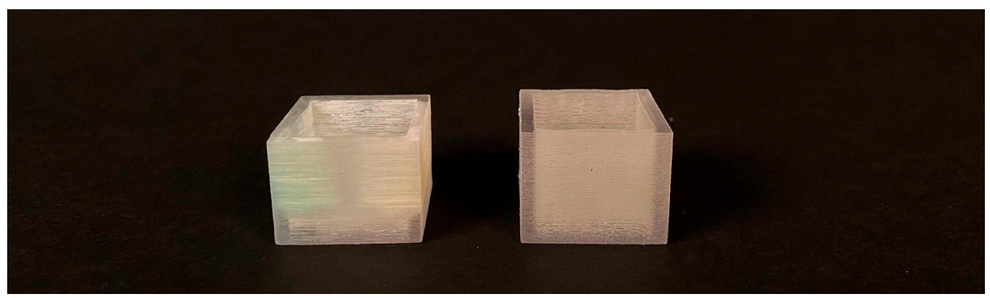

Figure 7: Gain in printing quality for 20x20mm cube using a voxel-based support structure of 55% liquid to 45% support. (left) A sample printed with 100% liquid support. (right) A sample printed with voxel-based 55% liquid to 45% support structure.

Bibliography

1. MacCurdy R, Katzschmann R, Youbin Kim, Rus D. Printable hydraulics: A method for fabricating robots by 3D co-printing solids and liquids. 2016 IEEE International Conference on Robotics and Automation (ICRA). IEEE; 2016. p. 3878–85.
2. Speijer Diez P. 3D printing with fluid analysis and guidelines Pablo Speijer-2021. 2022.
3. Speijer Diez P. 3D printed Fluidic systems [Internet]. Delft: Delft University of Technology; 2022 Mar [cited 2022 Apr 3]. Available from: http://resolver.tudelft.nl/uuid:708a9c8c-a1e6-49d7-9a1f-835b174265cd
4. Doubrovski EL, Tsai EY, Dikovsky D, Geraedts JMP, Herr H, Oxman N. Voxel-based fabrication through material property mapping: A design method for bitmap printing. Computer-Aided Design. 2015 Mar;60:3–13.

Appendix D: Grasshopper file of simulation

For using the simulation *Firefly* must be installed for the Arduino component. Note this plugin is only available for Windows OS. For a better display performance, the display settings for the Rhino viewport can be altered according to Figure 2.

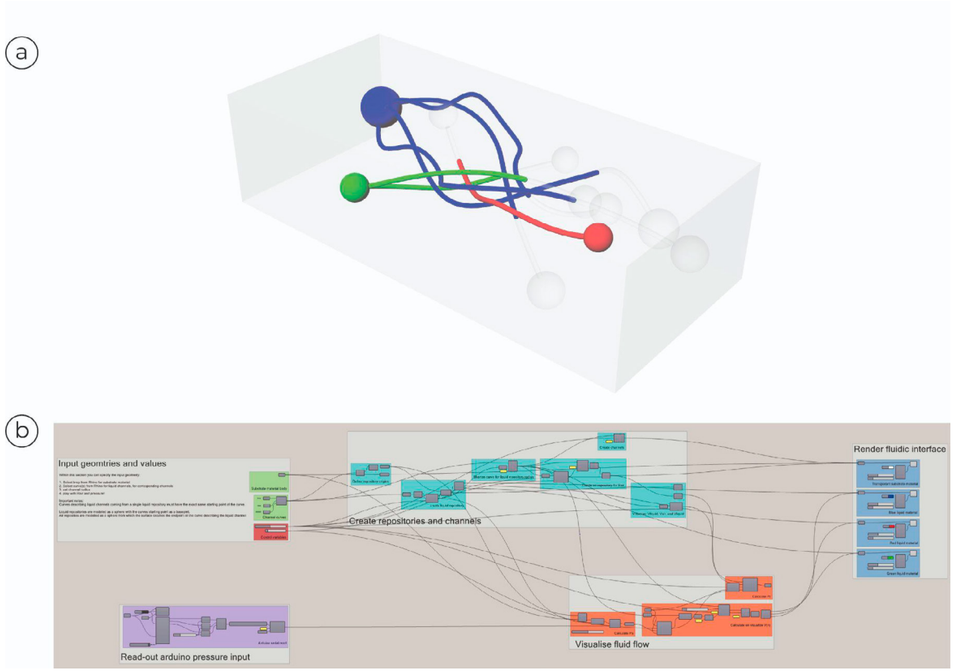

Figure 1: Grasshopper file of the simulation tool. (a) Rendered output. (b) Grasshopper code.

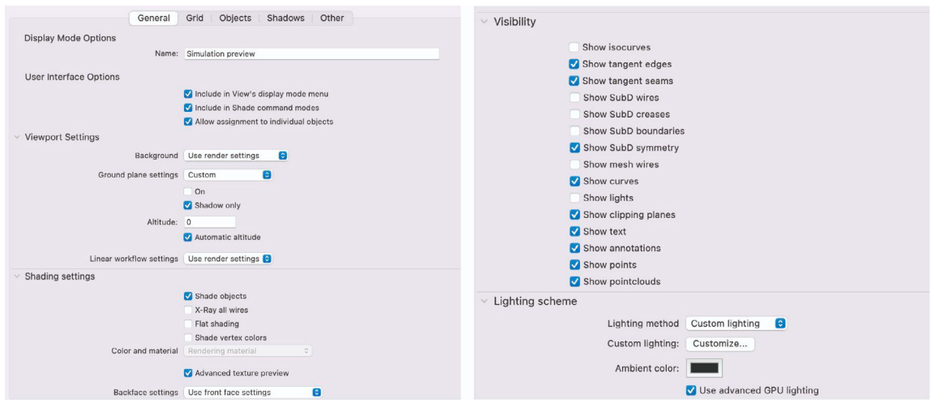

Figure 2: Display settings used for Rhino viewport during simulation.

Appendix E: Excel tool for determining $R_{(m)}$ and $h_{(m}$

A plotting tool is developed in excel to plot the effect of $R_{(m)}$ and $h_{(m)}$. The parameters can be adjusted within the orange section on the top left, together with $Fpress\ (max)$.

4 graphs are plotted to see the effect of $R_{(m)}$ and $h_{(m)}$ on the fluid flow of a fluidic interface.

Interpreting the results designers are able to obtain the initial values for the parameters for their design.

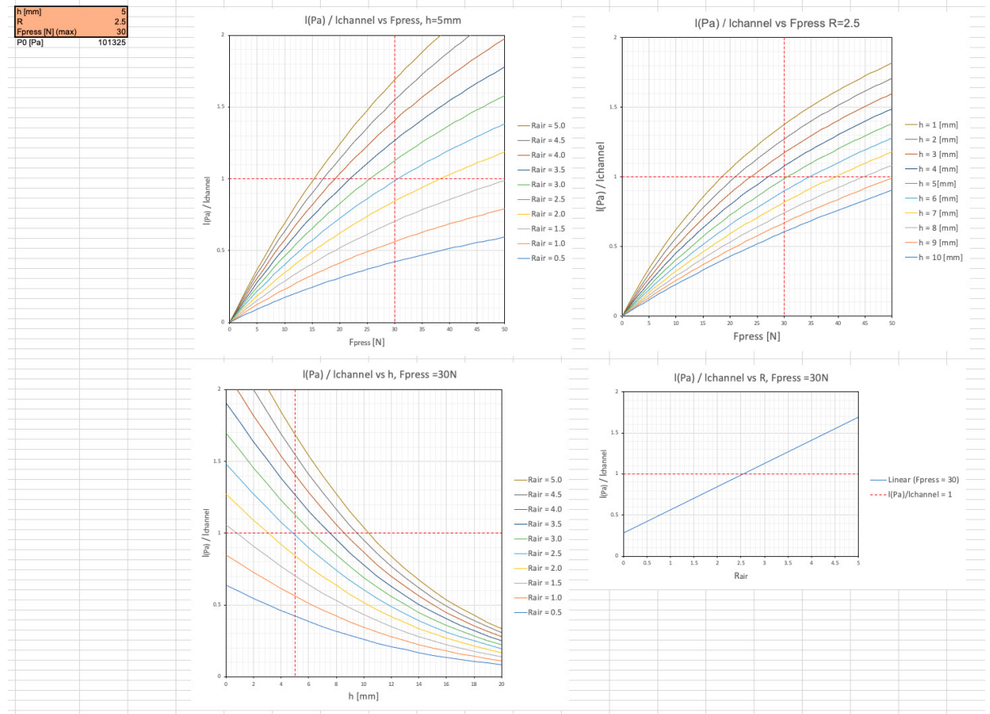

Figure1: Overview of Excel tool for plotting R(m) and h(m).

Appendix F: Data sheet Interlink Electronics FSR 402

INTERLINK ELECTRONICS
Sensor Technologies

FSR 402 Data Sheet

FSR 400 Series Round Force Sensing Resistor

Features and Benefits

- Actuation Force as low as 0.1N and sensitivity range to 10N.
- Easily customizable to a wide range of sizes
- Highly Repeatable Force Reading; As low as 2% of initial reading with repeatable actuation system
- Cost effective
- Ultra thin; 0.45mm
- Robust; up to 10M actuations
- Simple and easy to integrate

Industry Segments

- Game controllers
- Musical instruments
- Medical device controls
- Remote controls
- Navigation Electronics
- Industrial HMI
- Automotive Panels
- Consumer Electronics

Description

Interlink Electronics FSR™ 400 series is part of the single zone Force Sensing Resistor™ family. Force Sensing Resistors, or FSRs, are robust polymer thick film (PTF) devices that exhibit a decrease in resistance with increase in force applied to the surface of the sensor. This force sensitivity is optimized for use in human touch control of electronic devices such as automotive electronics, medical systems, and in industrial and robotics applications.

The standard 402 sensor is a round sensor 18.28 mm in diameter. Custom sensors can be manufactured in sizes ranging from 5mm to over 600mm. Female connector and short tail versions can also be ordered.

Figure 1 - Force Curve

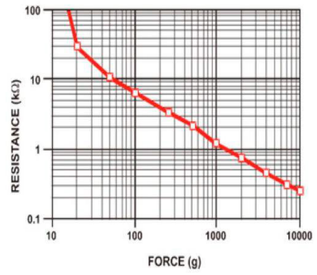

Figure 2 - Schematic

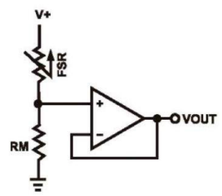

Interlink Electronics - Sensor Technologies

www.interlinkelectronics.com

INTERLINK ELECTRONICS
Sensor Technologies

FSR 402
P/N: 30-81794

Applications

Detect & qualify press
Sense whether a touch is accidental or intended by reading force

Use force for UI feedback
Detect more or less user force to make a more intuitive interface

Enhance tool safety
Differentiate a grip from a touch as a safety lock

Find centroid of force
Use multiple sensors to determine centroid of force

Detect presence, position, or motion
Of a person or patient in a bed, chair, or medical device

Detect liquid blockage
Detect tube or pump occlusion or blockage by measuring back pressure

Detect proper tube positioning

Many other force measurement applications

Device Characteristics

Feature	Condition	Value*	Notes
Actuation Force		0.1 Newtons	
Force Sensitivity Range		0.1 - 10.0[2] Newtons	
Force Repeatability[3]	(Single part)	± 2%	
Force Resolution[3]		continuous	
Force Repeatability[3]	(Part to Part)	±6%	
Non-Actuated Resistance		10M W	
Size		18.28mm diameter	
Thickness Range		0.2 - 1.25 mm	
Stand-Off Resistance		>10M ohms	Unloaded, unbent
Switch Travel	(Typical)	0.05 mm	Depends on design
Hysteresis[3]		+10%	$(R_{F+} - R_{F-})/R_{F+}$
Device Rise Time		<3 microseconds	measured w/steel ball
Long Term Drift		<5% per $\log_{10}$(time)	35 days test, 1kg load
Temp Operating Range	(Recommended)	-30 - +70 °C	
Number of Actuations	(Life time)	10 Million tested	Without failure

* Specifications are derived from measurements taken at 1000 grams, and are given as one standard deviation / mean, unless otherwise noted.

1. Max Actuation force can be modified in custom sensors.
2. Force Range can be increased in custom sensors. Interlink Electronics have designed and manufactured sensors with operating force larger than 50Kg.
3. Force sensitivity dependent on mechanics, and resolution depends on measurement electronics.

www.interlinkelectronics.com

Contact Us

United States
Corporate Offices
Interlink Electronics, Inc.
546 Flynn Road
Camarillo, CA 93012, USA
Phone: +1-805-484-8855
Fax: +1-805-484-9457
Web: www.
interlinkelectronics.com
Sales and support:
fsr@interlinkelectronics.com

Japan
Japan Sales Office
Phone: +81-45-263-6500
Fax: +81-45-263-6501
Web: www.interlinkelec.co.jp

Korea
Korea Sales Office
Phone: +82 10 8776 1972

Application Information

FSRs are two-wire devices with a resistance that depends on applied force.

For specific application needs please contact Interlink Electronics support team. An integration guide is also available.

For a simple force-to-voltage conversion, the FSR device is tied to a measuring resistor in a voltage divider configuration (see Figure 3). The output is described by the equation:

$$V_{OUT} = \frac{R_M V +}{(R_M + R_{FSR})}$$

In the shown configuration, the output voltage increases with increasing force. If R_{FSR} and R_M are swapped, the output swing will decrease with increasing force.

The measuring resistor, R_M, is chosen to maximize the desired force sensitivity range and to limit current. Depending on the impedance requirements of the measuring circuit, the voltage divider could be followed by an op-amp.

A family of force vs. V_{OUT} curves is shown on the graph below for a standard FSR in a voltage divider configuration with various R_M resistors. A (V+) of +5V was used for these examples.

Figure 3

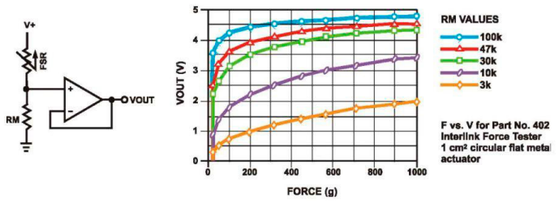

Part No. 402

- Active Area: 12.7mm
- Nominal thickness: 0.55 mm

Mechanical Data

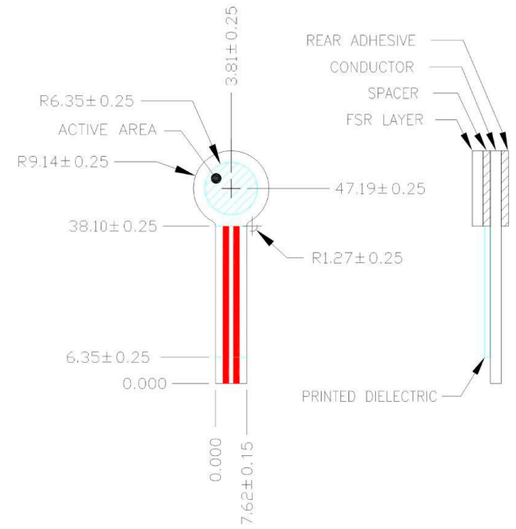

P/N: 94-00011 Rev. A

Interlink Electronics - Sensor Technologies

Expert Interview

FLUIDIC INTERFACES

I Introduction

- Introduce yourself: David van Rijn IPD master
- Graduation project, Willemijn & Zjenja, final stage. Next week greenlight & one month to graduate.
- Briefly inform project" 3D printed fluidic channels in 3D shapes.
  I would like to let you think freely without steering you too much upfront.
- My end result: a set of 3D printed samples.
- Final step I would like to interview 5 experts on these samples to explore further research opportunities and applications. Which could form a starting point for future research.
- Interview consists of 9 questions, on which we can elaborate. I would like to record audio if that's okay. Can I use your name in my report? Wil take around 25 minutes. And at the end there is some room for a free discussion.
- Do you have any questions for now?

Input
Fluids with different properties

Output
3D free shape

Together
Analog
Embedded
Reversible
Responsive

Interview sheet 1

II Interview questions

>>> *Start recording*

PART 1 / GETTING ACQUAINTED WITH SAMPLE

Show first sample

1. Without touching, what do you see?

Invite to touch, please think out loud!

2. What do you experience?

3. How do you think it works?

PART 2 / APPLICATIONS

Briefly explain working principle, get other samples

4. At this moment, what is interesting about these samples for you?

I am curious to know what, from your area of expertise, might be interesting applications...

5. So, could you quickly explain your expertise area?

6. Looking from this expert point of view: What do you foresee as promising applications for these fluidic interfaces?

7. What makes these fluidic interfaces fitting the promising application?

PART 3 / FUTURE

8. If you could change some properties, what would you like to change in order to create more value for promising applications?

9. From your point of view, what do you see as valuable research on fluidic interfaces?

III Ending

So the interview is over

10. Are there any thoughts or questions that come up in your mind that we haven't discussed yet?

>>> *End recording*

Interview sheet 2

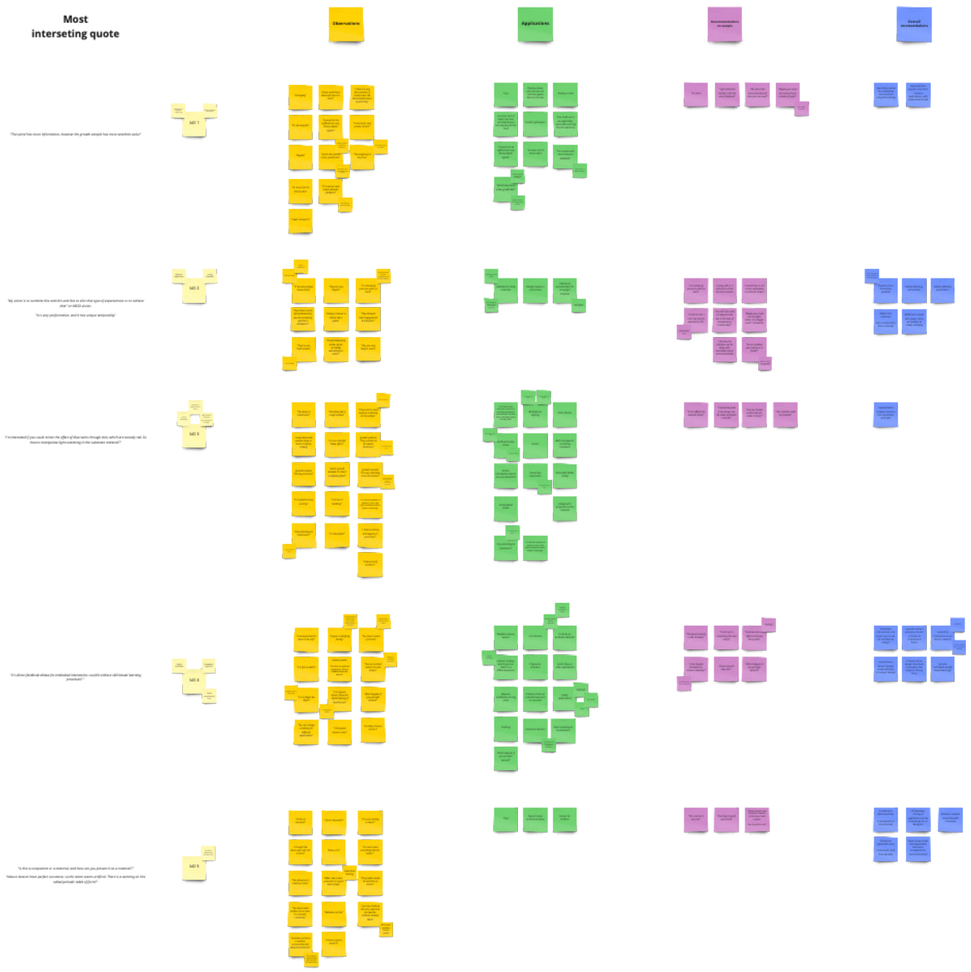

Figure1: Interview results per participant. Divided by (1) observations. (2) Applications. (3) Recommendations on samples. (4) Overall recommendations

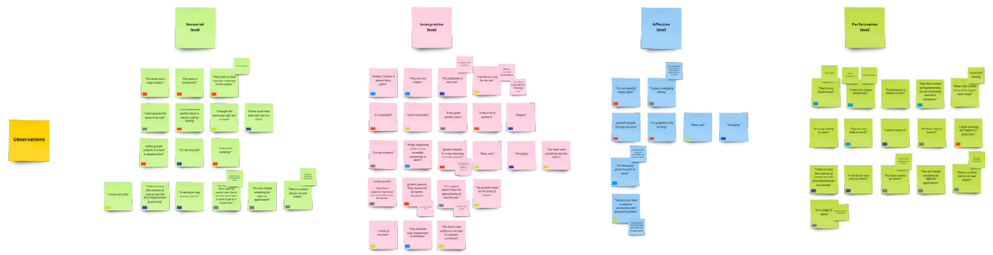

Figure 2: Observations according to four levels of experiential qualities as defined by Giaccardi & Karana [17] .

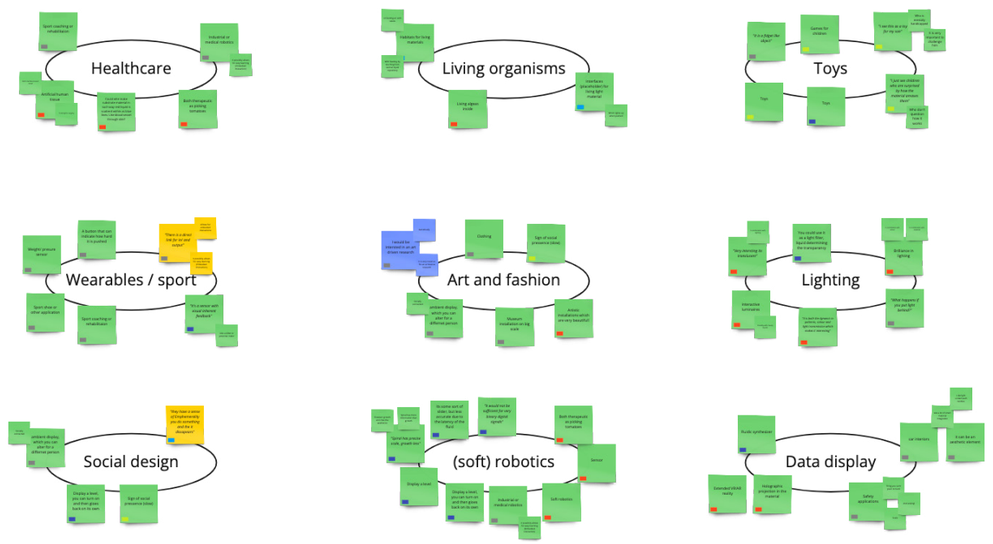

Figure 3: Applications found during interviews categorised by six application areas.

Master Thesis
MSc. Integrated Product Design
Faculty of Industrial Design Engineering
Delft University of Technology

08-12-2022
David van Rijn